WARSAW UNIVERSITY OF TECHNOLOGY

FACULTY OF MECHATRONICS

Ph. D. Thesis

Maciej Karaszewski, M.Sc.

Automated system for high resolution 3D shape digitization

Supervisor

Robert Sitnik, PhD.

Warsaw 2017

Abstract

Growing quality and accuracy of devices used for acquiring 3D shape of surfaces of objects, as well as their affordability and development of 3D visualization methods (augmented and virtual reality) led to their popularity in various applications. 3D models are currently used in, for example, reverse engineering, quality control, 3D printing, special effects in movies, 3D animation and, last but not least, in cultural heritage (CH) documentation. Some of those applications require very high spatial resolution of 3D models, which implies taking many (hundreds or even thousands) directional measurements of the object being digitized. Those measurements have to be integrated into complete 3D model. The whole process is very time-consuming and requires patience and precision from 3D scanner user. It significantly rises cost of professional digitization, but also introduces so called "operator influence" on the measurement result. The result of this influence is that no two 3D models of the same object, even obtained by the same person will not be identical (with regard to measurement noise). In many applications, for example when 3D data is used for comparing objects before and after restoration in CH, it is disqualifying.

This dissertation refers to the topic of automation of 3D shape digitization of objects which does not have any prior digital models. The process of digitization consists of following actions: calculating the set of 3D scanner poses which are required for full digitization of object (this issue differs significantly whether computer model of the object is or is not available), collision-free positioning of the scanner in calculated poses and integrating obtained directional measurements into complete 3D model. When automated, this process does not require operator assistance (apart from obvious actions like placing object within operating space of the system, putting rough object dimensions etc.). The work presented in this dissertation emphasizes the problem of obtaining 3D models with high spatial resolution (c.a. 2500 points per mm^2), required in many professional applications.

In this work, review of existing systems for automated digitization of 3D shape is presented. Those systems are divided into commercial and research ones. Further, elements of typical digitization station are presented: contactless, optical shape acquisition devices, positioning devices and control algorithms. In the following sections of this work, 3DMADMAC|AUTOMATED system for acquisition of 3D data, developed with author assistance, is presented. Its disadvantages are discussed, along with the proposed solutions which led to development of HD3D|AUTO system.

In the last section of this dissertation, results of HD3D|AUTO evaluations are presented. They consist of digitization of various objects including simple geometrical primitives, cultural heritage objects as well as technical ones (automotive parts). The performance of the system is compared to the typical semi-automated digitization processes conducted by experienced operators from Museum of King Jan III's Palace in Wilanów 3D Documentation Laboratory.

Keywords: **3D digitization, automation of 3D measurements, next-best-view**.

Streszczenie

Wzrastająca jakość i dokładność urządzeń pozwalających na akwizycję danych 3D reprezentujących powierzchnię obiektów, jak również spadek ich cen oraz rozwój metod wizualizacji 3D (rzeczywistość wspomagana i wirtualna) powoduje coraz szersze wykorzystanie ich w rozmaitych zastosowań. Modele 3D są aktualnie wykorzystywane między innymi do inżynierii odwrotnej, kontroli jakości ale również pozyskiwania modeli do coraz popularniejszego druku 3D, efektów specjalnych w filmach, animacji 3D a także do profesjonalnej digitalizacji zbiorów muzealnych. W niektórych zastosowaniach wymagane jest uzyskanie bardzo wysokiej rozdzielczości przestrzennej modelu, co wiąże się z koniecznością wykonania wielu (nawet setek czy tysięcy) pojedynczych (tzw. kierunkowych) pomiarów 3D obiektu, które następnie muszą być połączone w całościowy model 3D. Proces ten jest bardzo czasochłonny i wymaga od użytkownika skanera 3D cierpliwości i precyzji, co w znacznym stopniu podnosi koszt profesjonalnej digitalizacji, a także obarcza pozyskane dane tzw. wpływem operatora, powodującym że dwa modele 3D pozyskane z tego samego obiektu nigdy nie będą identyczne. Nierzadko dyskwalifikuje to dane z profesjonalnego zastosowania (np. porównanie obiektu przed i po konserwacji).

Prezentowana praca podejmuje temat automatyzacji procesu digitalizacji 3D kształtu obiektów rzeczywistych, dla których nie istnieje wcześniejszy model komputerowy. Proces digitalizacji obejmuje wszystkie czynności, począwszy od wyznaczenia zbioru położeń skanera 3D niezbędnych do akwizycji pomiarów kierunkowych (zagadnienie znacznie różne od przypadku kiedy istnieje model komputerowy skanowanego obiektu), bezkolizyjnego pozycjonowania tego urządzenia aż do połączenia danych w całościowy model 3D. Proces ten wykonywany jest bez uczestnictwa operatora (poza oczywistymi czynnościami takimi jak umieszczenie obiektu na stanowisku pomiarowym, określenie jego zgrubnych gabarytów, uruchomienie procesu itp.). Duży nacisk położono na zagadnienie pozyskania modeli o wysokiej rozdzielczości przestrzennej (rzędu 2500 punktów na mm^2), wymaganych w profesjonalnych zastosowaniach (np. dokumentacji konserwatorskiej).

Praca przestawia przegląd istniejących systemów automatycznej akwizycji kształtu 3D, z podziałem na systemy komercyjnie dostępne (głównie przeznaczone do kontroli jakości lub inżynierii odwrotnej) i zaprezentowane w literaturze naukowej. Omówione zostały również elementy typowego stanowiska automatycznej digitalizacji, takie jak bezkontaktowe, optyczne systemy akwizycji informacji o kształcie obiektu, urządzenia pozycjonujące oraz

algorytmy sterujące procesem pomiarowym. W dalszej części pracy przedstawiono opracowany przy udziale autora zautomatyzowany system akwizycji kształtu 3DMADMAC|AUTOMATED wraz z jego niedoskonałościami udoskonalonymi w drugiej wersji systemu nazwanej HD3D|AUTO. W pracy znajduje się również wynik procedur testowych nowego systemu, przeprowadzonych dla różnorodnych obiektów, będących zarówno prostymi bryłami geometrycznymi, obiektami muzealnymi jak i elementami technicznymi (części samochodowe). Zestawiono również wydajność systemu w odniesieniu do procesu digitalizacji obiektów zabytkowych wykonanych przez profesjonalnych operatorów półautomatycznego systemu digitalizacji 3D z Laboratorium Digitalizacji 3D w Muzeum Pałacu Króla Jana III w Wilanowie.

Słowa kluczowe: **digitalizacja 3D, automatyzacja pomiarów 3D, selekcja najlepszych kierunków skanowania**.

Contents

1. Introduction

The recent 15 years has been a time of growing popularity and applicability of three-dimensional techniques (Barrile, et al., 2015), (National Institute of Justice, 2016), (Taylor, et al., 2016), (Yashyna, et al., 2016), (Henry, et al., 2014), (Markets, 2016).Those techniques range from the acquisition devices, through presentation (like virtual (Roettgers, 2016), (Meeri, 2016) (Lee, 2016), (Rusli, 2015), (Ginsburg, 2016), (Cline, 2005) and augmented reality (Stuart, 2012), (Divecha, 2011), (Webley, 2010), (Wadhwa, 2013), (Katts, 2012), (Loy Rodas, 2014), (Davis, 2016) (Calhoun, et al., 2005), (Benford, et al., 1998), (TRoesner, et al., 2014)) up to 3D printing (Scopigno, et al., 2015) (Wittbrodt, et al., 2013), (The Economist, 2016) and other manufacturing methods like injection molding (Rosato & Rosato, 2012), CNC machining (Altintas, 2012) etc. Virtually all branches of 3D-related techniques have been heavily researched and developed which led to their growing applicability. Recently, the 3D printing is one of the hottest topics on the market, moving from the niche' to mainstream (Kerney, 2015), (Finocchiaro, 2012). Also, with such large players like Intel (Intel Corporation, 2016), Microsoft (Microsoft Corporation, 2016), Google (Google, 2016), HTC (HTC, 2016) and Facebook (Facebook, 2016), the virtual (VR) and augmented (AR) reality is bound to be the next step of multimedia, shifting from 2D images and videos to full 3D imagery both in entertainment and professional branches of industry.

While the technology utilizing 3D models is a hot topic in the research and commercial markets, one of the main problems in its development is the acquisition of such models. Generally, 3D content can be synthetic (i.e. computer generated) or natural (i.e. obtained with 3D digitization devices) (Sculpteo, 2016). Usually, creation of synthetic models is easier and does not require any hardware devices but PC computer. On the other hand, obtaining natural 3D models is hardly ever easy and requires some kind of 3D digitization device, specialized software and much work. Natural models are however required for many applications, such as reverse engineering (Durupt, et al., 2008), (Gibson, 2006), documentation of works of art (Bunsch, et al., 2011), industrial quality control (Ponomarenko, et al., 2009) etc.

The complexity of natural 3D models acquisition is a result of many factors which are more or less the same regardless of method used for this process. Figure 1 shows the schematic of such digitization process. To obtain digital 3D model of real-world object, one has to take multiple 3D measurements (from now on referred to as *directional 3D measurements*), changing the spatial relation between measurement head and digitized object to cover the

whole surface of the object. From each of such measurements, partial representation of object's surface is recovered. Joining all parts of the surface, complete model can be recovered. Usually, there are two stages of directional measurements integration – initial and fine. In the first one, rough transformation of data is found. In fine integration stage, the surface part is fitted into the 3D model with precision comparable to geometrical uncertainty of 3D measurement head used. There are many algorithms and methods of initial and fine integration of 3D measurement data (Bernardini & Rushmeier, 2002), (Hähnel & Burgard, 2002), (Munkelt, et al., 2013), (Richter & Döllner, 2014), but they are not data-agnostic which means that the result of their application is a function of input data (generalizing – the number of unique features on the object's surface). Some of those methods require additional markers to be placed on or in the vicinity of object scanned. Finding transformations between subsequent measurements in this case is based on locating those markers in obtained data, usually done automatically. Use of markers is however problematic or impossible (for example when digitizing cultural heritage objects). For specific tasks (for example quality control of some part), only single measurement is required or data integration process can be automated (Larue, et al., 2015), (Haas, 2016), (Dorai, et al., 1998), (Poussart & Laurendeau, 1989). In other cases, the initial integration of directional measurements is done manually or at least it is user guided. For fine integration, in most cases *Iterative Closest Point* (ICP) (Besl & McKay, 1992) algorithm is used.

Due to the skills and time which are needed to carry out manual digitization process, such operation is usually complicated and expensive. Because of this, natural 3D models are not so popular as digital ones, and most of the existing ones are of poor quality. In fact, those models are usually either acquired for amateur purposes by hobbyists (low quality) or for strictly professional purposes (high cost, poor availability). There is virtually no in-between space of high quality, rich collections of 3D models. Massive digitization of various objects (like works of art) is nowadays impossible due to the complexity and high cost of such process.

Start of digitization process

Place scanner in the working distance from the object

Make a measurement

Clean measurement data

Manually integrate new measurement with 3D model

Whole object digitized?
yes
no

Identify new position for scanner

Position provides new data?
yes
no

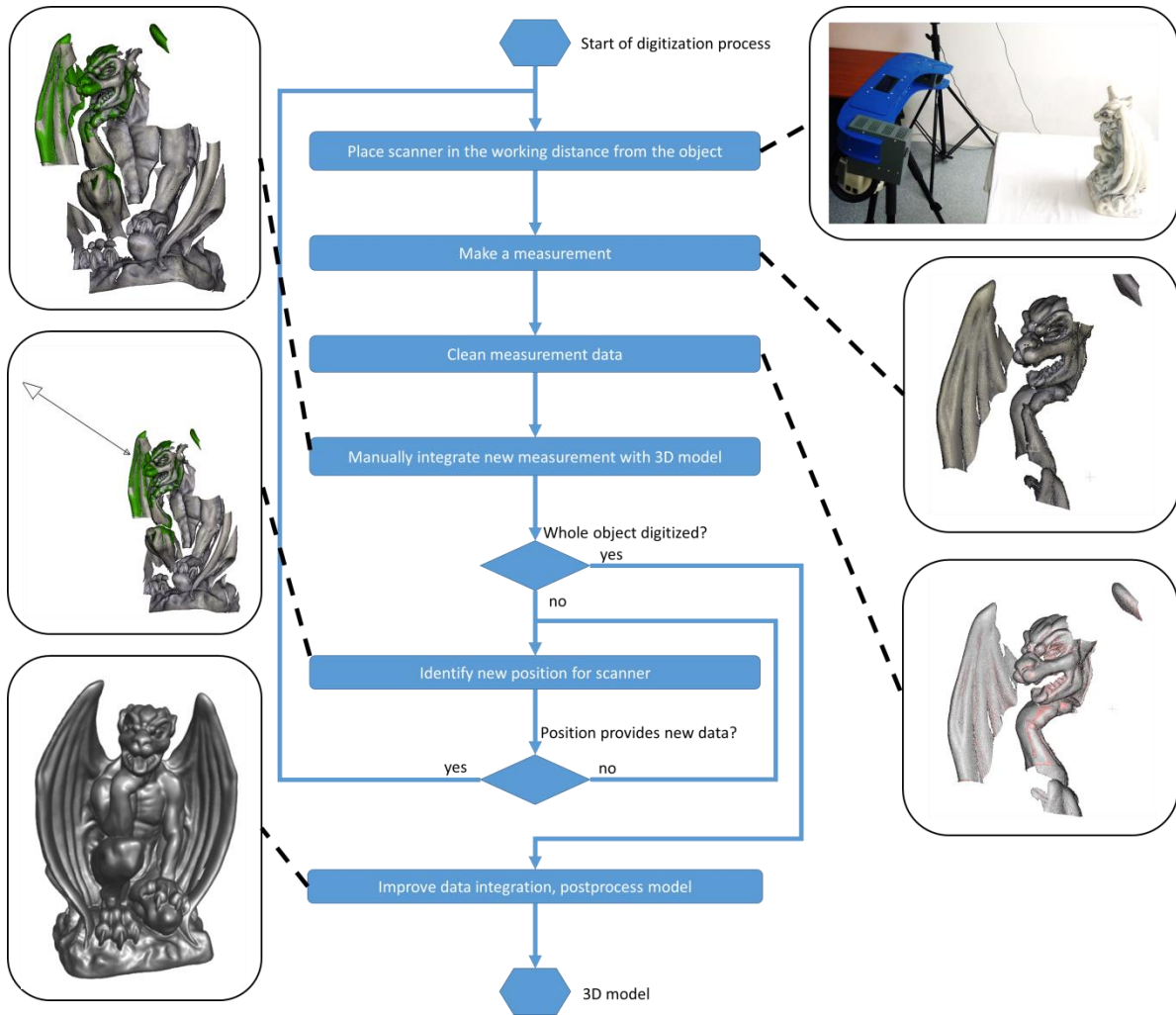Improve data integration, postprocess model

3D model

Figure 1. Manual 3D shape digitization process.

1.1 Motivation

Three dimensional models of objects contain significantly more information than photography, thus they are gaining importance in many professional applications. Some of the examples are: quality control (Yang & Ciarallo, 2001), (Martins, et al., 2005), (Zhao, et al., 2009), reverse engineering (Durupt, et al., 2008), (Gibson, 2006), (Scott, et al., 2003), (De Luca, et al., 2006), (Cheng & Jin, 2006), (Bagci, 2009), (Sokovic & Kopac, 2006), crime scene investigation (National Institute of Justice, 2016), (Hołowko, et al., 2016), (Sansoni, et al., 2009), medicine (Thali, et al., 2007), (Glinkowski, et al., 2010), (Sansoni, et al., 2009), cultural heritage documentation (Taylor, et al., 2016), (Bunsch, et al., 2011), (Remondino, 2011), (Sansoni, et al., 2009). Those applications usually require high resolution measurements. For industrial purposes, the resolution and accuracy of measurements are determined by the tolerances of parts being controlled. Crime scene investigation and medicine scans usually have resolution of 100 points per mm^2 (Figure 2a) or less (Witkowski, et al., 2008), (Banks, 2008), (Hołowko, et al., 2016), (National Institute of Justice, 2016), (Little, et al., 2000). Cultural heritage applications, on the other hand demand much better resolution. While up to now there are no worldwide standards regarding the creation of professional 3D heritage documentation, two independent studies conducted in United Kingdom (MacDonald, 2010) and in Poland (Bunsch, et al., 2011) have determined that the optimal resolution of surface sampling for most materials used in works of art is about 2500 points per mm^2 (i.e. the distance between sampled points is 0.02 mm - Figure 2b).

Some pilot digitization projects use even higher resolution (up to 10000 points per mm^2 – 0.01 mm distance between points). Such sampling density allow to do research on the micro changes in the material caused, for example, by aging, temperature or humidity influence etc. (Markiewicz & Zawieska, 2015), (Bunsch, et al., 2011). For most mentioned applications, measurement data should also include high resolution color information (Stanco, et al., 2011).

Manual 3D shape digitization processes cannot be used for mass production of high resolution 3D models. Besides of being expensive, both in terms of costs and time, they are often unfeasible for professional applications. To obtain high-resolution 3D scan, precise measurement head has to be used. Such devices have very small working volume (Karaszewski, et al., 2012), requiring many directional measurements (even thousands (Bathow & Breuckmann, 2011)) to completely cover the surface of the object being digitized.
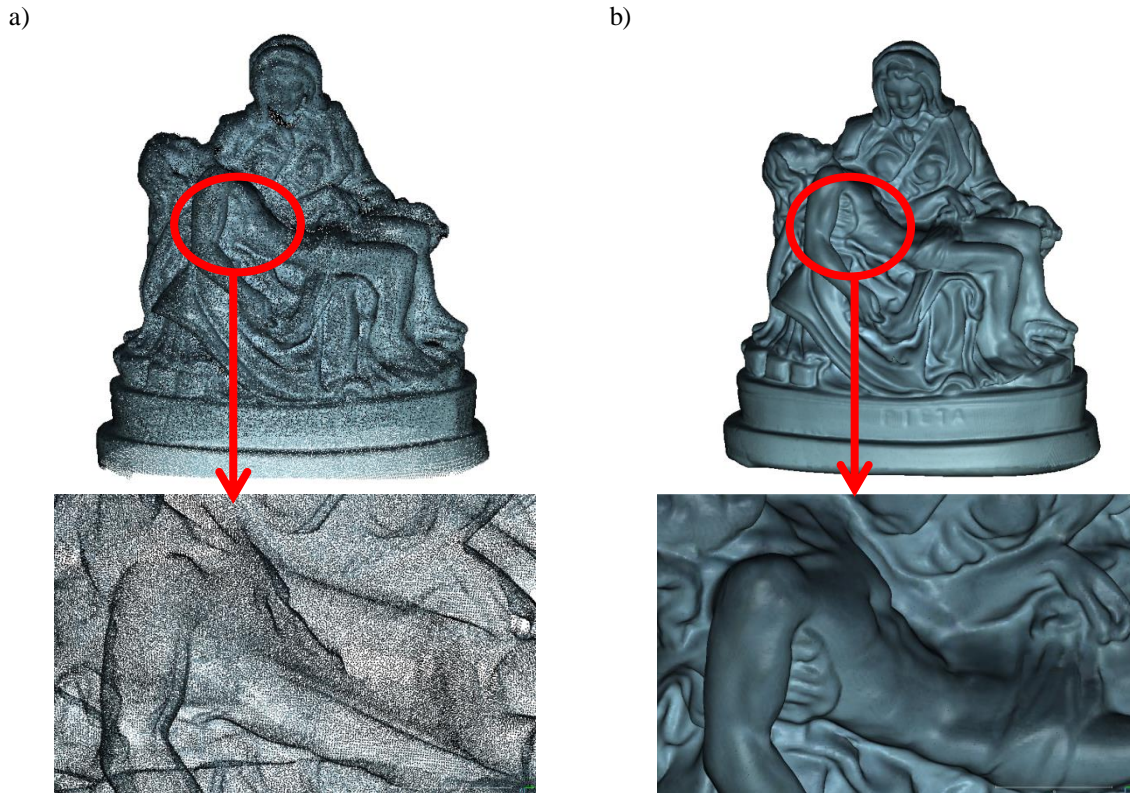
a)   b)

Figure 2. Comparison of surface representation for 3D scan with a) 100 points per mm^2, b) 2500 points per mm^2.

Conducting the process of few hundreds directional measurements is almost impossible for human operator because planning how to position the scanner in relation to the object to cover its whole surface is not a trivial task. Moreover, it is almost sure, that obtained 3D model will have errors, discontinuities etc. which require additional measurements to be fixed. Re-measurement is sometimes impossible or at least very difficult (for example when the object was borrowed from museum collection for limited time) (Bunsch, 2010). The process of joining large number of directional measurements is also a significant problem, both to the operator (skills, time, 3D perception) and processing software (displaying and manipulating large datasets) (Remondino, 2011), (Bathow & Breuckmann, 2011), (Schäfer, et al., 2011), (Kai-Browne, et al., 2016). Usually, it is assumed that no more than hundred directional measurements per 3D model can be integrated by skilled operator (Karaszewski, et al., 2012).

Besides the unfeasibility of manual digitization processes of large number of directional measurements, the so-called operator's influence on the measurement result is a problem. This influence is introduced during the stage of using 3D sensor (by selecting sensor poses) and during the integration of the data (Bunsch, 2010). Because the model is built manually (or semi-manually), with operator providing at least initial transformation of each directional measurement result, the outcome is not determined. Each time it is slightly different as

human's operations are never identical (McAlinden, et al., 2011), (Ajmal, et al., 2010), (Beraldin, et al., 2003), (Bianchi, et al., 2004), (Beraldin, et al., 2007). Such 3D model is unacceptable from the metrological point of view, as it is impossible to isolate the real characteristics of the object from the inaccuracies introduced by operator. Moreover, those inaccuracies are hard to quantify as they tend to change for each operator, his / her disposition, fatigue etc. Because of this, removal of operator's influence on the result of digitization process (i.e. manual data integration) is crucial.

Another source of operator's influence on the final 3D model is the assumed data processing scheme. Selection of algorithms, their controlling parameters and even order of operations may lead to significant differences in obtained data (Bunsch, 2010). The only solution to this problem is to design and strictly follow rules of constructing data processing chain. This should be done by experienced specialists, taking into account particular object's parameters and characteristics.

 Combining the above stated observations, it becomes clear that influence of human operator should be minimized in the 3D shape digitization process. Instead, some kind of automation should be introduced, on all stages of the process, starting from the acquisition, through integration to final data processing. Moreover, the data processing schemes should be designed for variety of object classes to be used as templates depending on the particular digitization subjects. This solution should allow to overcome the obstacles introduced by manual operations to the popularization of high quality, natural 3D model acquisition.

Automated digitization system, the next step in evolution of 3D digitization techniques is a device which utilizes some kind of positioning devices (minimally – rotary stage, usually – 6 axis robot arm and rotary stage) for positioning the 3D sensor during measurement process (Papadopoulos-Orfanos & Francis, 1997), (Kriegel, et al., 2012), (Ko, et al., 2007). If the positioning system has any coupling (i.e. it returns information about its spatial configuration), it can be used to fit directional measurements into complete 3D model without any user interaction. More than that, the whole digitization process can be completely automated – the 3D sensor can be positioned in a set of positions calculated by some kind of algorithm basing on the knowledge about the digitized object (the nature of this knowledge may vary from rough object dimensions only to the complete 3D model, for example CAD file). To allow for completely automated digitization, the measurement system has to use some kind of collision-avoidance methods, either software or hardware-based. To sum up, the automated 3D digitization system should have following components:

- 3D measurement head (based on any technique as long as the results returned are given in coordinate system bound to the head's chassis). Exemplary 3D sensors are structured-light scanner, laser triangulation and time-of-flight camera.

- Positioning system which can be built of any general positioners (rotational or translational ones) with encoders returning the nodes' positions. Exemplary positioners are 6axis robot arm, translation or rotation stages.

- Software with modules for calculating:
    - set of sensor's positions which are required to digitize the surface of the object,
    - collision-free trajectories of sensor's movement between those positions,
    - directional measurements' position and orientation in global coordinate system of 3D model,
    - the noise and other measurement errors which should be filtered out from the data,
    - any operations forming the processing chain leading to the final 3D model format (for example data simplification, triangulation etc.).

- Optional hardware collision-detection module.

The system capable of completely automated, high-resolution 3D digitization of a real world objects would be a significant step forward in the topic of obtaining 3D models for professional purposes like cultural heritage documentation and reverse engineering.

1.2 Research claims

The aim of this work is to develop an automated, high-resolution digitization system which can be used for broad range of objects which do not have prior digital models. The system should have no significant constraints to type of used measurement head, nor to used positioning system construction. It is assumed however, that the measurement head outputs data in the coordinate system fixed to its frame and can have working volume significantly smaller than the size of digitized object (for example 20 times smaller). Also, the range of positioning system should allow for complete object digitization and its inaccuracy has to be small enough to ignore it during calculations of set of head's positions for measurements and to allow for fine integration of data with ICP algorithms. The developed device should be controlled with algorithms which provide high degree of 3D model's completeness (comparable with skilled operator), require less time for digitization than operator-guided system and provide collision-free positioning of measurement head. Also, the controlling software should provide methods to automatically process the data to the form required by end users (noise-removal, simplification, triangulation etc.).

The claim of this research is that automated 3D digitization system will make it possible to obtain high resolution 3D models of objects, simultaneously lowering cost, shortening time of such process and eliminating influence of operator on measurement result.

Detailed research objectives are divided into research and application fields. The research objectives are:

- Development of the method allowing for calculation of a set of measurement directions to be used for obtaining high-resolution 3D model of an unknown object with high surface coverage. During calculations, collision-avoidance between scanner, positioner and digitized object should be considered. From now on, above mentioned process of identifying set of measurement directions will be referred to as *Next Best View*s calculation or *NBV*;
- Evaluation of the developed NBV method for various classes of objects in comparison to other, most popular NBV algorithms.

The application field objectives assume construction of the automated digitization system, with high-resolution, color 3D scanner, 6axis robot arm and rotary stage. This system will be used for digitization of few representative cultural heritage objects as well as technical parts in order to test and prove the potential of the new NBV method in future applications. The selection of the objects is dictated by the high demands to the 3D models in professional cultural heritage documentations – high resolution and high level of surface coverage (Bunsch, et al., 2011) with color information directly mapped onto measurement data.

1.3 Document outline

The dissertation is divided into six chapters. Chapter 2 contains a review of various systems used for automated 3D shape digitization which are available commercially or were presented in literature. This review is summarized by theoretical evaluation of those systems capabilities according to the requirements stated in 1.1 section of this document. Chapter 3 focuses on the elements of the automated 3D digitization system: measurement head, positioning systems and controlling algorithms (Next Best View calculation). A survey of those topics is presented. Chapter 4 is focused on the proposed new digitization system. This chapter is divided into three sections, the first one describes the hardware-related elements of the system, the second one – the first novel algorithm for NBV calculation, the last one – the second, two stage method used for calculating a set of measurement direction in high resolution digitization. The sections describing algorithms are summarized with the evaluation of their performance in relation to popular solutions. Chapter 5 presents exemplary results of automated digitization process for a set of test objects. Final chapter concludes the work giving directions for the future research.

2. Automated digitization systems – a survey

During recent years, automated digitization systems were developed both by research institutions and by companies manufacturing 3D scanners and sensors. While systems constructed for research purposes are focused rather on the problem of digitization of unknown objects (i.e. ones without the previously acquired computer model), commercial devices are made for industrial quality control of parts and elements which have CAD models. This differentiation is crucial when considering algorithms calculating the set of sensor poses required for digitization, considering the occlusion of sensor's working volume, collision avoidance etc. In this chapter, the most important systems are presented, along with the evaluation of their capability to be used in the process of mass, high-resolution 3D shape digitization process.

The systems presented in this chapter are:

1. LaserDesign Rexcan DS3,
2. LaserDesign CyberGage360,
3. ShapeGrabber Ai310,
4. GOM Atos ScanBox,
5. FARO Factory Robo-Imager,
6. ZEISS T-Scan and Comet,
7. Creaform3D ScanMaster,
8. Perceptron Robotic Scanning,
9. RoboScan,
10. Automated digitization system by Khalfaoui,
11. Automated digitization system by Kriegel,
12. CultLab,
13. Automated digitization system by Wu.

In this review, simple digitization systems like MatterAndForm scanner (Matter and Form, 2016), Structure Sensor (Occipital, 2016), XYZPrinting daVinci 1.0 AiO (XYZ Printing, 2016), 3DSystems Sense (3D Systems, 2016) etc. are omitted because they do not provide data of quality acceptable for any professional purpose. Those devices are designed rather as toys or gadgets than measurement devices.

2.1 Commercial systems

In this chapters, commercially available systems are described. Automated 3D measurement devices are present in many manufacturers portfolios. Usually, they are designed with industrial applications in mind, most often inspection and quality control with measurement plans (i.e. set of scanner poses required to digitize the object) created on the basis of CAD models of parts or manually, by skilled operators.

2.1.1 LaserDesign Rexcan DS3

Rexcan DS3 is a portable, automated 3D digitization system for scanning small objects like jewelry, dental elements and tiny industrial parts (Figure 3). This device is aimed at semi-professional users, offering high quality 3D scans for moderate price (LaserDesign, 2016). With its twin-camera structured light measurement head, it allows for surface sampling with up to 2500 points per mm^2 (i.e. 0.02 mm distance between measurement points). 3D scanner uses blue light technology and it is not clear whether it captures color information also.
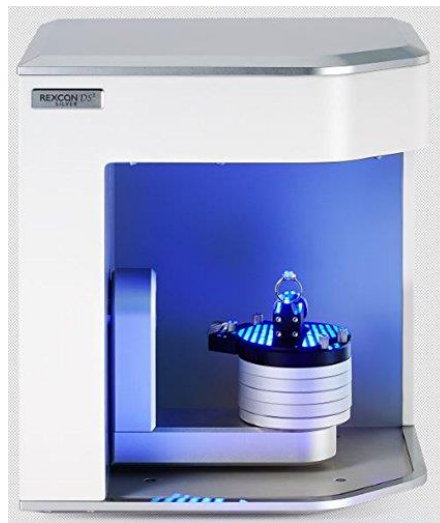

Figure 3. LaserDesign Rexcan DS3 (image source: LaserDesign webpage).

The positioning system used in this device is very simple and has only two degrees of freedom. It is composed of rotary table which can also swivel. With these movements and two camera head, high surface coverage can be obtained for not too complicated objects, but only within very small working volume (user can choose two modes: 50 mm x 50 mm x 50 mm or 120 mm x 120 mm x 120 mm, the second mode yields lower spatial resolution). It is said that the 3D model is returned as STL file (triangle mesh) which, by definition, does not include color information.

There is no direct information about the measurement process itself, but taking into account press materials and demonstration videos (LaserDesign2, 2016), it seems that scanning is performed from predefined set of poses. When there is need to re-measure some part of the object surface, operator can select it and order measurement (unless the required position is not within the reach of positioning tables).

When considering usability of Rexcan DS3 system for massive digitization of objects for cultural heritage purposes (or multimedia ones), the digitization speed has to be emphasized. DS3 manufacturer claims that the complete 3D model creation takes only 3 – 4 minutes (LaserDesign, 2016) albeit this for sure depends on the complexity of the surface and the re-measuring necessity. Declared 2500 points per mm^2 is a spatial resolution high enough even for professional purposes. However, the system lacks fully automated operating mode, in which it would not require operator to assess the completeness of the model or to order additional measurements. Moreover, the limited freedom of positioning system movements does not allow for obtaining high surface coverage for moderately complicated objects.

2.1.2   LaserDesign CyberGage360

Another LaserDesign system made by its subsidiary, CyberOptics Corporation, the CyberGage360 (LaserDesign3, 2016) is a turnkey solution for non-contact automated 3D scanning inspection (Figure 5). This device is intended to be used in factory near-production-line environments, mainly for quality control and inspection. LaserDesign has a product line of such devices, differing in accuracy, resolution and allowable size of measured details, CyberGage360 however uses the sensor with Multi-Reflection Suppression (MRS) technology (Figure 4) which allow for obtaining measurement data with less noise and higher resolution.

The object digitized is placed onto the tray which is supported by three moveable pillars (Figure 5). Such configuration allows for adjusting the position of the object easily but within very limited range. Two MRS sensors observe the working volume (one from the top, the other – from the side). Using such configuration, the full 3D scan can be performed in 3 minutes (LaserDesign3, 2016). The measurement process can use predefined or operator – generated set of tray positions. Directional measurements are automatically integrated and converted to triangle mesh to be compared with CAD model of inspected part.
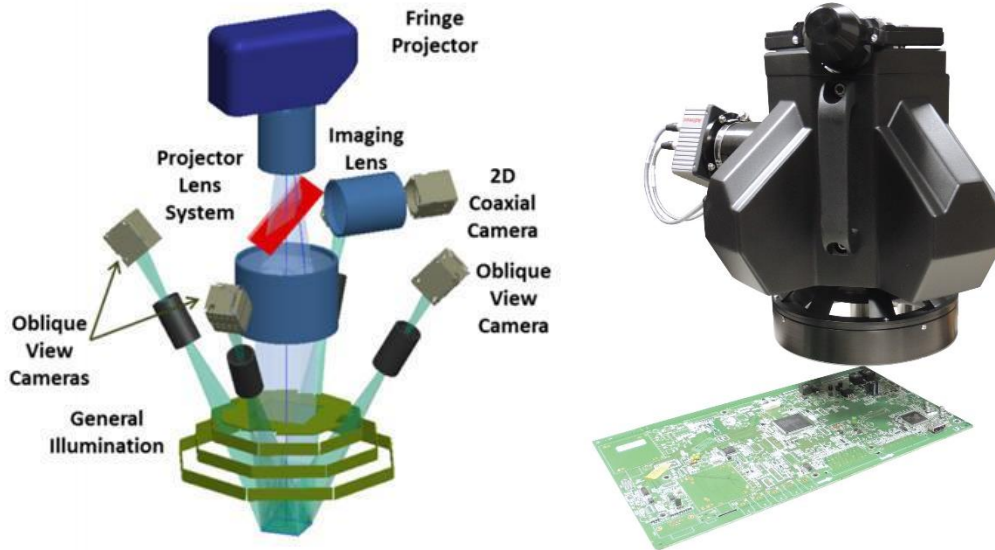
Figure 4. MultiReflection System: schematic and measurement head (image source: LaserDesign webpage).

Figure 5. LaserDesign CyberGage360 (left) and its working chamber (right). Three moveable support pillars are visible near the bottom (images source: LaserDesign webpage).

While the MRS technology is very interesting and probably allows for better quality scans when compared to classic structured-light measurement heads, the sensor does not capture color information. The positioning system does not have large operation range therefore the size of measured objects has to be small. Moreover, it seems that the movements are too limited to deal with measurement of complicated, self-occluding surfaces. Finally, the offline programming for each part makes the system incapable of fully automatic digitization of unknown, real-world objects.

24

2.1.3 Shapegrabber Ai310

Shapegrabber, a subsidiary of Quality Vision International offers a line of automated digitization stations (Shapegrabber, 2016). Those solutions are based on laser profilometer 3D sensors (Figure 6), integrate acquisition, alignment and processing stages in one control application. The positioning modules used in those systems are composed of rotary table on which object is placed and vertical column along which laser scanning head is moved. The larger system has additional horizontally moving scanning head. For the smallest device, Ai310 (Figure 6), maximum measurable object size is defined as cylinder with 300 mm height and 200 mm diameter (Shapegrabber, 2016), for larger model – 800 mm height and 1250 mm diameter. The resolution of 3D scan is customizable but can be as high as 100 points per mm^2 (distance between points of 0.1 mm).

Figure 6. ShapeGrabber Ai310 (left) and its laser profilometers (right) (images source: ShapeGrabber website).

This 3D measurement solution is designed for inspection and quality control purposes only. Measurements plans are created offline, by the operator. Further operation and data processing (which can include analysis of deviations and decision whether scanned part is correct or should be rejected) is operator controlled. Whole GD&T analysis is performed in Geomagic Control software suite (Geomagic, 2016).

Due to measurement head which is used in these systems, there is no color information in measured data. Also, regardless of advertising the system as automated station, operator is required. There is no possibility to measure unknown objects automatically. Finally, the

limited possibility of scanning head positioning (only two or three degrees of freedom) does not allow for obtaining high surface coverage.

2.1.4   GOM Atos ScanBox

The well-known manufacturer of optical measurement hardware, GOM offers a line of automated 3D digitization systems, aimed at various applications which differ with measured objects size, scanning resolution etc. GOM Atos ScanBox comes in 5 variants (GOM, 2016), namely Series 4, 5, 6, 7 and 8 (Figure 7).
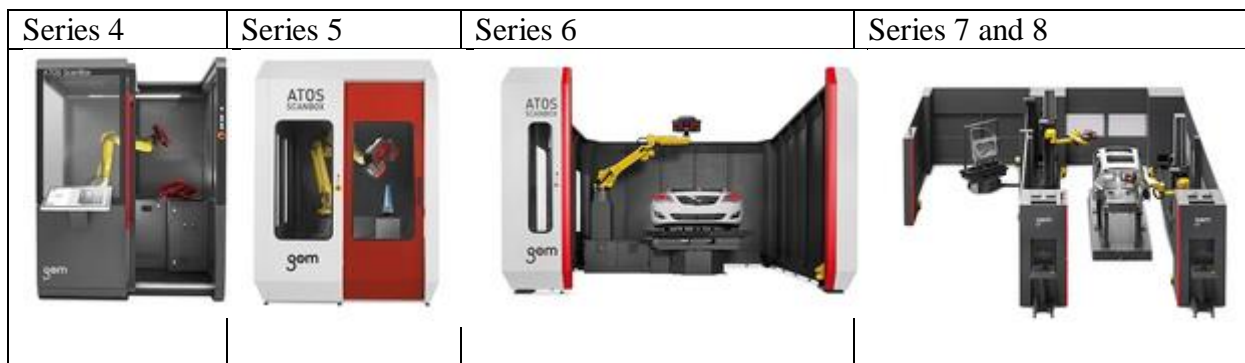
Series 4	Series 5	Series 6	Series 7 and 8

Figure 7. GOM Atos ScanBox systems product line (images source: GOM website).

ScanBox systems differ mainly with the range and complexity of the positioning system. Series 4 is the smallest of the offerings, it can digitize objects up to 500 mm x 500 mm x 500 mm. Measurement head can be adjusted to have working volume as small as 80mm x 60 mm x 60 mm, providing spatial resolution of about 400 points per mm^2 (0.05 mm between points) (GOM, 2016). Series 5 devices are capable of measuring objects up to 800 mm x 800 mm x 800 mm with 400 points per mm^2 resolution. The enlarged version of Series 5 device is able to digitize objects up to 2000 mm long. Series 6 system is designed for measuring large and heavy objects. Series 7 and 8, contrary to the previously described devices have positioners with 8 degrees of freedom (Series 4,5 and 6 have 7 DOF) (GOM, 2016). Their intended use is quality control of very large parts in production environments.

GOM Atos ScanBox product line is a very complex offering for almost all kind of quality control applications. Regardless of the series, the measurement head is always GOM Atos II structured light scanner (GOM2, 2016). This is one of the best 3D sensors available on the market, providing very fast measurement (1-2 seconds for single measurement) with adjustable resolution (up to 2500 points per mm^2). In highest resolution configuration, working volume of this scanner is about 38mm x 28mm x 15 mm. This device is using pattern projector and two cameras (up to 8 megapixels each) (GOM2, 2016). Output data is cloud of points in native GOM's format but it can be exported to standard ones (ascii, ply etc.) or

converted and saved as triangle mesh (stl, ply). GOM Atos does not capture color information during measurement.

The software controlling ScanBox systems is proprietary GOM application suite. It allows to create measurement plans basing on the sensor's configuration and CAD model of the inspected part. The inspection may include full object measurement, measurement of its selected features or control points. The suite includes ScanBox simulator in which operator can test the created measurement plan before executing it. During control process, measurements are automatically integrated and the 3D model is aligned to CAD model. After the digitization process is completed, the analysis module (GOM Inspect) calculates the differences between measured detail and CAD model (Figure 8) using methods certified by National Metrology Institute of Germany (PTB) and the National Institute of Standards and Technology (NIST).
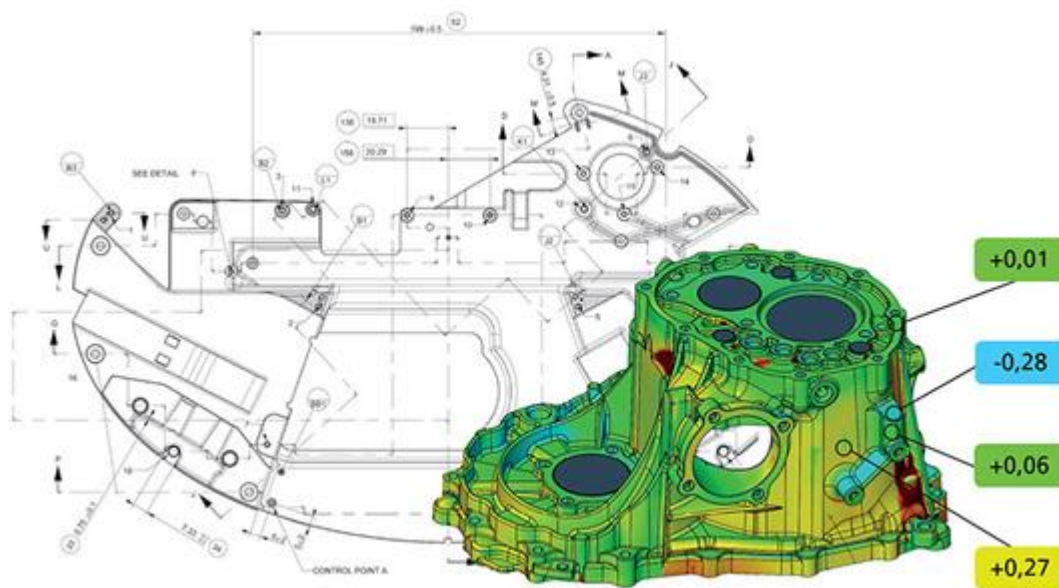
Figure 8. Shape differences between measured detail and CAD model in GOM Inspect application (image source: GOM webpage).

GOM Atos ScanBox is a complete, turnkey solution for quality control applications, and, taking into account a list of references given by GOM, applied by many manufacturers in various fields of industry. Regardless of those positives, it however lacks some crucial features to be useful in the process of mass digitization of real world objects for cultural heritage documentation and other, similar applications.

The first significant problem is the lack of color information in measurement data. While irrelevant for many applications, especially industrial ones (like quality control), this is clearly a drawback for creating real world objects' models for multimedia or cultural heritage purposes where more often than not the color is as important as shape.

The second disadvantage of GOM Atos ScanBox is its inability to measure objects without CAD models. Taking into the account the main applications of ScanBox product line it is understandable because they were designed for quality control and assessing deviations between measured parts and their CAD models. Unfortunately, when thinking about the massive digitization of unique, real world objects, the ability to measure them without their digital models is a must.

2.1.5 FARO Factory Robo-Imager

FARO, the US-based manufacturer of contactless measurement devices, recently updated its product portfolio with Factory Robo-Imager system (FARO, 2016). It is currently available only for early adopters, therefore FARO does not reveal many details of the system publicly. However, the main features are given in promotional materials (FARO2, 2016). This device is a successor to the FARO Factory Array Imager (Figure 9), a 3D scanner which can be fixed to robot arm which provide its repeatable positioning in relation to object digitized. This system however does not use any measurement planning aids, the robot arm positions are taught by operator, in the manner similar to classic applications of robotic devices (FARO, 2016).

Factory Robo-Imager (Figure 10) is an automated 3D shape digitization system intended for inspection and quality control (FARO3, 2016). It is rather designed for smaller parts than GOM Atos products, probably not larger than about 300 mm x 300 mm x 300 mm (FARO3, 2016). Measurement head is a well-known FARO Cobalt 3D (FARO4, 2016), blue light structured-light scanner. Positioning system is of classic design with 6axis robot arm and rotating stage on which the object is placed. The system contains also the console for operator which allows manual control of positioning system.

According to FARO, the system is capable of 3D measurements of objects for inspection and quality control purposes. There is no direct information about the creation of measurement plan but basing on advertisement and promotional materials (FARO2, 2016), one can assume that the possibilities are similar to GOM's offering – measurement of the whole object or only interesting parts or features, all options based on CAD model of the object. Automated

measurement of unknown objects is not mentioned; thus it can be assumed that it has not been implemented yet.

Figure 9. FARO Factory Array Imager (image source: FARO website).

The great advantage of FARO Factory Robo-Imager is its mobility. The system is integrated into a mobile cart which can be easily transported to any location. Very intriguing is the lack of any safety fence around the system (Figure 10) which is required for systems with robotic arms.

Figure 10. FARO Factory Robo-Imager (image source: FARO website).

Measurement capabilities of Factory Robo-Imager system are directly related to FARO Cobalt measurement head used in this device. This 3D scanner is a blue-light structured light 3D sensor using two 5 megapixel cameras. It has interchangeable lenses which allows for

customizing its working volume and spatial resolution. The maximum resolution of the system is only about 60 points per mm^2 (0.13mm distance between points) obtained for working volume 260 mm x 200 mm x 90 mm (FARO4, 2016). Measurement results are returned as clouds of points without color information, but can be converted to triangle meshes.

FARO Factory Robo-Imager is comparable to GOM ATOS ScanBox series 4. It is also a turnkey solution for inspection and quality control for various fields of industry. In such environments, the once designed measurement plan (which is either taught by operator or created on the basis of CAD model of inspected part) is run for each analyzed element. However, similarly to GOM ATOS ScanBox, the system lacks the possibility of automated digitization of objects without their CAD models or operator guidance. Therefore, it cannot be used in mass 3D digitization process of unique, real world objects. Moreover, as the measurement head is incapable of capturing color information, its applicability to any multimedia related digitization processes is discussable.

2.1.6   ZEISS T-Scan Automated and Comet Automated

One of the best-known manufacturers of measurement systems and devices, ZEISS Optotechnik, offers two automated digitization systems (Figure 11), named T-Scan Automated (Zeiss Optotechnik, 2016) and Comet Automated (ZEISS Optotechnik2, 2016). They are designed for "recurring measurement tasks for the fast acquisition of 3D geometry and surface data (…) in production-related quality assurance processes" (Zeiss Optotechnik, 2016). ZEISS advertises its solution as ideal for quality control, inspection, tools and molds making.

Figure 11. ZEISS T-Scan (left) and ZEISS Comet (right). Images source: ZEISS Optotechnik website.

Both systems offer high resolution 3D measurements and automated data integration. The Comet station include additional optical tracking system of position and orientation of measurement head which allows for precise directional measurements integration regardless of actual robot accuracy. T-Scan system has measurement resolution up to 178 points per mm^2 (distance between points: 0.075 mm). Working depth of the sensor is about 50mm and laser line width up to 125 mm, with 1317 sampling points. As this sensor is laser triangulation sensor without color camera, it does not provide color information.

ZEISS Comet station on the other hand, is a structured-light based system. What is rather unique, it is not constrained to one robotic arm type or even manufacturer – ZEISS can integrate this system with any robot (ZEISS Optotechnik2, 2016) which is compatible with their VISIO software package (ZEISS Optotechnik3, 2016). The measurement head itself offers medium resolution data output: 30 points per mm^2 (distance between points of 0.18 mm) but has working volume of 600 mm x 450 mm x 400 mm (ZEISS Optotechnik4, 2016). There is no information about color capturing capabilities.

Figure 12. ZEISS Comet sensor on various robotic arms (image source: ZEISS Optotechnik webpage).

ZEISS offers T-Scan and Comet stations in standard configurations (Figure 12) which can be customized to any customer needs. The adaptation includes not only positioning systems (apart from robotic arms other devices can be used, for example portal machines similar to Coordinate Measuring Machines), but also the sensor itself (probably working volume and accuracy) and controlling software. Stations can be integrated with existing manufacturing lines. The information about the scanning process itself is limited but generally only offline teaching and CAD-based plan generation are mentioned.

While ZEISS offering is probably one of the best solutions for quality control and inspection tasks, its applicability to mass digitization of real-world objects is rather discussable. The reasons are exactly the same as with previous systems – mediocre resolution, the lack of color information returned by the sensor (probably this feature can be customized by ZEISS) and the inability of measuring unknown objects fully automatically.

2.1.7 Creaform3D ScanMaster

Another of integrated, automated 3D inspection system is Creaform3D ScanMaster (Figure 13) utilizing MetraSCAN 3D R-Series laser sensor (Creaform3D, 2016). Contrary to most of the existing solutions, ScanMaster does not rely on tool coordinates returned by robot – additional optical tracker is used for locating measurement head and robot segments in global coordinate frame (Creaform3D2, 2016). This solution allows for high precision of initial data fitting regardless of the type of robot used. That is why ScanMaster can utilize big, less precise robot arms to allow for large working volumes (the smallest system has 0.9 m × 0.9 m × 1 m but the largest one can measure parts which are 3m long). The system may include turntable (of 1.3m diameter) but also can be used without it, depending on customer requirements.
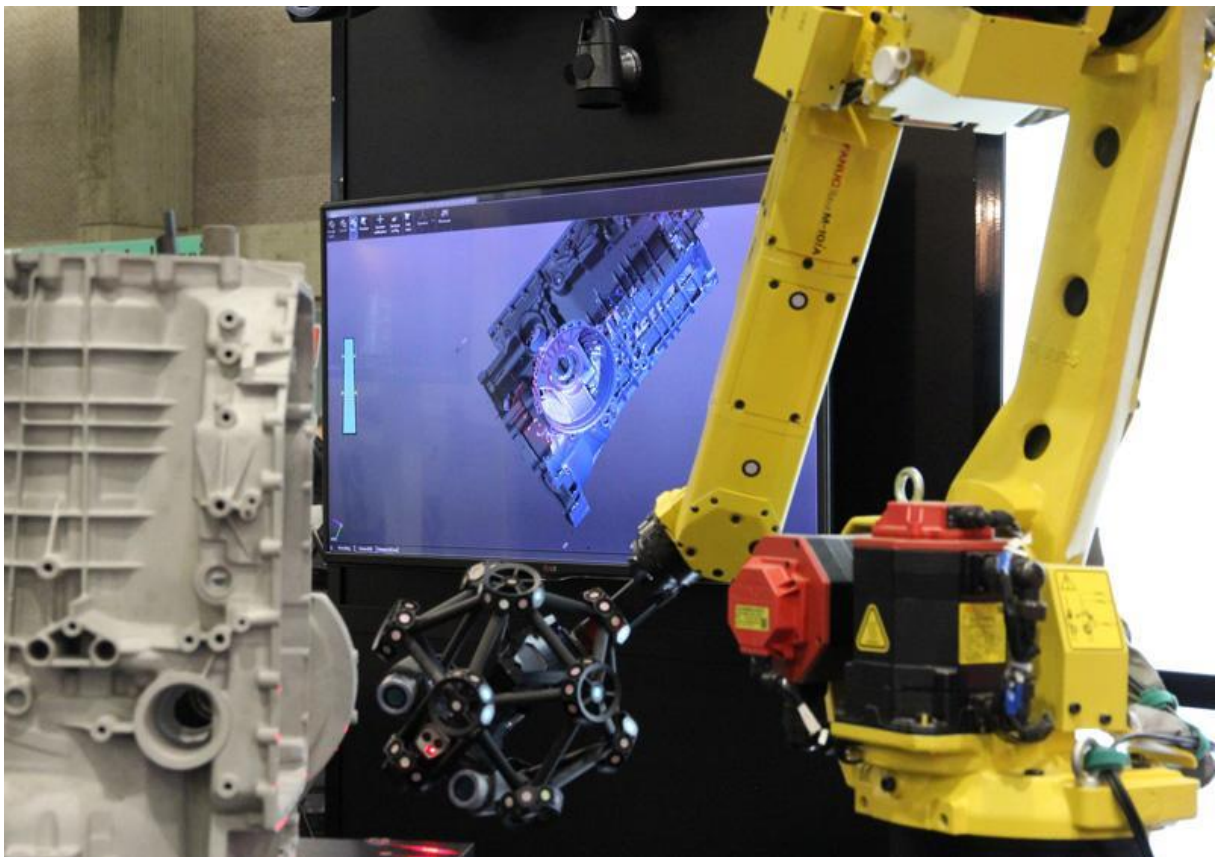
Figure 13. Creaform3D ScanMaster with MetraSCAN sensor fixed to Fanuc robot arm (image source: Creaform3D webpage).

MetraSCAN 3D sensor is rather unique device compared to other manufacturers offerings. Using laser triangulation principle, this device combines seven laser lines to allow for faster and more precise data acquisition. Futuristic shape of this device (Figure 14) allows for placing multiple markers which are tracked with additional optical system to determine sensor position.

Creaform3D assures that the MetraSCAN sensor is capable of obtaining 144 point per mm^2 resolution (average distance between points of 0.08 mm) with accuracy of up to 0.085 mm in real-life, shop-floor conditions (regardless of instability, vibrations, thermal variation, etc.). This device is not capable of capturing surface color data.

Figure 14. Creaform MetraSCAN measurement head (image source: Creaform3D webpage).

ScanMaster system was developed for industrial inspection. There is no possibility to measure object without offline-created measurement plan which is constructed around CAD model. The output data is saved to common formats accepted by popular geometrical dimensioning and tolerancing (GD&T) (Concheri, et al., 2001) applications like Geomagic (Geomagic, 2016), SmartProfile (Kotem Software, 2016) etc.

Due to no color information, medium sensor resolution and incapability of measuring unknown objects, the system cannot be used for mass digitization of cultural heritage objects.

2.1.8 Perceptron Robotic Scanning

Perceptron, one of the most well-known manufacturer of metrology equipment, developed its own robotic measurement station (Figure 15). It is based on Perceptron Helix, laser-based structured light sensor. Measurement resolution is not disclosed however accuracy is said to be 50 microns (Perceptron, 2016), possibly thanks to its internal temperature compensation routines. Scanning system uses robotic arm but no further details are given, however on some video materials large Fanuc robot is visible. Thanks to laser projector, no surface coating is required. Integration of directional measurements is based on tool transformations returned by robot arm. No information is given whether Perceptron system can be equipped with rotating table for object placement.

Apart from the physical device, Perceptron solution includes advanced software package which is capable of simulating whole scanning process (Figure 16) and can be used to create measurement plans, execute them, assess the correctness of parts (by GD&T calculations) and create reports. Perceptron claims that the whole system can be used by production personnel (running inspection and reporting) without any special skills. Manufacturer states that "influences of human error are not present in the measurement results" (Perceptron, 2016).
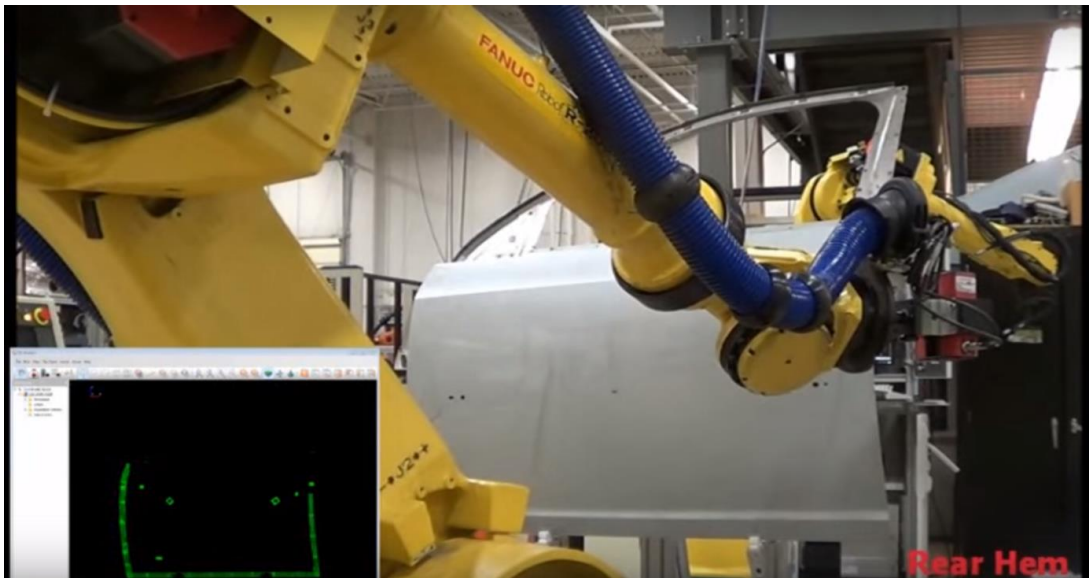
Figure 15. Perceptron Robotic Scanning system measuring car doors (image source: Perceptron 3D webpage).
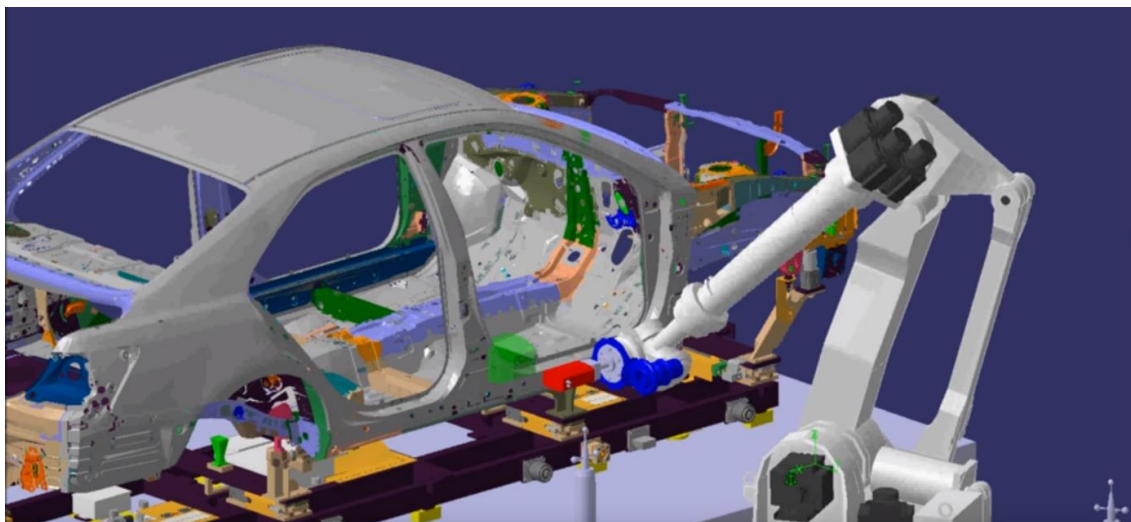
Figure 16. Perceptron Robotic Scanning simulation software (image source: Perceptron website).

The system is designed with inspection in mind – it does not have any capability to automatically create measurement plan for parts with CAD models, not mentioning ones without it. Its laser-based sensor does not capture color information. Because of those reasons, Perceptron Robotic Scanning system, while well suited for industrial quality control is not a good solution for mass digitization of cultural heritage objects.

2.2 Research systems

Systems presented in this section of the document were developed during scientific research or pilot 3D scanning programs. They are not commercially available, and they do not have as high technology readiness level as systems presented in previous chapter. Controlling software however is more advanced and is usually directed at measurements of unknown objects rather than measurements based on CAD models.

2.2.1 RoboScan

RoboScan is the first of the non-commercial automated digitization systems presented in this dissertation. It was designed by a group of researchers from Istituto di Scienza e Tecnologie dell'Informazione lead by Marco Callieri. The main aim of the system is the digitization of works of art.

The system uses Konica Minolta Vivid 910 3D Laser Scanner (Konica Minolta, 2017) sensor of medium resolution (distance between points about 0.55 mm in tele mode, 1.3 mm for wide mode) capable of capturing color information with shape data. The sensor has large working volume (350mm x 250mm x 450mm). It is mounted to the wrist of large ABB robot-arm (ABB, 2016), while the object to be digitized is placed on the rotating stage (Figure 17).

Figure 17. RoboScan system (image source (Callieri, et al., 2004)).

RoboScan system was presented in paper by Callieri (Callieri, et al., 2004) in 2004 and up to now no new information appeared. To the best of my knowledge, it has not been commercialized nor used in other research which is rather strange as its presented performance and some properties are very interesting.

The main strength of the RoboScan station is its ability to digitize unknown objects, without giving any detailed information apart from their rough size (defined with height and radius of encompassing cylinder). Using this data, initial scanning positions are calculated (or rather chosen from the predefined set) – placing 3D sensor on the surface of the cylinder or sphere with parameters calculated basing on object's dimensions. Sensor is aimed at object's center. Using such setup and 3D sensor of large working volume, significant part of object surface is digitized. Afterwards, rather ingenious model analysis procedure is run to identify holes in the model. Such areas are then used as targets for 3D sensor which is positioned accordingly. The process of identifying holes and re-measuring them is continued until satisfactory level of surface coverage is reached.

Identification of holes in the model is done in a very clever way, without any analysis of 3D data. Partial model is converted to triangle mesh and then rendered using OpenGL. Both sides of each triangle from the mesh use different colors (for example blue for outer side and red for inner one) and when the model is rendered, the inside of the object can be identified by searching for red pixels in the image. Inner side of the mesh is visible only if there is a hole in the model lying between virtual camera and identified inner triangle. Rendering multiple views from numerous vantage points, most of the holes in the model can be easily identified. Of course, the accuracy of such process is a function of the number of the vantage points and their placement, however with modern PC hardware it is easy to perform such computations for few thousands virtual camera positions in very short time.

Unfortunately, the calculation of sensor placement required to digitize given hole in the model is rather straightforward and does not take into account the problem of occlusions. To measure any part of the surface, it has to be lighten by the projector and observed by detector (for structured-light scanner). When any optical path is blocked by for example another part of the object, the expected measurement cannot be performed. RoboScan control algorithms does not analyze this problem thus some holes in the model can be still present regardless of their identification and re-measuring.

Moreover, the method of using predefined set of poses for initial scanning gives acceptable results only when working volume of measurement head is large (at least comparable with object). In other case, for most objects the partial 3D model will not be created correctly not allowing for the analysis and re-measuring. Because of this, when the high-resolution, small working volume head is used, only very small objects can be measured with RoboScan system.

The presented system is much better suited for automated digitization of unknown objects than previously shown commercial devices. In fact, for many applications its parameters are satisfactory. However, for the professional 3D documentation it lacks the capability of capturing high-resolution models due to the deficiencies of the controlling algorithms.

2.2.2 Automated digitization system by Khalfoui

Another of "research" type systems, presented in paper by Khalfoui (Khalfaoui, et al., 2013) is composed of robotic arm (Kuka KR16) and rotating stage. Sensor used for digitization is Steinbichler CometV scanner (Figure 18) of large working volume (480 mm x 360 mm x 250 mm) and low resolution (1.4MPix. detector). Output data is returned as triangle mesh.

Khalfoui's system was presented in paper and to the best of my knowledge it has not been used in any digitization project nor commercial product. It is hard to find any information about it apart from mentioned paper.

The configuration of positioning system is conventional. Robot arm has significant range of operation, which is further extended by rotating stage. There is no information whether table is controlled by robot controller or separately.

The system is capable of digitizing unknown objects. This is done by two-stage Next Best View algorithm. In the first stage, digitization is performed using Mass Vector Chain method (Yuan, 1995). After obtaining partially completed model, discontinuities in it are identified. For each hole in the model, measurement direction is calculated. Center of working volume is set in the gravity center of discontinuity, while observation direction is calculated by averaging normal vectors of points lying on the edge of the hole. While simple in principle, this method is clearly designed for use with large working volume scanners. For such devices, it allows to obtain good results.
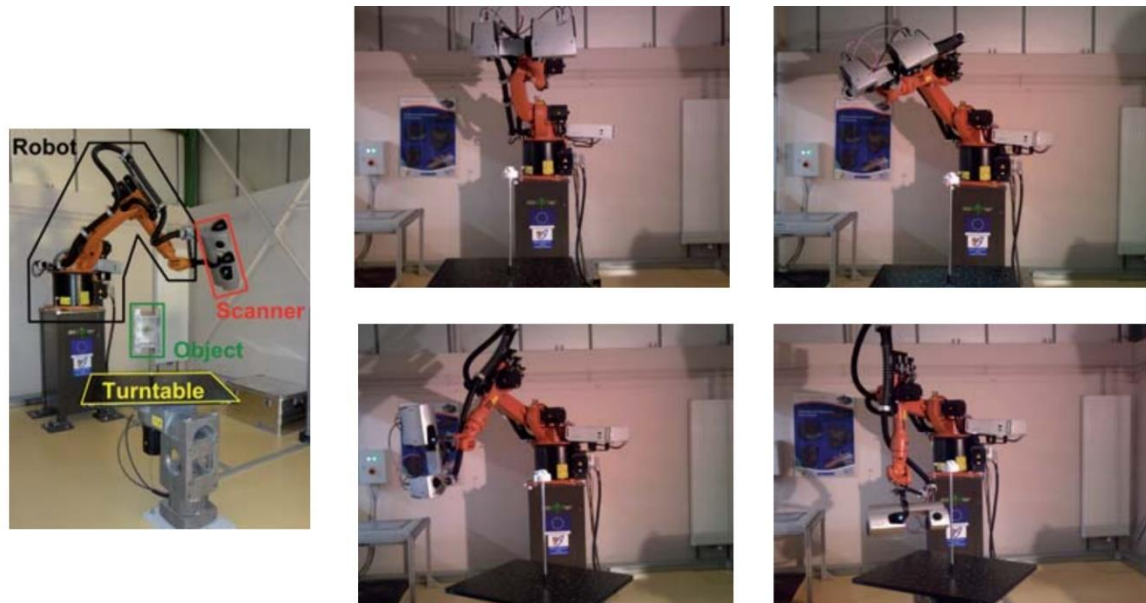
Figure 18. Automated digitization system by Khalfoui (Image source: (Khalfaoui, et al., 2013)).

Unclear information is given about the accuracy of initial data alignment – Khalfoui states that the relation between robot and scanner coordinate system is not calibrated precisely ("after the coarse registration all the point clouds have the same orientation, but there is a gap between them. This spacing is due to the estimation error of the transformation between the robot flange and the scanner origin" (Khalfaoui, et al., 2013)).

Judging from the details of the system given in the paper, this system is very limited in terms of used sensor and proposed Next Best View algorithm. As it was described above, 3D sensor has large working volume. Next Best View method utilizes Mass Vector Chain paradigm which work only when digitized object size is at least comparable with working volume of the sensor. Therefore, using high resolution sensor with small working volume limits digitization capabilities of Khalfoui's system to very small objects.

2.2.3 Automated digitization system by Kriegel

Digitization station presented by Kriegel in the series of papers (Kriegel, et al., 2011), (Kriegel, et al., 2012), (Kriegel, et al., 2015) utilizes robot arm (Kuka KR16) without any rotating table (Figure 19). Kriegel states that his system is designed for cultural heritage objects, therefore it does not use a table because such objects cannot be moved from their exposition place (Kriegel, et al., 2011). This statement has not been confirmed by specialists from Museum of King Jan III's Palace in Wilanów 3D Documentation Laboratory (Bunsch, 2010), moreover, using robotized system directly at the expositions would not be possible. Nevertheless, Kriegel uses only robot arm for scanner positioning. This choice severely

impacts positioning possibilities and even with objects which are small in relation to robot operating range, not every proposed scanning path is reachable (Karaszewski, et al., 2013). The other significant difference from Callieri and Khalfoui systems is measurement head. In this case, 3D sensor is laser stripe profiler. This sensor is rather poor choice for cultural heritage objects documentation – it has very small linear resolution (224 points per stripe length which is about 300mm, resulting in approximate distance between points of 1.34 mm). Additionally, only geometry information is collected, there is no information about surface color.
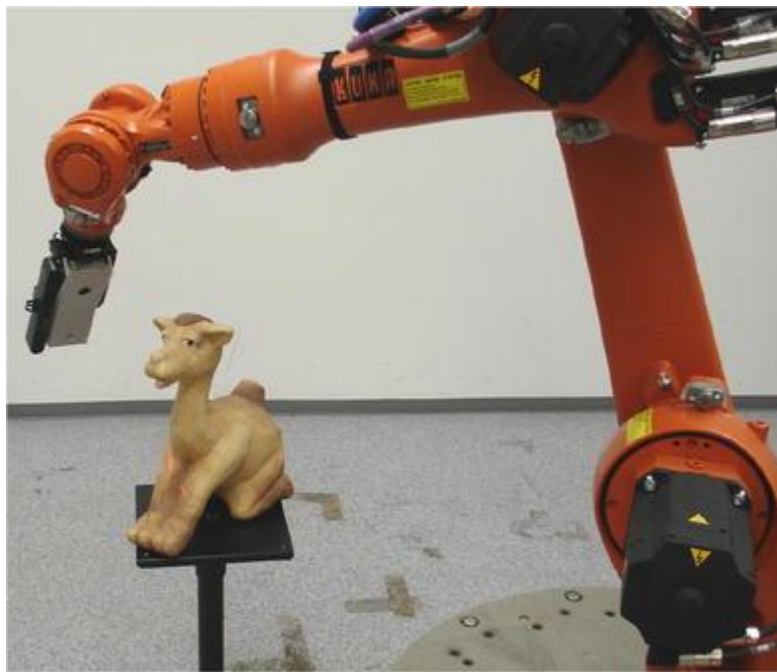
Figure 19. Automated digitization system by Kriegel (image source: (Kriegel, et al., 2012)).

Similarly, like previously mentioned "research" digitization systems, Kriegel's station does not appear to be used in any digitization project nor commercially available system. Therefore, it is hard to assess its capabilities by analyzing output 3D models produced by this device. Judging by characteristics presented in the paper, along with one exemplary model shown there, the system is rather poorly suited for using in professional digitization processes. Inability to capture color information limits its applicability to industrial objects rather than cultural heritage ones.

2.2.4   CultLab3D

In the recent few years, the topic of massive 3D shape digitization aimed at documenting cultural heritage received much attention among researchers in European Union. This was caused by many disasters like destroying of 2000 year old statue of lion in Palmyra, Syria by

Islamic State jihadists, collapse of Cologne historical archive, fire in Anna Amalia Library in Weimar etc. CH digitization – related research was also boosted by EU framework programs (FP7 (European Commision, 2016) and HZ2020 (European Commision, 2016)). On the wave of this topic popularity, CultLab3D system was developed by research team lead by Pedro Santos from Competence Center Cultural Heritage Digitization at the Fraunhofer Institute for Computer Graphics Research IGD (CultLab3D, 2016). CultLab3D was designed as complete system for 3D digitization, composed from hardware devices but also from software modules for semantic enrichment and data export conforming with CIDOC-CRM schema (Doerr, 2005) and Europeana, using Europeana Semantic Elements (Doerr, et al., 2010).

The hardware-side of CultLab3D system is based on automated pipelined 3D scanning with high quality color acquisition and reflectance properties. Accuracy of 3D geometry is poor ("millimeter accuracy" as stated on website (CultLab3D, 2016)). Exemplary results given on project website (even those named as "high quality" (CultLab3D, 2016)) are of very limited spatial resolution (no more than 500k triangles for typical object). In some other materials, it is said however that accuracy is submillimeter and 3D models are of about 10M triangles (CultLab3D, 2016). This is not a surprise as the digitization is made using two stations (Figure 20) – the first using cameras and lighting rings which can change their alignment, the second one – using large working volume structured light scanner mounted on vertical column or robot arm (depending on system version). Geometrical data is reconstructed from images acquired on the first station using photogrammetry. Object is moved before 3D scanner by rotating the table (Santos, 2014). No information was published regarding the control of measurement direction (with 3D scanner) apart from the CultLab3D leaflet (CultLab3D, 2014) where the statement "we compute an optimized, iterative view planning for the robotic arm to resolve remaining occlusions of the virtual model". It seems that the main aim of robot controlled measurements is the measurement of places, where ring-based digitization left discontinuities only. It is hard to assess controlling algorithm performance, all the more that no paper with any technical details was published.

The rather unique configuration of the whole system which uses conveyor belt for transport of cultural heritage objects reflects the aim of its developers – mass digitization. Unfortunately, the results are usable only for general audiences, not for professional users as they demand much better results.
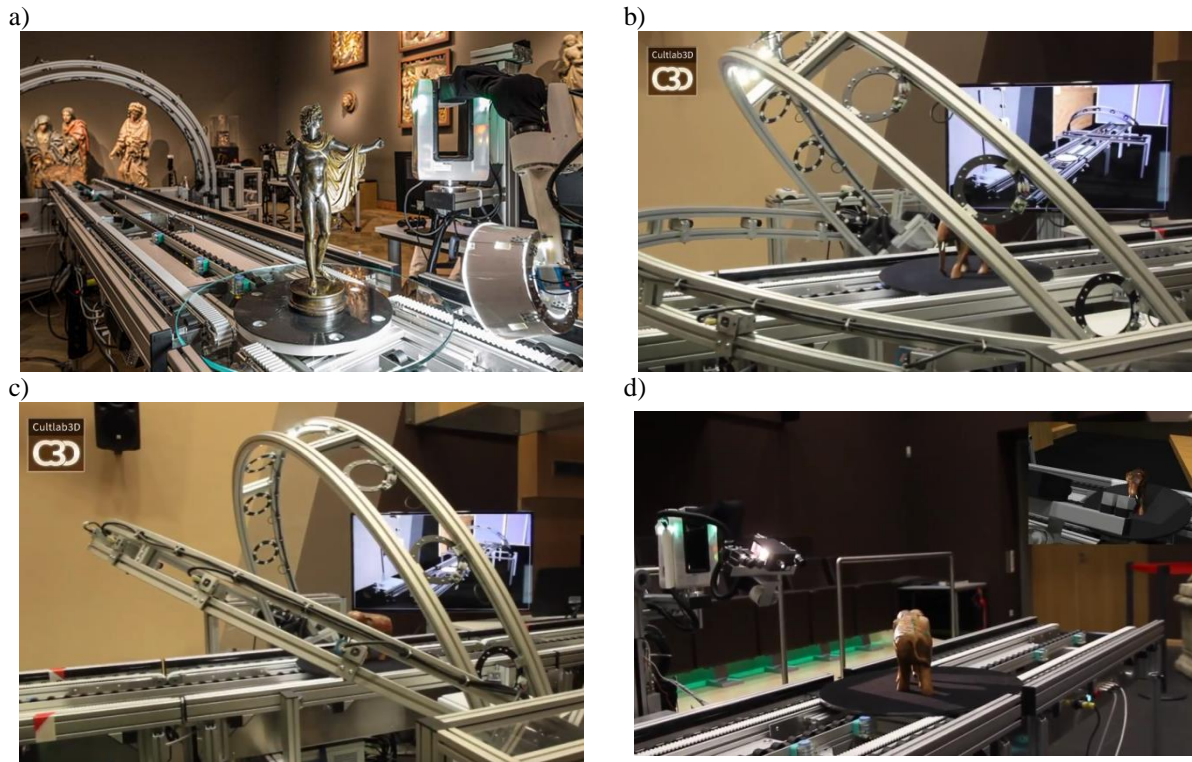
Figure 20. CultLab3D scanning system: a) overview with conveyor belt visible, b, c) shape, texture and reflectivity measurement station; d) structured light scanner with rotary table and vertical column. Images source: (CultLab3D, 2016).

2.2.5   Automated scanning system by Wu

The 3D scanner produced by Artec, a well-known manufacturer of inexpensive 3D scanning systems was used by research group led by Wu (Wu, et al., 2014) in automated scanning system using rather unique positioning system - humanoid robot . Digitized object is placed in the palm of one hand of this robot, while 3D scanner (Artec Spider (Artec, 2016)) is fixed to the other. "Hand" holding object can rotate in a manner replacing rotary table in typical systems (Figure 21).

The system is designed to measure unknown objects, i.e. ones without CAD models. No offline-generated measurement plan is needed; subsequent scanner positions are calculated basing on the information collected during previous directional measurements. At the beginning, several "blind-scans" are performed to initially digitize part of the object (Figure 22). For this purpose, working volume of scanning head has to be significant, comparable to the size of the object, otherwise, the collected information will be very fragmentary.

After blind-scanning, Poisson-surface-based algorithms is run reconstruct iso-surface from this partial data. As a result, an extrapolated 3D model is obtained. Regions which does not occur in previously made measurements become new scanning targets (Figure 23). The process continues until no such regions can be identified.

Figure 21. Wu's automated scanning system (image source: Artec3D YouTube Channel).
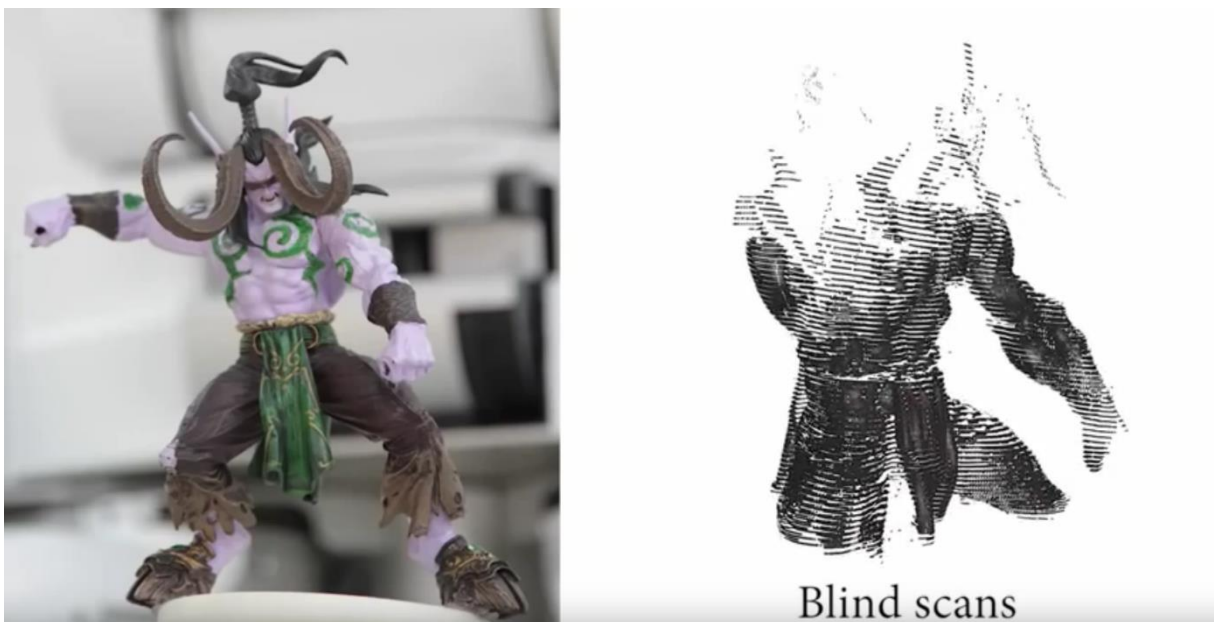
Figure 22. Initial digitization with Artec Spider scanner (image source: Artec 3D YouTube channel).

Wu disclosed that the positioning system has only five degrees of freedom. Probably the movements of scanner are constrained by the construction of used robot. Also, the role of Microsoft Kinect sensor visible on the "head" of the robot (Figure 21) is unclear, but it is possible that it is used to track the position of the scanner during measurements (this could mean that the precision of the positioners is very poor). Wu claims however that the above described NBV method was also tested with unnamed robotic arm and turntable, used in typical manner (Figure 24).

a)   b)
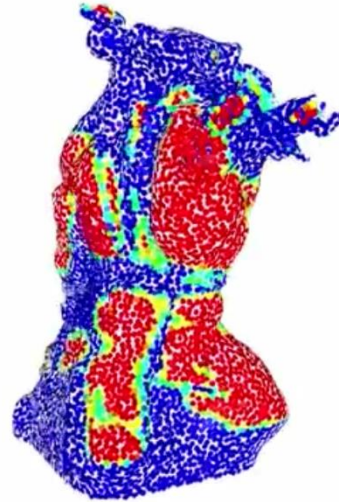
Figure 23. Partial model (a) and reconstructed iso-surface (b) (image source: Artec 3D YouTube channel).

Figure 24. Artec Spider mounted to robot arm (image source: Artec 3D YouTube channel).

Wu's automated scanning system is very interesting proposition for the mass digitization purposes. From the previously presented devices, it is the first one which is capable of obtaining high-quality 3D models of unknown objects automatically. Moreover, the Artec Spider 3D scanner captures color information. Unfortunately, the spatial resolution of this head is not high (maximum 100 points per mm^2 – average distance between points is about 0.1 mm). Color information is also of low resolution (images are taken with 1.3MPix camera 90 mm x 70 mm area (Artec, 2016)). While this is more than enough for typical, consumer and prosumer digitization purposes, fully professional 3D documentation requires higher resolution which require measurement heads with smaller working volumes. Such devices are however incompatible with Wu's NBV algorithm.

2.3 Summary of existing automated 3D measurement systems

In the previous sections of this dissertation, many automated 3D digitization systems were presented. They include devices which are commercially available and some research ones, which, to the best of my knowledge, are not. The division between commercial and research system is also a division between those systems capabilities – commercial stations are designed with industrial application in mind and they may be used for inspection and quality control purposes only. Their capability of obtaining 3D models of unknown (i.e. not having CAD model) objects is nonexistent because controlling software is unable to create measurement plan of such unknown object. There is possibility to scan such objects using mentioned systems but only if operator guidance is provided. Completely autonomous operation is not possible.

Most of commercially available systems utilize 3D sensors which are unable to capture color information. It is understandable as this data modality is rather not used in industrial applications. But while for industrial inspection such limitation is acceptable, for digitization of cultural heritage objects, or in general, for multipurpose scanning, it poses a severe problem.

On the contrary, research are designed to allow for unknown objects digitization. As it is shown in the publications, automatic digitization is indeed possible. Moreover, apart from Kriegel's system (Kriegel, et al., 2011), those devices capture color information (or even additional modalities like surface reflectance profile (Krzesłowski, et al., 2011)). Those parameters make such systems theoretically able to mass digitization of cultural heritage objects for non-professional purposes. However, the lack of any information about application of any of those systems indicates that their performance in real digitization projects is not as good as their authors stated.

Moreover, all of presented systems use 3D detectors of large working volume in relation to digitized objects size. Such sensors have limited resolution ($1 - 100$ points per mm^2), much worse than required for professional applications (2500 points per mm^2) (MacDonald, 2010), (Bunsch, et al., 2011). Sensors capable of obtaining high resolution data have very limited working volume and algorithms used for measurement plan generation in these systems are not able to work correctly with them.

Conclusions which can be drawn from the review of automated 3D digitization systems is that currently there is no system capable of massively digitizing real world objects which do not have computer model with precision and modality (i.e. at least geometry and color) required by professional users such as art historians and conservators. On the other hand, the demand for such system exist, especially now when many dangers such as natural disasters, climate change, terrorists and fundamentalists attacks threaten the world cultural heritage (Logan, 2007), (Schäfer, et al., 2015), (Erič, et al., 2013), (De Reu, et al., 2013), (Du, et al., 2015).

3. Modules of digitization systems – a survey

The automated 3D digitization system is a device composed of several important hardware and software modules. Most important components are shown at Figure 25.
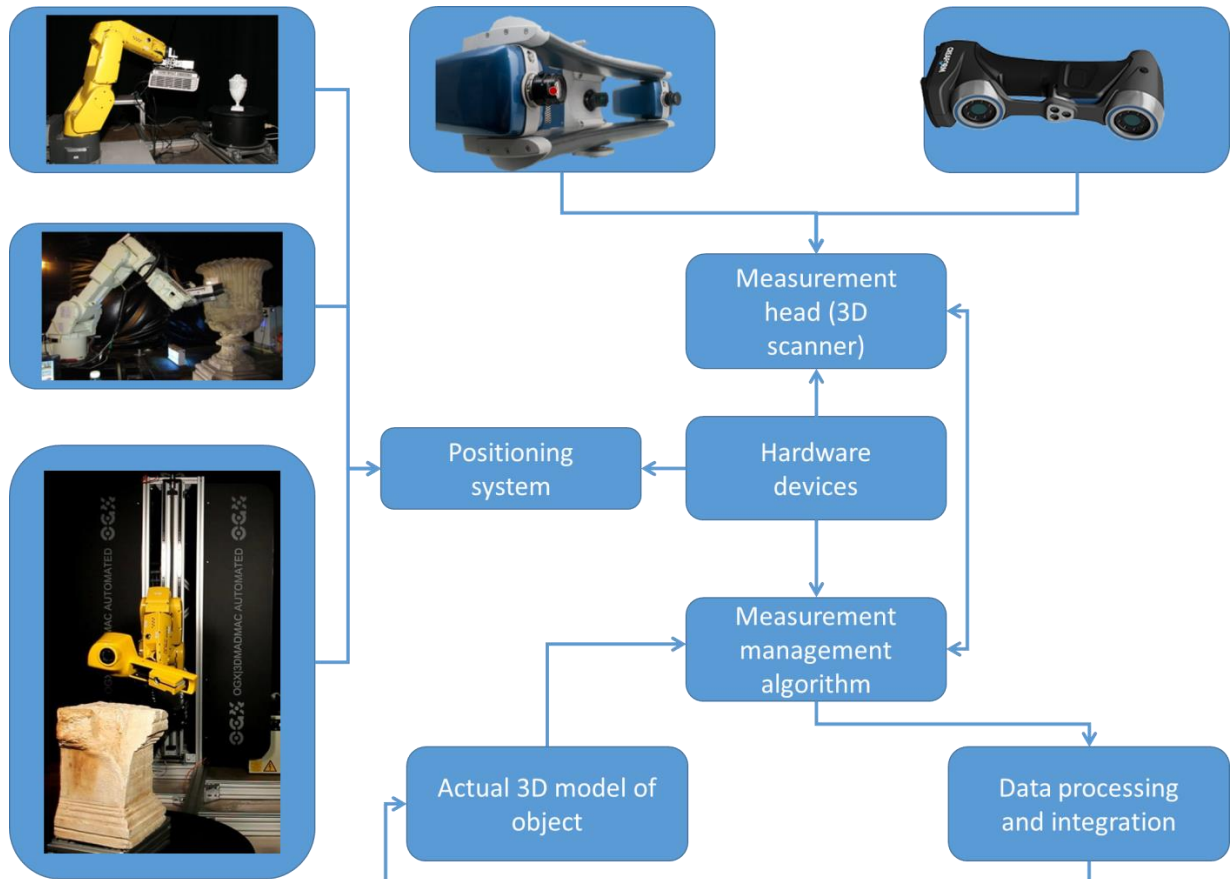
Figure 25. Modules of automated 3D digitization system.

The first module is a 3D measurement head. In all solutions which are known to me, the head is a contactless, optical sensor using one of few measurement techniques: photogrammetry, laser triangulation, time-of-flight or structured-light. Those methods will be characterized in section 3.1 of this dissertation, along with the assessment of their usability in high-resolution, color 3D measurements.

The second module of automated 3D digitization station is the positioning module. It is usually composed of robot arm and rotary table, but more exotic solutions exist, offering various advantages over the classic setup. Those systems are presented in section 3.2 of this work.

The final group of important modules of 3D digitization station is software controlling the whole process which is probably the most complicated part of the whole system. Software packages can be very complicated and advanced, offering various functionality, but from this work perspective (automated, high-resolution digitization), the most important task is measurement plan calculation. Measurement plan is a set of positions in which 3D sensor has to be placed to measure as much surface of an object as possible. This topic is widely researched for long time. Review of the most popular methods, along with assessment of their performance for high-resolution, small working volume measurement heads is presented in section 3.3 of this document.

3.1 Contactless, optical 3D shape measurement methods

There are numerous methods of optical 3D shape measurement, which differ in possible resolution and accuracy of measurement, working volume, hardware requirements and limitations, complexity etc. In this chapter, four such methods are presented:

- Photogrammetry,
- Laser triangulation,
- Time of flight,
- Structured light.

All methods are briefly presented, along with exemplary commercial devices which utilize them. Applicability of each method to mass digitization of cultural heritage (or similar) objects is discussed at the end of this chapter.

3.1.1 Photogrammetry

Photogrammetry is a technique developed almost at the same time as analog photography. It is also one of the least demanding in terms of hardware – all what is needed is a camera (contemporary digital one, but originally analog cameras were used). If the object is photographed from at least two different vantage points (or two or more cameras placed in different places), its area which is visible on both images can be reconstructed in 3D. This process requires so called internal camera calibration (i.e. finding parameters which describe image projection done in camera: focal length, principal point shift and lens aberrations, usually distortion only). Moreover, the transformation between vantage points has to be known. Using this set of data, coordinates of all points identified on images from different views may be calculated (Luhmann, et al., 2006). Unfortunately, point pairs have to be identified precisely on images (Figure 26). This necessity significantly limits applicability of photogrammetry – in the past points were matched manually by operator, nowadays characteristic points are identified by key-point detectors and characterized by various descriptors like SIFT (Lowe, 2004), SURF (Bay, et al., 2006), RIFT (Lazebnik, et al., 2005), ORB (Rublee, et al., 2011) etc. The result however is dependent on the input data (occurrence of characteristic points in images). For objects with simple or repeatable texture, automatic processing is impossible. The reconstructed 3D model contains only 3D coordinates of characteristic points, the areas between are usually interpolated (Luhmann, et al., 2006).

Photogrammetry can be very precise technique. The quality of camera calibration parameters is the most important factor. Moreover, precision of corresponding points location is crucial. Multiple methods have been developed for identifying characteristic points in images and describing them with unique feature vectors. Some of the best known algorithms are SIFT (Lowe, 2004), SURF (Bay, et al., 2006) and ORB (Rublee, et al., 2011). For highest accuracy, special markers are introduced into the scene. With such markers, the accuracy of photogrammetric 3D reconstruction can reach the level of 0.1 * pixel size in object space (Fraser, 2015).
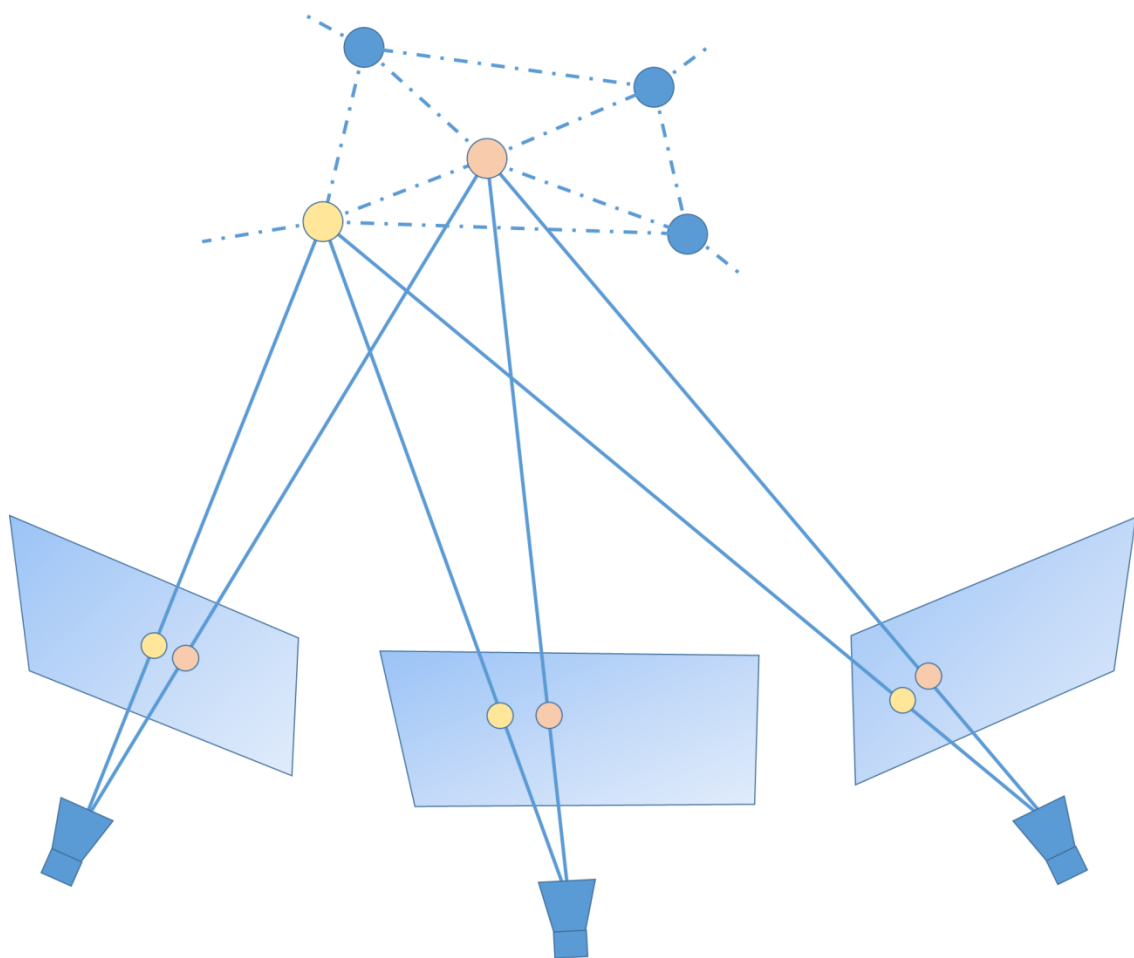
Figure 26. Photogrammetry principle.

Photogrammetry has recently evolved into a method called Structure from Motion (SfM) (Westoby, et al., 2012). The difference between those two techniques lies in the lack of calibration of internal and external camera parameters before measurements (in SFM). Using RANSAC algorithm (Hartley & Zisserman, 2003) in a process called Bundle Adjustment (Triggs, et al., 1999), those parameters are found by correlating a set of images taken from different vantage points. The number of those images is significantly greater than for pure

photogrammetry (usually hundreds or even thousands) (Turner, et al., 2012). As all parameters are found basing on images only, the output model is produced in arbitrary scale which has to be scaled to metrological units. This is usually done by placing some kind of calibration unit in the scene (for example ball-bar of known length). This process impacts accuracy of the method, moreover, the results are sometimes heavily distorted in areas, where photo density was lower or not well illuminated (Rüther, et al., 2012), (Koppel, 2012).

Photogrammetric or SfM models usually contain geometry and color information. It is relatively easy to use multispectral imaging devices (instead of typical RGB detectors) (Raju, et al., 2011) which allow for obtaining high quality spectral information (usually in visible, near infrared and near UV range).

3.1.2 Laser triangulation

Laser triangulation method is a very popular technique used for digitizing 3D shape of objects. It is commonly used in industrial inspection systems thanks to its simplicity and robustness with surfaces of various characteristics. Due to high intensity of laser light, measurements may be performed in daylight (Dorsch, et al., 1994).

Mathematical principle of laser triangulation method was developed by W. Snell van Royen in 1615 year (Haasbroek, 1968). With the advent of lasers, CCD / CMOS detectors and computers it became very simple to implement.

Typical scheme of laser triangulation measurement is shown in Figure 27. Laser light is aimed at the surface of object. The bright dot is observed by camera placed in some distance from laser source and its position in image coordinates is calculated by analyzing captured image. Using this coordinates and information about physical setup of the system (distance and angle between camera and laser source), distance between the bright point on the surface and system can be calculated.

This method can be modified for example by using aspheric cylindrical lens (Powell lens) which forms laser light into a stripe (Coherent Inc., 2012). This way, coordinates of multiple points lying along projected stripe can be calculated and if the head or object moves perpendicularly to the stripe direction (Figure 28), the whole surface can be digitized (MakerBot, 2016).

Most advanced laser triangulation systems use multiple laser stripes set at different angles (Zeiss Optotechnik, 2016). This way, single measurement is almost full-field one. Small head or object movements allow for high resolution surface digitization.

Due to the nature of laser light (high coherence (Harris, et al., 1998)), analyzed image contains speckles which form due to interference on unevenness of surface. This phenomenon causes measurement noise especially in multiline systems. Speckles can be eliminated by lowering light coherence for example using so called laser choppers (Dorsch, et al., 1994).
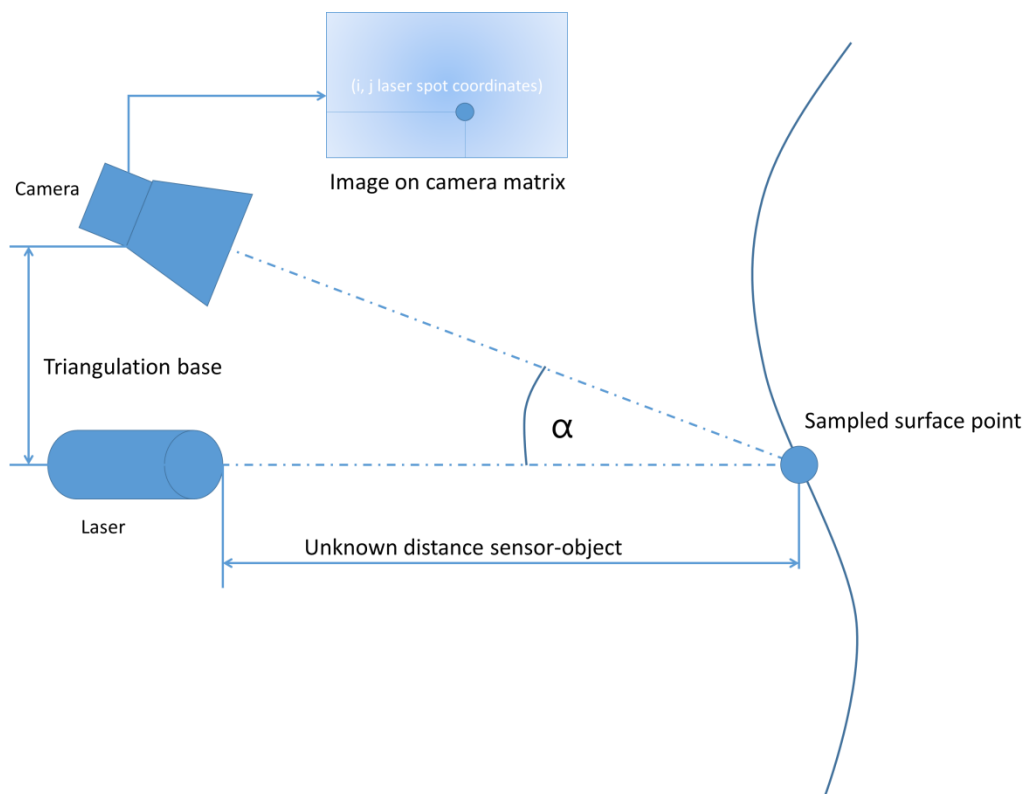
Figure 27. Laser triangulation principle.

Because of significant size of laser dot and width of laser stripe (usually not less than 0.8mm), laser triangulation sensors are not capable of digitizing small details (Curless & Levoy, 1995). Also, they do not capture color information.

Triangulation sensors are manufactured by Konica Minolta (Konica Minolta, 2016), Creaform (Creaform3D, 2016), NextEngine (NextEngine, 2016), Zeiss (Zeiss Optotechnik, 2016) and many more companies (Figure 29).

a)

b)

c)

d)
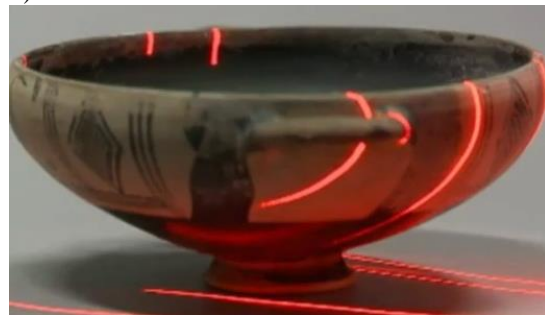
Figure 28. Typical laser triangulation system: (a) (b); with single laser stripe and rotating table providing movement of object (MakerBot Digitizer (MakerBot, 2016)) images source: MakerBot webpage; c) multi-stripe system (Creaform Handyscan (Creaform3D, 2016), image source: Creaform webpage); d) multi-stripe laser scanner (NextEngine), image source: NextEngine webpage.

a)   b)   c)   d)

Figure 29. Laser triangulation 3D scanners: a) Konica-Minolta-range-7-3D-Scanner; b) Creaform Handyscan; c) NextEngine 3D scanner HD; d) ZEISS/Steinbichler T-Scan (images sources: manufacturers' webpages).

3.1.3 Time of flight technique

Time of flight technique is a method which, similarly to the laser triangulation became popular with the development of laser sources and fast electronic detectors. Its principle is very simple – to measure distance between the device and object, time required for light pulse to travel from the device to the object and back is measured (Figure 30). With ultrafast detectors and correctly assessed speed of light in environment conditions, the distance can be calculated straightforward.

In classic time of flight devices, one point is measured at the time. When rotating mirror is put in front of the 3D sensor (i.e. light emitter and detector) at 45° angle, scanned points form a circle with axis identical to mirror rotation axis. If the whole device is put on rotating table (which moves after full rotation of mirror), such scanner can measure everything contained within a sphere centered at its position (apart from the parts blocked by chassis of the device etc. - Figure 31).
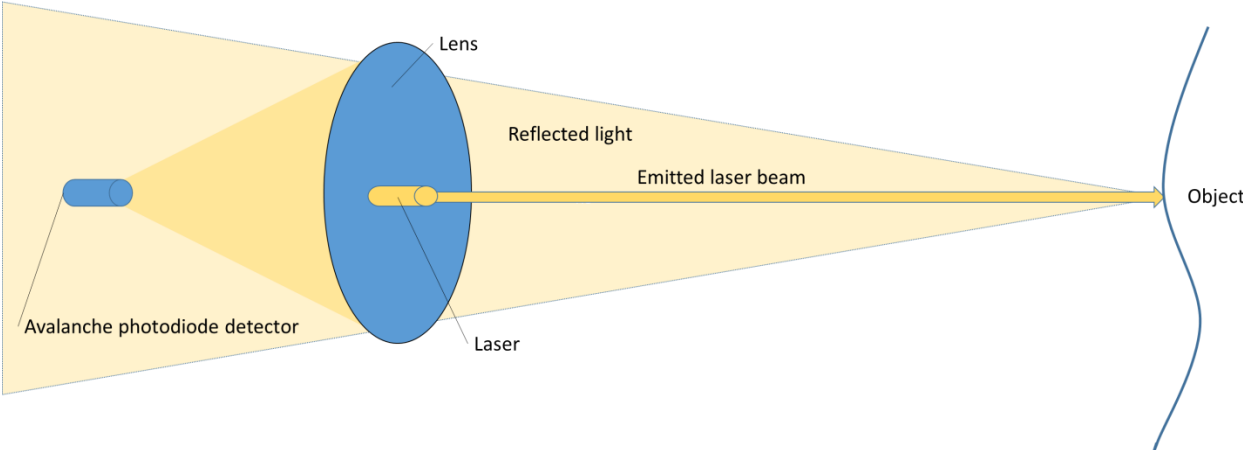
Figure 30. Time of flight principle.
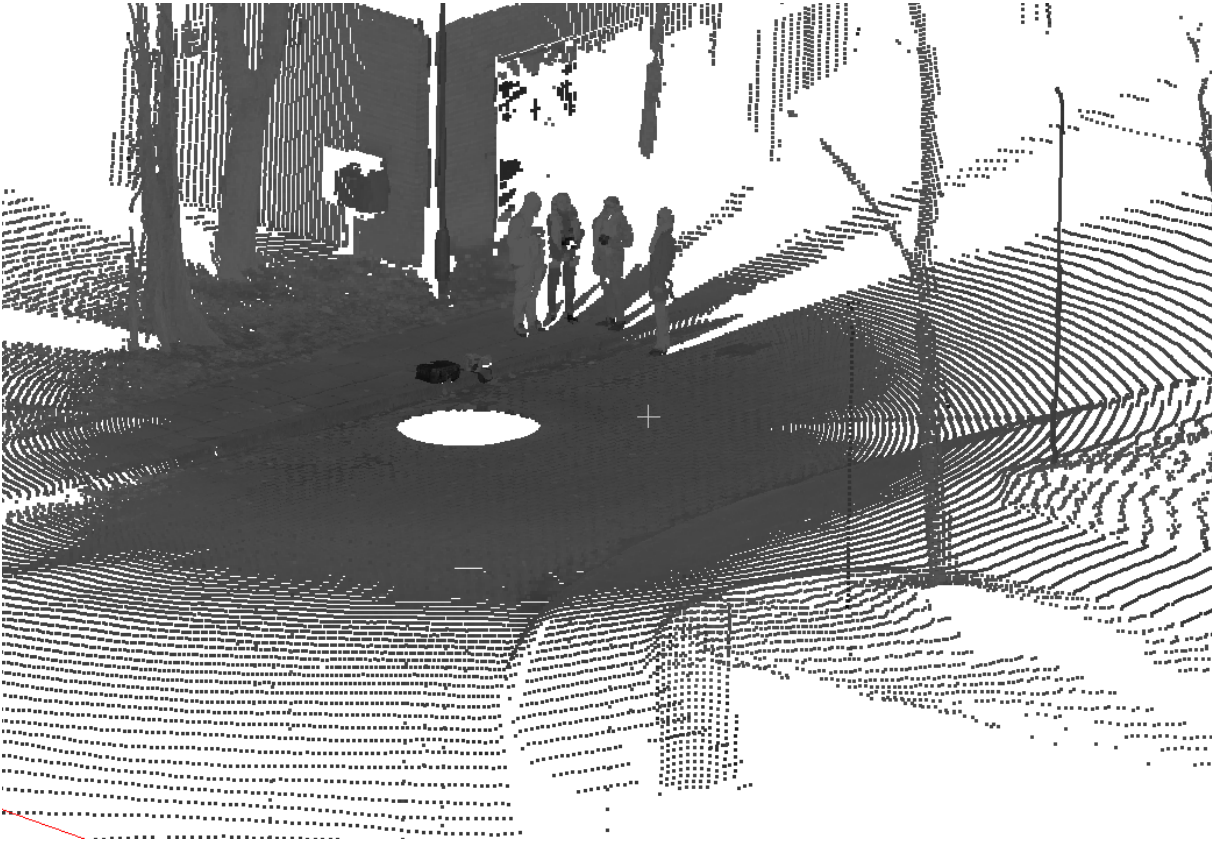
Figure 31. Exemplary measurement taken with time of flight scanner (Faro Focus).

Light sources used in time of flight devices should provide very narrow beam. This is crucial for obtaining noise free data – wide beam means multiple reflections from objects placed in its radius but at different lengths. This problem can be mitigated by using sophisticated phase modulation of light (Gokturk, et al., 2004) or other techniques (Buller, et al., 2005). Nevertheless, the only source used in classic time of flight scanners is laser, usually infrared one. Lasers are the only emitters capable of providing powerful light pulses which stay narrow for long propagation distances. Best devices may have operating range up to few thousands meters (Fröhlich & Mettenleiter, 2004). Apart from beam quality, main factor affecting accuracy of measurements in time of flight devices is the variability of environment conditions between device and object (temperature, humidity, pressure) which affect the speed of light and are very difficult to compensate (Hebert & Krotkov, 1992).

Best known time of flight scanners are manufactured by Riegl (Riegl, 2016), Leica Geosystems (Leica Geosystems, 2016), Faro (Faro, 2016), Trimble (Trimble, 2016) (Figure 32).

a)   b)   c)   d)

Figure 32. Time of flight scanners: a) Riegl VZ1000, b) Leica HDS; c) Faro Focus 3D; Trimble TX8 (images sources: manufacturers webpage).

In the recent years, development of advanced CMOS detectors allowed for creation of matrix time of flight detectors (May, et al., 2006). Their principle of operation is still the same as for previously described sensors, but the light is emitted in wider angle (covering full working area). Time of flight propagation is measured by each pixel individually, thus providing full field 3D information (Lange, 2000). The accuracy and distance of such sensors are currently mediocre, with best systems providing few millimeter accuracy (Dorrington, et al., 2010), (Basler, 2016). The main advantages of such sensors however are: very short time of measurement, high tolerance of surface characteristics and small size of the sensor (which often is comparable to typical camera used for industrial inspection - Figure 33).

Figure 33. Time of flight matrix detector (Basler ToF - left) next to standard industrial camera (Basler Aviator - right) (images source: Basler webpage).

3.1.4 Structured light technique

Contrary to previously presented methods, structured light technique term covers very wide range of measurement techniques. Those techniques use some kind of lighting system which projects patterns on object and one or more detectors (nowadays CCD/CMOS cameras) placed in some distance from the projector. The angle between projector and detector affects performance of the system (optimally this angle should be between 35° and 40°) (Woo, et al., 2002). Physically, this setup is similar to laser triangulation technique but instead of constant light from laser in structured light system, a pattern or changeable set of patterns is used.

Raster, which is projected onto object, is seen as deformed by the camera (because of its different vantage point). By the analysis of this deformation, geometry of surface of the object can be recovered. For systems, which use pattern only for addressing projector pixels, the accuracy is comparable to triangulation systems, however the data is collected for full field instead of point or line(s) without any head movement.
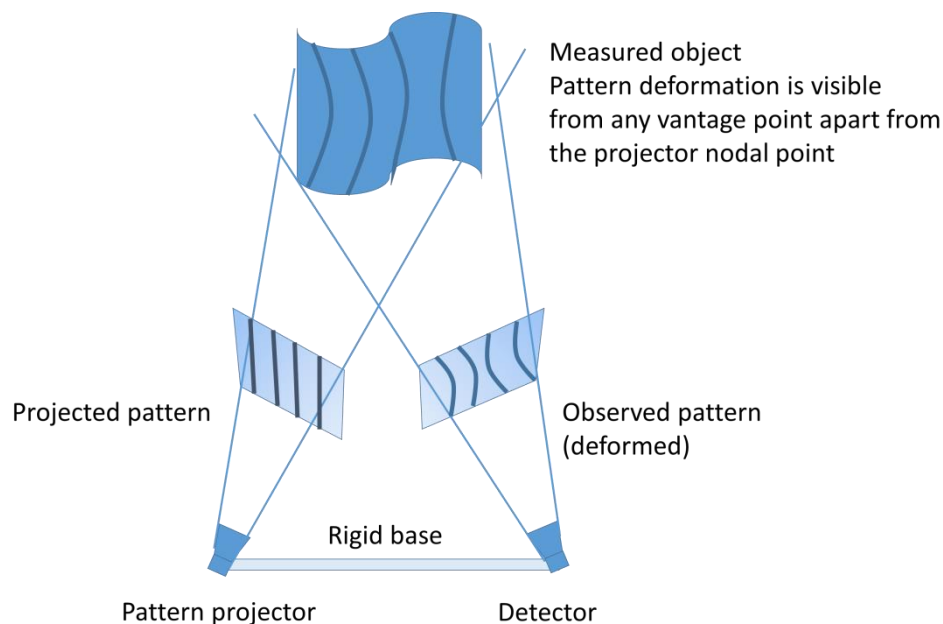
Figure 34. Typical structured light system composed of pattern projector and detector fixed to rigid base.

Precision of measurement depends inter alia on used patterns. The most accurate systems use sinusoidal fringes and phase shifting technique. In this configuration, accuracy may reach tens of micrometers (Georgopoulos, et al., 2010), (Sładek, et al., 2011), (Krzesłowski, et al., 2011). Sinusoidal fringes are usually used with Grey codes (Bitner, et al., 1976) which provide additional information about shape which is used in phase unwrapping processing stage. The necessity of projecting Grey codes (or similar patterns) and few (3-6) sinusoidal images causes long measurement time during which measurement conditions and objects state should be constant. Any changes cause inaccuracies or noise. For this reason, this method is suitable for stationary objects in controlled environment conditions.

Due to the possibility of projecting (and observing) patterns on small area (using macro lenses), measurement resolution may be high. Moreover, small details of objects can be digitized. However as typical projectors used in structured light systems (DLP or DMD) do not offer light intensity comparable to laser sources, measurements cannot be performed outdoors, especially in sunlight.

Color information can be easily acquired, usually using projector (with white image) as an illumination source. Color data is directly mapped onto geometry because the same camera is used for bot purposes. Moreover, as demonstrated in literature, color does not need to be limited to RGB color-space, it may be extended to multispectral imaging (infrared, visible and ultraviolet) (Mansouri, et al., 2007), (Krzesłowski, et al., 2011).

High precision obtained with structured light technique caused its popularity among professional 3D measurement systems. Multiple solutions exist, the best known ones are: GOM Atos II (GOM2, 2016), Aicon SmartScan (Aicon 3D Systems, 2016), Faro Cobalt (FARO4, 2016) and Steinbichler (Zeiss) Comet (ZEISS Optotechnik4, 2016) (Figure 34). In Poland, the most known structured light scanners are produced by Smarttech (Smarttech, 2017) and Evatronix (Evatronix, 2017).

a)   b)   c)   d)
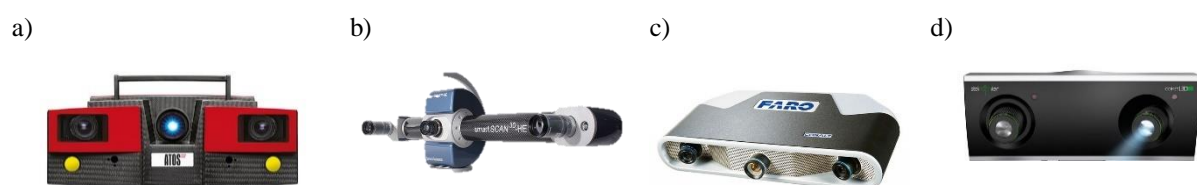
Figure 35. Most popular structured light 3D scanners: a) GOM Atos II; b) Aicon SmartScan; c) Faro Cobalt; d) Steinbichler Comet (images sources: webpages of manufacturers).

3.1.5 Summary

Presented methods of optical, contactless measurements are the most popular ones utilized in commercial and research 3D scanning devices. They all have their advantages and disadvantages and there is no universal method which works perfectly for all types of digitized surfaces. When choosing a system for a given type of object, one has to analyze surface properties (reflectivity, color etc.), required resolution, time for digitization, working conditions (vibrations, dirt, lighting parameters) and available budget. Passive methods, like photogrammetry and especially Structure from Motion can be considered as low cost alternative but obtained results heavily depend on the object itself (number of characteristic points). Contrary, active methods are not constrained by this requirement, but cost of hardware is usually much higher.

Scope of this work is an automated 3D system for massive digitization purposes of cultural heritage objects. As it was said in the first chapter, for such purposes high resolution (2500 points per mm^2 or better) is required as well as good quality of color sampling. Moreover, the measurement method should be as safe to objects as possible. For some works of art, conservators pose heavy limitations to light exposure and density of energy focused on surface of objects (Bunsch, 2010), (Karaszewski, et al., 2013). For this reason, laser based devices are not applicable as lasers deliver high energy light. Even structured light systems using commercial DLP projectors sometimes provide too much light and have to be modified to stay within allowed level of lighting energy.

Overall, laser triangulation and structured-light technique provide required level of resolution and accuracy. The commercial devices using first method usually do not have capability to capture color information directly mapped on measurement results but could be implemented. This feature is natural in structured light systems which can capture color information with the same sensor as used for capturing images of deformed patterns and in fact most of such devices obtain geometry and color information at once. Laser-based systems can be easily used even in direct sunlight while for structure light devices measurements should be performed indoors, optimally with weak or no ambient light. On the other hand, laser triangulation systems have mechanical moving parts which in certain conditions is a disadvantage. Also, structured light devices are better suited to imaging small details than laser triangulation sensors. Table 1 concludes the statements given above.

	Photogrammetry	SfM	Laser triangulation	Time of flight (classic)	Time of flight (matrix)	Structured light
Resolution	-	-	+/-	+/-	-	+
Accuracy	+	+/-	+/-	-	-	+
Good result regardless of characteristic points	-	-	+	+	+	+
Fast measurement	+	-	-	-	+	-
Price	+/-	+	+/-	-	-	-
Low energy emitted on analyzed surface	+	+	-	-	+/-	+/-
Color information without parallax	+	+	+/-	+/-	+/-	+

Table 1. Comparison between optical measurement techniques.

Considering all those observations, I have chosen structured light technique as the one which is best suited for stated requirements. In this realization, 3D scanner is built using CCD color camera and DLP projector, used for projecting sinusoidal patterns (phase shifted) and Gray codes.

3.2 Positioning systems

This chapter contains brief review of positioning devices which are used in automated measurement system. Those systems are not limited to 3D digitization stations but also include other similar setups (for example Coordinate Measuring Machines – CMMs).

3.2.1 Robotic arms and rotating stage

The most popular positioning system for automated 3D measurements is definitely robotic arm, usually with rotating stage. Typical robot arms have usually six degrees of freedom providing high flexibility of movements (Figure 36). Moreover, such devices are widely used in industrial applications and are precise, highly-reliable and commercially available at moderate prices. Using industrial communication standards (Profinet (Pigan & Metter, 2008), EtherCAT (Büttner, et al., 2003) etc.), integration with computer software is usually easy.

a)

b)

c)
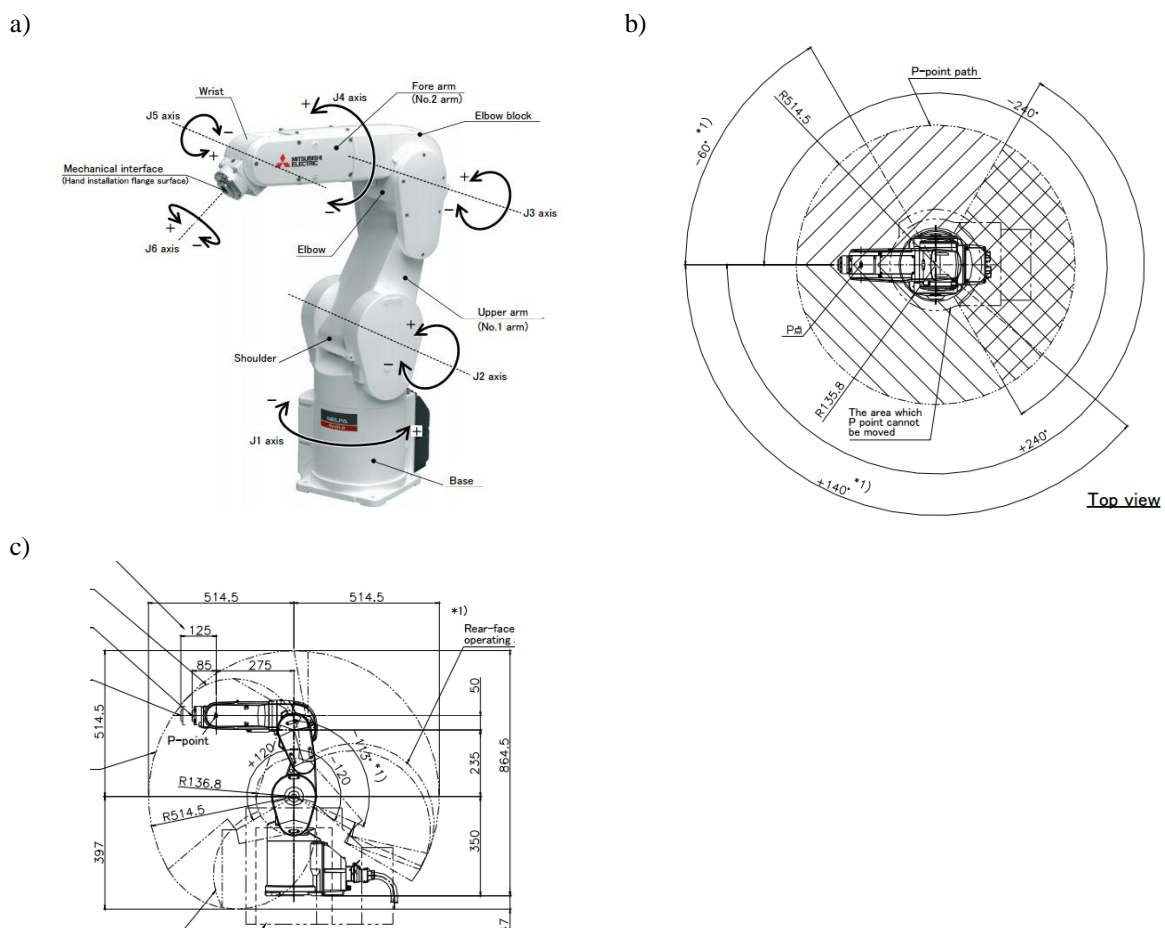
Figure 36. Typical 6-axis robot arm (Mitsubishi Electric RV-4FL): a) overview; b, c) operating range (Images source: Mitsubishi Electric webpage).

Rotating stage is often added to give possibility to measure objects from all directions (Figure 37). Without it, even using robot arms with large operating range it is hard to place the

scanner behind the object. Stages are often connected to robot controller as seventh axis. This way, they are controlled as they would be part of robot arm.
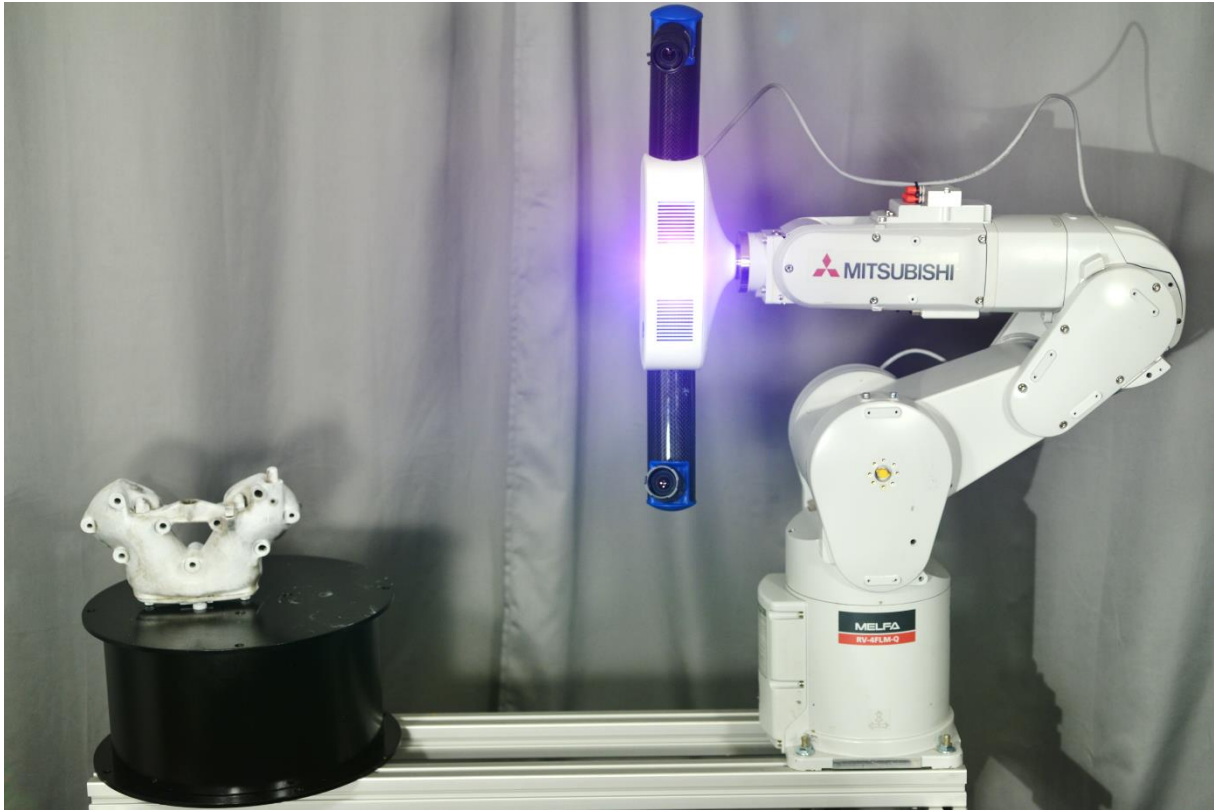
Figure 37. Typical setup of robot arm and rotating stage (PragmaVision SLScan2xR, image source: manufacturer's materials).

To the best of knowledge of author, there is no preferred manufacturer of robotic arms. Fanuc, Kuka and ABB robots are often used but I have not found any information whether it is caused by some advantages over other manufacturers or they are just less expensive.

3.2.2 Rotating and translating tables

The physical realization of positioning system is in fact of low importance for 3D scanning results, as long as it provides required accuracy. Thus, commonly used setup with robot arm can be replaced by set of rotating stages linked with rigid links. When six or more degrees of freedom are required, robot arms are most popular as they provide commercially available, cost effective and precise solution. However, there are some applications where smaller number of degrees of freedom is required (for example scanning of paintings, facades, cylindrical objects with low surface complexity etc.). In those cases, simple positioners are often used. Custom solutions can be better suited for the task, like for example in SAPO system (Karaszewski, et al., 2013) where two long linear positioners are used to allow for

paintings digitization (Figure 38). In this system, paintings with dimensions of up to 2m x 2m can be scanned. Such requirements cannot be realized with robot arm due to its limited range.

Figure 38. SAPO system with linear XY positioners (left) and its measurement head (right).

As it was said, custom solutions are used in specific tasks rather than universal digitization systems. One notable exception is Popodopoulos-Orfanos system (Papadopoulos-Orfanos & Francis, 1997) which used laser sensor mounted on three connected linear tables (providing X,Y and Z shift), while an object was placed on the rotary stage.

3.2.3   Drones and mobile robots

Practically all previously presented digitization systems and positioners are stationary. Digitization objects are placed on the tables or fixtures and 3D head is positioned around it by positioners. There are however systems which use mobile platforms with 3D sensors used to create maps (3D model) of environment. Examples of such systems include ground-based mobile platforms like Pioneer 3DX with stereo-vision, laser rangefinders or full-fledged time of flight scanners (Figure 39).

During last few years, new branch of mobile mapping systems appeared. Those devices are based on unmanned aerial vehicles (UAV) such as helicopters, fixed-wings or multirotor drones. Due to limited payload (especially when compared to ground vehicles), they usually have only one 3D sensor. Most often it is specially constructed laser rangefinder (Figure 40).

Figure 39. Mobile, ground-based 3D mapping platforms: a, b) Pioneer 3DX with stereovision (a) and rangefinder (image source: http://www.ti.uni-bielefeld.de); c) Topcon IP-S2 Compact+ with multiple rangefinders (image source: manufacturers webpage); d) custom platform with Riegl VZ-400 time of flight scanner; e) custom platform with time of flight scanner and rangefinders (image source: http://cyberspaceandtime.com).
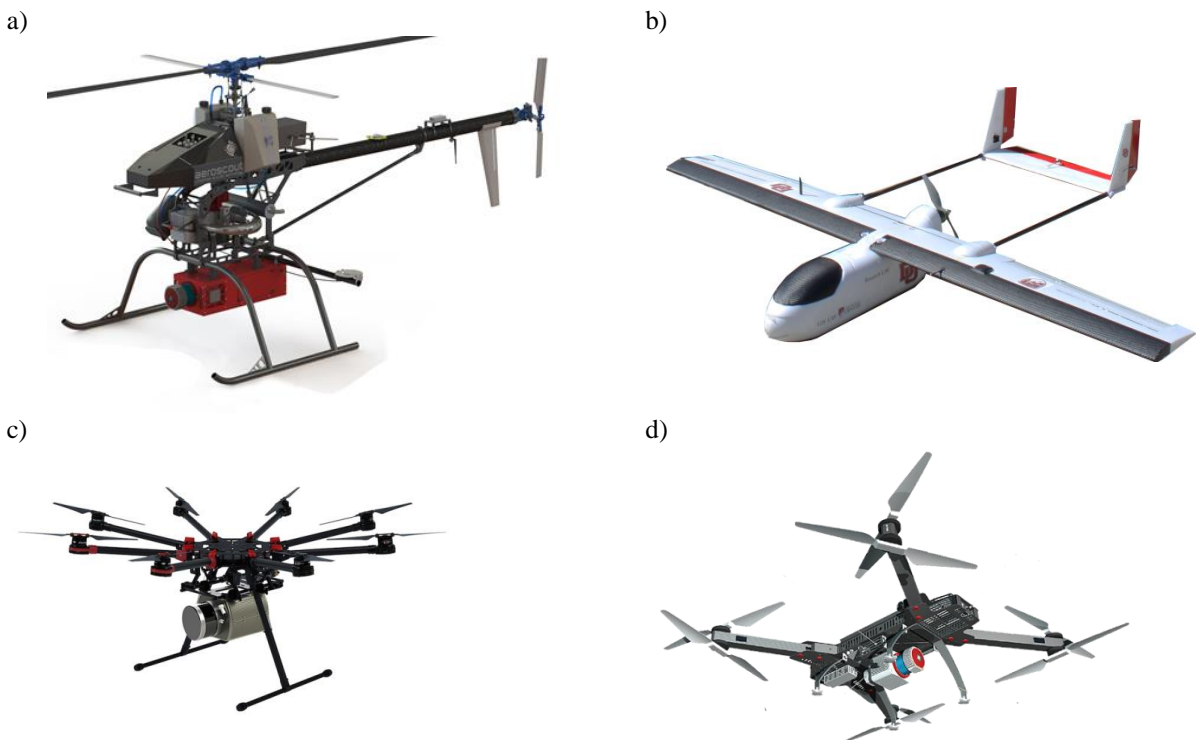
Figure 40. Airborne 3D mapping platforms: a) Aeroscout Scout B1-100; b) Aerial Data Systems MDAP fixed-wing drone; c) Phoenix Aerial Scout S1000; d) Riegl Ricopter with VUX-1UAV lidar rangefinder (images sources: manufacturers' webpages).

Usually, mobile platforms are used for different digitization targets at completely different resolution and accuracy levels than stationary systems. Nevertheless, while the topic of calculating a route along which such a device should travel to allow for 3D mapping is similar in nature to Next Best View topic, the differences in positioning systems parameters are so significant, that the algorithms from fixed systems cannot be applied to mobile platforms and vice versa.

Low positioning accuracy, vibration, limited movability (for example fixed-wing drones cannot turn "in-place", changing observation angle requires changing of elevation angle of a drone which in turn changes its height etc.) are factors which have to be considered during measurement planning. On the other hand, working volume of lidar and time-of-flight sensors is usually large, making it easier to capture data from interesting area.

3.2.4   Summary

The aim of my work is to design station capable of high resolution, high precision 3D shape digitization. Basing on this, the elements of such system have to provide adequately precise operation, many degrees of freedom as well as significant operating range for reasonable price. For this reason, for positioning system, I have chosen industrial robot arm. To provide additional degree of freedom, robot is accompanied by rotary table. Such configuration is similar to the one used in commercially available digitization stations.

3.3 Next Best View algorithms

Calculation of Next Best Views has been an active topic for many years. Various researchers have been working on this problem, usually with one of two purposes in mind: digitization of unknown objects (without any information apart from rough size) or digitization of objects with digital models (usually CAD ones). This division was of course caused by different needs of industry – the demand for CAD-based methods was higher due to the possibility of using automated 3D digitization systems in industrial inspection and quality control. In this dissertation, I focus mainly on the first group of NBV algorithms, i.e. ones which are used in unknown objects' digitization as such system is the topic of my dissertation. In this work, the review of both groups of algorithms is presented because some concepts which were introduced in CAD-based analysis can be applied to my automated digitization system.

3.3.1 Next Best View methods based on CAD models

Traditionally, quality control in manufacturing was performed using touch-probes and coordinate measuring machines (Woźniak & Dobosz, 2003), (Kamrani, et al., 2015), (Fan & Leu, 1998), (Kweon & Medeiros, 1998), (Wu, et al., 2004). Such devices, while offering extremely high precision, do not allow fast measurements (only one point is sampled at a time (Zhao, et al., 2009)). The need of fast quality control in industry and rising precision of optical, non-contact measurement devices led to development of inspection systems which use optical 3D sensors instead of touch-probes (Zhao, et al., 2009), (Ko, et al., 2007), (Kamrani, et al., 2015), (Chen & Li, 2005). Usually such sensors provide full field measurement (even millions of sampled surface points per measurement), significantly speeding up the whole inspection process. In the case of quality control, computer model of digitized part is available and is used for measurement strategy planning.

There is a significant difference in measurement planning principles for quality control and object documentation (like in cultural heritage-related applications or reverse engineering). The main purpose of 3D scanning in quality-checking applications is to obtain measurements on which critical object features may be located (Germani, et al., 2010). Therefore, full 3D model is almost never completed as it is unnecessary and require more directional measurement than needed for quality control. Moreover, strategy is usually determined by some expert knowledge, which defines the best way to scan a feature or determine its deviation (Gao, et al., 2006), (Zhao, et al., 2009), (Yang & Ciarallo, 2001; Germani, et al., 2010). The situation is different when considering objects with freeform surfaces, for which

the only way to determine dimensional correctness is to compare measured surface with CAD-one (Sheng & Xi, 2000), (Prieto, et al., 1999). For this purpose, at least the part of the object which contains freeform surface has to be digitized completely.

In this review, I do not present tolerance-, or feature- based measurement strategy methods. They cannot be applied to unknown object digitization as they require more than geometry containing CAD model – namely important features definitions, tolerances etc. (Sheng & Xi, 2000), (Zhao, et al., 2009), (Germani, et al., 2010). In the further section of this review, I present few important and often - referenced freeform inspection methods.

One of the most popular works on the topic of CAD-based surface digitization process is the method of Martins et al. (Martins, et al., 2005). This method works for any CAD model as basing on the geometrical information (in the form of triangle meshes, parametric surfaces etc.) voxel description of measurement volume is constructed. Size of the voxel is determined by operator and should be related to the size of the details which should be inspected. Initially all voxels receive "*empty*" flag. After model loading, those voxels which encompass surface of the model are marked as "*target*". For each voxel, its central point and normal vector (calculated as average vector of all geometrical features in voxel) are stored. Using fixed set of 3D sensor (there is no clear explanation how this set is generated), visibility of each voxel from each sensor pose is determined. Afterwards, poses which allow to measure possibly high number of voxels are selected and sent to measurement system. This measurement strategy method has two obvious disadvantages. While voxel model is easy to use and allow for fast calculation of visibility, collisions etc., it does not allow for analysis small features of object. Moreover, as for each voxel one, averaged, normal vector is calculated, it does not allow to present well surfaces with high surface gradients. The second problem is related to fixed set of possible sensor poses. If the set is too simple (for example sensor is placed on sphere or cylinder surface), it will not allow to obtain good shape representation for sensors with small working volumes. On the other hand generation and analysis of very complex sensor poses is computationally prohibitive.

Another of popular systems for freeform surfaces digitization was presented by Prieto et al. (Prieto, et al., 1999). Their algorithm is restricted to surfaces defined as NURBS. Using laser-sweep sensor, the system calculates measurement trajectories by calculating sensor pose which allows for perpendicular observation of current part of the CAD surface (using its normal vector for analysis) from strictly controlled distance (to provide required measurement resolution). There is no clear information how the subsequent viewpoints are selected,

probably they are just inserted along the NURBS patch with regard to sampling density. Voxel model of environment is also created to allow for collision and occlusion detection. The proposed collision-free trajectory calculation algorithm is based on adding additional points in some distance from collision point. Occlusions are mitigated by allowing non perpendicular observation direction. While the paper is vague on some details, the presented method is sound and probably can be modified to non NURBS digital models.

A measurement strategy method, similar to proposed by Prieto was introduced by Sheng and Xi (Sheng & Xi, 2000). In their work, computer models were not limited to NURBS surfaces. The system identifies similarly oriented parts of the surface (i.e. having normal vectors oriented in the same way). For each of such groups a bounding box is calculated. Center of this bounding box becomes a target for 3D sensor, while the observation vector is inverted surface normal. Those two features form directional measurement pose. The method works well for sensors of large working volume (at least comparable with largest of created bounding boxes). Authors do not present however any extension of their algorithm which could allow for using sensors of smaller working volume.

An interesting method for identifying sensor positions leading to obtain good quality digital representation of an object with CAD model was proposed by Yang et al. (Yang & Ciarallo, 2001). Basing on the model, they calculate a set of edges along which digitization should be performed to fulfill 3D sensor placement requirements (observation angle, distance, no occlusions). This allows for minimization of measurement errors caused by non-optimal observation angle etc. Yang also consider many other error sources like positioning inaccuracy and quantization. All those sources were combined into one function over digitization space. To find proper solution for an object, measurement poses were selected by genetic algorithm which simultaneously minimized errors and kept sensor constraints within acceptable limits.

3.3.2 Next Best View methods without CAD models

This review is based on work of author published in Journal of Photogrammetry and Remote Sensing (Karaszewski, et al., 2016). Twelve most popular algorithms were implemented and their performance was for three measurement heads. Those devices had different working volumes: large (significantly greater than digitized object), medium (comparable to digitized object) and small (significantly smaller than object). In further sections of this paper, this

relation between scanner working volume and object is referred to as Object Size to scanner Working Volume (OSWV). The criteria of evaluation were as follows:

- number of measurements required by method (less is better),
- time of digitization (shorter is better),
- total positioning distance (approximated as the sum of distances between start and end of positioning trajectory for each directional measurement; shorter is better),
- surface coverage (calculated without base of the object; larger is better).

Surface coverage was calculated by comparison of obtained models with their digital sources (STL files). For all objects but aluminum gusset, this comparison is not perfect because their physical forms were printed on 3D FDM printer (this process introduces slight shape changes), however this inaccuracy can be neglected because it is the same for all compared methods (the same objects were used).

The selection of the NBV algorithms was dictated by their popularity. In this document, they are presented in chronological order of their publication:

1. The Determination of Next Best Views by Connoly (Connoly, 1985).
2. A Mechanism of Automatic 3D Object Modelling by Yuan (Yuan, 1995).
3. Automatic 3-D Digitization Using a Laser Rangefinder with a Small Field of View by Papadopoulos-Orfanos) (Papadopoulos-Orfanos & Schmitt, 1997).
4. A solution to the next best view problem for automated surface acquisition by Pito (Pito, 1996).
5. Constraint-Based Sensor Planning for Scene Modelling by Reed (Reed & Allen, 2000).
6. A Next Best View System for Autonomous 3-D Object Reconstruction by Banta (Banta, et al., 2000).
7. RoboScan: An automatic system for accurate and unattended 3D scanning by Callieri (Callieri, et al., 2004).
8. Vision Sensor Planning for 3-D Model Acquisistion by Chen (Chen & Li, 2005).
9. A Surface-Based Next Best View Approach for Automated 3D Model Completion of Unknown Objects by Kriegel (Kriegel, et al., 2011).
10. An efficient method for fully automatic 3D digitization of unknown objects by Khalfaoui (Khalfaoui, et al., 2013).

11. Towards fully automatic reliable 3D acquisition: From designing imaging network to a complete and accurate point cloud by Ahmadabadian (Ahmadabadian, et al., 2014).

12. Volumetric Next Best View Planning for 3D Object Reconstruction with Positioning Error by Vasquez-Gomez (Vasquez-Gomez, et al., 2014).

Short descriptions of each algorithm are given in the next part of this section.

3.3.2.1 The Determination of Next Best Views (Connoly)

The algorithm presented by Connoly (Connoly, 1985) is one of the first developed for the automation of the 3D digitization process. It is quite simple, mostly because of the limited computing power available and thus not very promising. It is mentioned and was tested because it introduces some of the most important ideas used by many researchers of NBV topic: so-called voxel space for describing measurement space with two classes of voxels (unknown and occupied) and NBV criterion, which defines a NBV algorithm as the one which tries to identify the positions of the sensor that will allow it to cover the maximum number of unknown voxels.

In Connoly's algorithm, 3D sensor can be only placed on a sphere encompassing the object with center of this sphere placed in the center of the object (this configuration resembles planetary system thus its name: *planetarium*).

Connoly presented also a second algorithm in which instead of voxels, the algorithm analyses the number of border walls (i.e., walls between the unknown and occupied voxels). The vertex that has the maximal adjacent wall area (calculated along XYZ coordinates) is identified and the average normal vector of those walls is selected as the viewing vector. Neither algorithm considers occlusions of the sensor view, collisions nor the OSWV ratio.

3.3.2.2 A Mechanism of Automatic 3D Object Modelling (Yuan)

NBV algorithm proposed by Yuan in 1995 (Yuan, 1995) is the first which uses more advanced mathematics rather than heuristics. It is based on the observation that for any convex object, the total Gaussian mass of its surfaces is equal to zero (Horn, 1984). Yuan stated that Gaussian mass of object may be approximated by so called total mass vector chain which can be calculated as an average of all point normal in the model. Next position of the measurement device is then found by placing it in a direction that is opposite to the mass vector. This method is extended to handle concavities in the measured object using a simple occlusion avoidance algorithm (Yuan, 1993). Unfortunately, in the state presented in the

paper, algorithm cannot be fully automated and require operator's intervention. There is no information about collision detection. One disadvantage of this method is clear—sensor positions are selected to be on the opposite side of the object than the previous ones; therefore, the positioning time and distance travelled by the measurement head will be significantly greater than average. As the head is placed with working volume in the barycenter of collected model, with large OSWV values it is dubious if surface of the object lies within sensor working volume.

3.3.3   Automatic 3-D Digitization Using a Laser Rangefinder with a Small Field of View (Papadopoulos-Orfanos)

Papadopoulos-Orfanos and Schmitt presented an idea of NBV algorithm which, contrary to previously described methods, had been developed specifically for 3D sensors with very small working volume (Papadopoulos-Orfanos & Schmitt, 1997). Operating depth of the laser sensor which authors use starts at 50 mm from the sensor and ends at 100 mm. The main aim of the algorithm is to digitize an object without any danger of collision between object and scanner. Developed method is very simple and consists of two stages. In the first one table on which object is placed rotates around its vertical axis in user defined increments. Between those movements, three linear stages move the head in XYZ directions (zigzagging in XY plane at distance z_1, then closer to object at distance z_2) until part of surface is sampled. In this XY position sensor does not move any more towards rotating stage axis. Authors coined the name of *space carving* for this method as it resembles carving material by sculptor. While this solution is very simple and does not take into account occlusions or any other problems which occur for most real-world objects, I wanted to include it in this review as it was the first method developed for a sensor with very small working volume and the first which covered the problem of collision avoidance.

3.3.4   A solution to the next best view problem for automated surface acquisition (Pito)

The paper by Pito (Pito, 1999) is definitely the most popular manuscript related to NBV problem. Researcher presents a method which is considerably more advanced that any previously published ones. Numerous problems which occur during digitization process are considered: surface observation angle, self-occlusions and requirement for overlaps between subsequent measurements (i.e., their size and placement). Collision avoidance during positioning is not covered however.

Pito's algorithm is based on the analysis of partially reconstructed 3D model in the form of triangle mesh. Border edges (i.e. triangle edges which occur only once) are identified thus locating holes in the model. From those edges, so-called patches are artificially created. Patches are oriented by analysis of source edge neighborhood and directed towards the center of a partially reconstructed 3D model. All patches are divided into groups by similar orientation. For such groups, sensor position which offers the most perpendicular and occlusion-free view of the group is selected (from the static set of possible sensor positions).

3.3.5   Constraint-Based Sensor Planning for Scene Modeling (Reed)

The paper by Reed and Allen (Reed & Allen, 2000) presents a NBV algorithm which closely resembles Pito's solution presented above. Their method also works on triangle meshes representing partially scanned object. Contrary to Pito's patches, here solids are created from directional measurements by their extrusion towards the center of the object. Those solids, are then intersected with each other forming triangles which can be identified as *measured* or *occluded. Occluded* groups are then used as digitization targets – 3D sensor is oriented in a way which assures perpendicular observation of groups surface. Unfortunately, sensor positions are limited to so called *viewsphere* which is a sphere with user-defined radius centered in the center of the object. This significantly constraints the OSWV ratio for which this method can be used. Collision avoidance is not covered by authors.

3.3.6   A Next Best View System for Autonomous 3-D Object Reconstruction (Banta)

The algorithm presented by Banta et al. (Banta, et al., 2000) is an evolution of original method developed by Connoly (Connoly, 1985). Main assumptions are as follows:

- Sensor may be placed in any point on the surface of a sphere with a user-defined radius that is centered at the center of the object.
- Sensor always aims towards the center

What is important, Banta does not analyze partial model of object at all (apart from the third NBV method, see below), obtained data is used only to update state of voxel into working volume is divided into. Those voxels may have one of three states: unknown, surface or occluded.

There are three methods of selecting Next Best View described in the paper: by localizing unknown voxels, clustering unknown voxels and by detecting edges in range maps obtained from directional measurements. For all methods, Banta uses occlusion detection (occlusion by

surface voxels). For occluded viewing directions, observation angle is iterated (by moving sensor on the viewsphere surface in the vicinity of its original position) until line of sight is occlusion-free. No information is given on collision detection.

3.3.7 RoboScan: An automatic system for accurate and unattended 3D scanning (Callieri2004)

The algorithm presented by Callieri in 2004 is a part of automated system for 3D digitization (Callieri, et al., 2004) presented in Chapter 2. This method is two-staged. At the beginning, an incomplete 3D model of an object is obtained by performing several directional measurements with sensor in static set of positions (i.e., on the surface of the cylinder circumscribing the object, or the plane in case of planar objects). Discontinuities in obtained model are then identified and set as a target for measurements in the second stage of the process. The method used for the detection of discontinuities is unique because it is based on analysis of images of 3D model rendered from different vantage points. During analysis, the number of pixels with color bound to the back surface of the model (which are visible only if there are holes in the model) is calculated. The paper does not specify, how the vantage points used for rendering are calculated, probably they are simply randomly chosen. There is no clear information about collision avoidance during NBV calculation.

3.3.8 Vision Sensor Planning for 3-D Model Acquisition (Chen)

The algorithm presented by Chen and Li (Chen & Li, 2005) is based on the analysis of partially measured model. It searches for so called best exploration direction which is assumed to be the direction in which the model changes the least (i.e. shape gradient is minimal). For this direction, the surface trend is approximated by polynomial fitting. Afterwards, position of 3D sensor is calculated to maximize area which is observed perpendicularly and without occlusions. In the paper, no details are given to the method used for detecting occlusions however. Also, it is not clear whether occlusions are only detected or mitigated for example by iterating the observation angle. Collision detection and avoidance is not covered in the paper.

3.3.9 A Surface-Based Next Best View Approach for Automated 3D Model Completion of Unknown Objects (Kriegel)

Algorihtm which was developed by Kriegel works on triangle meshes which represent partially digitized object. Like in Pito's method, unmatched triangle edges are located with the distinction to left, right, top and bottom groups. For each border edge, a quadric surface is fitted to its neighborhood. For such surface, sensor position is calculated in a way which

assures perpendicular observation of the surface. Similarly to Pito's solution, the overlapping areas of directional measurements is considered. The percentage of overlaps can be set by the operator. Kriegel states that the method is universal and should work with any 3D scanner, however there is no information about occlusion handling and collision detection.

3.3.10 An efficient method for fully automatic 3D digitization of unknown objects (Khalfaoui)

Khalfaoui et al. (Khalfaoui, et al., 2013) base their NBV algorithm on the detection of borders of partially measured models. In Khalfaoui's method, it is done separately for each of the directional measurements by analyzing the angle between the recovered surface's normal and current observation vector. This way, places which are not perpendicular to observation angles are located and marked as *barely visible*. Those areas are then clustered and compared with *barely visible* areas from other directional measurements. If any of such areas is not covered by *well visible* points, it becomes a target for next directional measurement in which sensor is placed to be perpendicular to it. There is no discussion about occlusions, collision avoidance during sensor positioning nor influence of scanner working volume on the results of algorithm application.

3.3.11 Towards fully automatic reliable 3D acquisition: From designing imaging network to a complete and accurate point cloud (Ahmadabadian)

The NBV method described by Ahmadabadian (Ahmadabadian, et al., 2014) is two staged and consists of initial model acquisition with very rough sensor (of large working volume) and this model analysis for digitization with photogrammetric head. In the first stage, Primesense 3D scanner is used, controlled by ReconstructMe software package (ReconstructMe, 2015). Object, placed on the rotary stage, rotates slowly in front of the sensor and its very rough 3D model is obtained. Afterwards, this model is virtually inscribed in ellipsoid which represents a set of possible photogrammetric head positions during the second stage of digitization. From this set of positions, a small subset is selected by identifying those ones which provide perpendicular observation of objects surface. There is no information about occlusion handling nor collision detection. Moreover, there is no discussion about possible size of scanner working volume, however using constrained set of its positions on ellipsoid probably limits applicability of this algorithm for sensors with small working volume.

3.3.12 Volumetric Next Best View Planning for 3D Object Reconstruction with Positioning Error (Vasquez-Gomez2014)

The last of presented methods, algorithm proposed by Vasquez-Gomez et al. (Vasquez-Gomez, et al., 2014) is an evolution of algorithm developed by Connoly (Connoly, 1985) described in earlier. The main assumptions are as follows:

- Scanning head may be placed on the viewing sphere (in Vasquez-Gomez version, it is not an exact sphere, but its approximation - result of a multistage tessellation of an icosahedron).

- Working volume is represented as voxelspace. Few types of voxels are present: unknown, used, empty, occluded, and occplane which are voxels through which surface of object comes through.

- Each voxel is characterized by its normal vector and quality (calculated as the maximum cosine of the observation of points inside).

The main novelty of Vasquez-Gomez algorithm is the assessment of the information gain for each of proposed sensor positions. This assessment is done with Bresenham's raytracing algorithm (Bresenham, 1965), considering many properties like surface observation angle, overlaps, and distance between analyzed and current positions of the 3D sensor. No information about the collision avoidance is given. Moreover, limiting allowable sensor positions to viewing sphere significantly impacts this algorithm's performance for large OSWV values making it rather impractical for sensor with small working volume.

3.3.13 Summary

Twelve well known Next Best View algorithms were briefly presented in the previous section. As it was said before, their performance was evaluated for different measurement heads (Table 2) and various objects (Table 3). The most important difference between those heads is their working volume. System named MK (Microsoft Kinect) has very large working volume, SL1 – medium one and SL2 – very small volume (the system is capable of taking measurements with more than 2500 points per mm^2).

Using presented systems, the usability of each of the tested algorithms depending on the object digitized and ratio of the object's size to the 3D sensor's working volume was assessed. This knowledge is summarized in Table 4 where the performance of all algorithms for different OSWV values is evaluated.
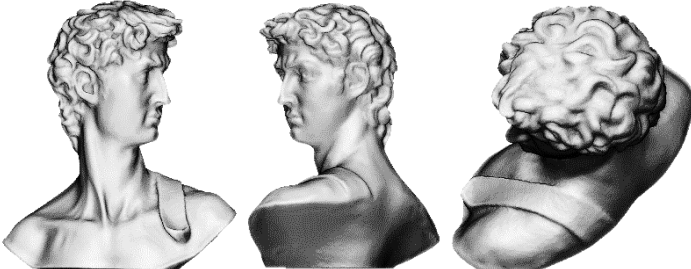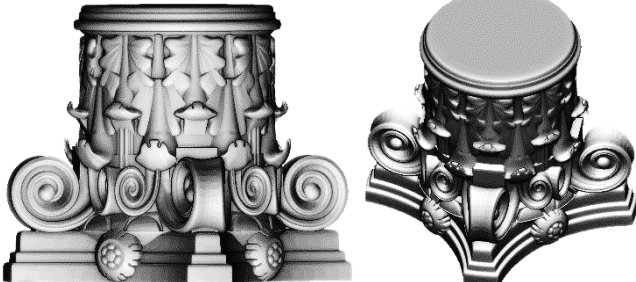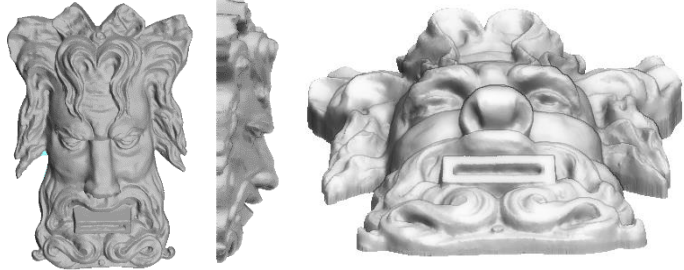
Measurement head	Photo	Working volume (mm)	Minimum working distance (mm)	Approximate OSWV ratio
MK (on top)		Large (500 × 500 x 500)	400	<< 1.0
SL1 (below)		Medium (180 × 120 × 110)	400	1.0
SL2		Small (50 × 50 × 12)	500	>> 1.0

Table 2. Measurement heads used for algorithms evaluation.

Name	Visualization	Characteristics
David's bust (DB) (Thingiverse, 2015a)		Simple object with some cavities (especially in the hair region). No self-occlusions, and few sharp edges.
Corinthian column (CC) (Thingiverse, 2015b)		Axially-symmetric object, many cavities, self-occlusions, and sharp-edges.
Luisville Public Library downspout (LD) (Thingiverse, 2015c)		Semi-planar object. On the front side, moderately deep cavities occur. Few sharp edges are present.
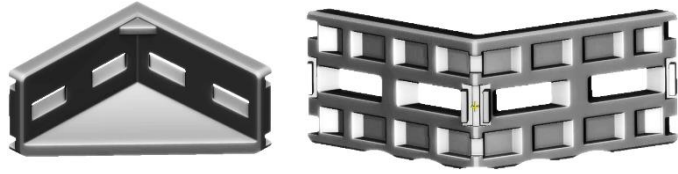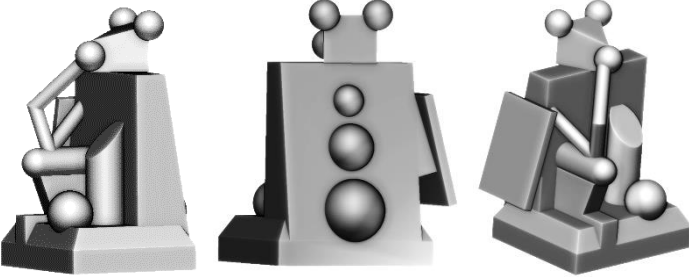
Aluminum profile gusset (AG)			Many sharp edges, holes, and cavities.
Artificial object for measure-ment test-ing (AO)			Sharp edges, large plane areas, and self-occlusions. No cavities.

Table 3. Objects used for testing NBV algorithms performance.

Method	OSWV << 1	OSWV ≈ 1	OSWV >> 1
Connoly1985	+	-	--
Yuan1995	++	-	--
Papadopoulos – Orfanos1997	++	++	+
Pito1999	+	-	--
Reed2000	+	+	+
Banta2000	++	-	--
Callieri2004	++	+	+
Chen2005	++	++	++
Kriegel2011	+	++	++
Khalfaoui2013	++	++	+
Ahmadabadian2014	++	+	--
Vasquez-Gomez2014	++	-	--

Table 4. Performance of tested algorithms for different OSWV values.

The final conclusion of conducted survey of NBV algorithms was that there is no single perfect method for all OSWV ratios and object types. Two of presented methods –Vision Sensor Planning for 3-D Model Acquisition (Chen)) and A Surface-Based Next Best View Approach for Automated 3D Model Completion of Unknown Objects (Kriegel) performed well for most cases, yielding good surface coverage in acceptable number of measurements. Kriegel's algorithm does not have occlusion-mitigating procedure therefore the completeness of 3D models is lower especially for sensors with small working volume. Methods developed by Khalfaoui, Callieri and Ahmadabadian require significantly more measurements than the best ones. While for Khalfaoui's algorithm, this is probably caused by the requirement for almost perpendicular measurement of each are of object, for the latter two algorithms it is caused by rough scanning from the predefined set of sensor poses. Especially for large OSWV values, this means that initial 3D model is of very low quality and require significant number

of hole-fitting measurements. Ahmadabadian's method is also burdened by the constraining set of possible sensor positions to ellipsoid.

Interestingly, Automatic 3-D Digitization Using a Laser Rangefinder with a Small Field of View (Papadopoulos-Orfanos) method yields acceptable results (surface coverage) despite its relative simplicity. The number of directional measurements is unfortunately much higher than for other methods.

Methods basing on constrained set of poses (*viewsphere* etc.) perform poorly with growing OSVW ratio. OSWV = 1 seems to be a threshold of their applicability. Overall, 3D models obtained with methods developed by Connoly, Pito, Reed, Banta, Vasquez − Gomez are of lower degree of surface coverage than the best performing methods.

One problem which was signalized in the first chapter of this work, namely collision detection, is almost totally ignored by authors of presented algorithms. Apart of Papadopoulos-Orfanos, they isolate the problem of collision awareness from NBV planning. While this is acceptable for sensors with large working volume (which usually have large standoff distance), short standoff distance of high-resolution sensors renders them unusable. I have conducted above described tests of NBV algorithms using CAD models of scanning targets for collision detection. In the process of unknown objects digitization this is however impossible. The only possible solution is to measure unknown space encompassing the object to check if it is free of any parts of the object which could collide. Unfortunately, this leads to the necessity of taking multiple "empty" measurements (especially with sensors of small working volume) which in effect resembles "brute-force" Papadopoulos-Orfanos algorithm.

The conclusion which arises from this survey is that no currently developed NBV method can be efficiently used with sensors of small working volume in systems for massive, automatic, unattended digitization of unknown objects. Best of existing methods yield good results even with large OSWV setups, however they require rough model of scanned object to ensure collision-free positioning. Also, such model should be provided to allow for analysis of occlusions during NBV planning.

The acquisition of initial model using high resolution head does not provide good results. When constrained set of poses (which can be predefined and collision free) is used, obtained model of object is heavily incomplete; depending on the particular case can be even unusable. Using more advanced method of sensor placement for initial scanning require additional information to provide collision-free positioning.

To conclude this chapter and observations contained within it, following statements can be formulated:

- to allow for automatic, high-resolution 3D shape digitization of objects without their CAD models, two stage process should be performed,
- in the first stage, initial 3D model should be obtained using low quality sensor of large working volume and efficient NBV algorithm,
- in the second stage, high-resolution measurements should be made. Set of sensor poses should be calculated using initial model as existing computer model.

4. Automated, high resolution 3D shape digitization system

Automated 3D digitization system is a complex device composed of many subsystems, both hardware and software. The most important ones are:

- 3D measurement head.
- Positioning system.
- Software with modules for calculating:
    - Set of sensor's positions required to digitize the surface of the object.
    - Collision-free trajectories of sensor's movement between such positions.
    - Directional measurements' position and orientation in global coordinate system of 3D model.
    - The noise and other measurement errors which should be removed from the data.
    - Any operations in processing chain leading to the final 3D model format (for example data simplification, triangulation etc.).
- Hardware collision-detection module.

In the course of author's work on the problem of automated, high resolution digitization of unknown objects, he was a member of a team which developed and built such system for Museum of King Jan III's Palace in Wilanów 3D Documentation Laboratory, Warsaw (Sitnik & Karaszewski, 2010). Few different versions of the system, named 3DMADMAC|AUTOMATED are used in the Laboratory of 3D digitization in this institution. Basing on those systems, the author has constructed his own test station which was used for further development and testing of inverse kinematics (IK), collision – avoidance methods as well as NBV algorithms.

The main concepts of 3DMADMAC|AUTOMATED system are presented in the following subchapter with emphasis put on the original Next Best View algorithm. It is presented along with the discussion about its advantages and disadvantages. The next subchapter in this section contains description of new version of digitization system HD3D|AUTO, developed to overcome 3DMADMAC|AUTOMATED limitations. Modifications were made to almost all subsystems – measurement head, positioning system control algorithms, collision detection and avoidance and finally, methods for calculating measurement head positions in fully automated digitization process.

4.1 3DMADMAC|AUTOMATED

The automated digitization system designed for professional cultural heritage documentation should be able to provide high resolution 3D models (at least 2500 points per mm^2) containing geometry and color information (MacDonald, 2010), (Bunsch, 2010), (Bunsch, et al., 2011). Used sensor should be also safe for works of art therefore laser based sensors were excluded (Bunsch, 2010). For those reasons, structured light scanner had been chosen as 3D scanner. In the first prototype of the station, named 3DMADMAC|AUTOMATED, it was a custom-built device, composed of high quality High Definition DLP projector and one DSLR camera (Canon D50). Using macro lenses, this system was capable of obtaining even 10000 points per mm^2 measurements (Sładek, et al., 2011) but usually was adjusted to 2500 points per mm^2. In such configuration, working volume was about 50 mm x 50 mm x 20 mm. Due to the use of DSLR camera, color reproduction was very good. Comparison of measurement results for different spatial scanner resolutions are presented in Figure 41.
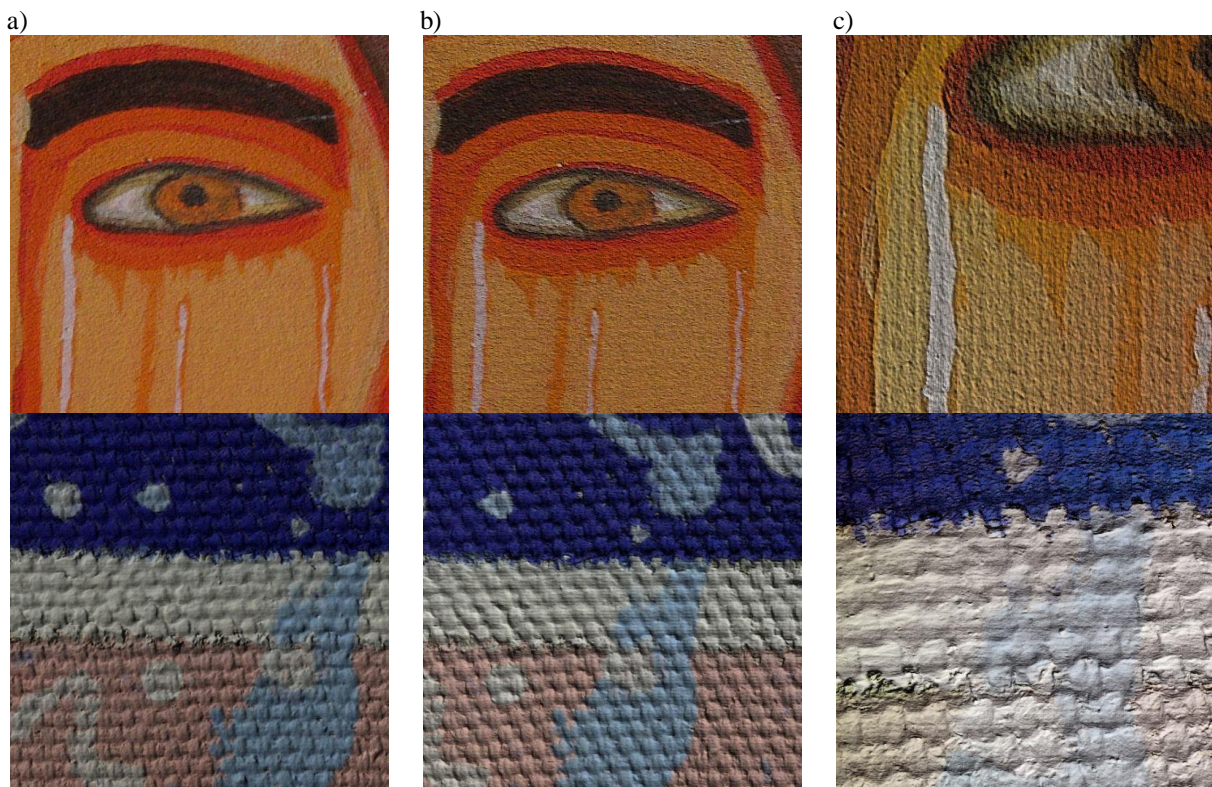
Figure 41. Comparison of surface details at: a) 100, b) 2500, c) 10000 points per mm^2.

To provide flexible positioning, robotic arm (Fanuc LRMate 200i (Fanuc Ltd., 2016)) was chosen as a main positioner for 3D sensor. Its operating range was however insufficient to allow for scanning typical objects from all directions and because of this, additional rotary stage was introduced. In this configuration, objects were placed on the stage while sensor was

fixed to robot wrist. To extend operating range, the robot itself was fixed to vertically moveable column (Figure 42). In this configuration, the system was capable of measuring objects of 1.2 m. diameter and 2.5 m. height.

The system was designed to be universal – measurement head could be exchanged to any 3D full-field measuring device, Fanuc robot to any other robot or even a set of rotational and translational nodes. This feature was possible because I had implemented my own Inverse Kinematics (IK) module (described in further section of this chapter), based on Cyclic Coordinate Descent paradigm (Sciavicco & Siciliano, 1996). With control over kinematics of positioners, the collision detection was possible at the stage of analyzing movement. Typical robotic arms usually do not have software collision detection module; they only react when physical collision occurs (servomotor current surge is detected). This is clearly not acceptable in a system used for cultural heritage documentation.

Few versions of the prototype system were constructed – usually in robot-table configuration (without vertical column). Those systems (Figure 44) were built around small robot arms (Fanuc LRMate 200i and Kawasaki RS005L (Kawasaki Robotics, 2016)), using rotary stage controlled by General Electric PacRX3i controller (General Electric, 2016) or small stages manufactured by Labster (Labster, 2016). Typically, they were used for digitization of small or medium sized works of arts: biscuit figurines, ancient Greek vases and other objects (Figure 43).

a)

b)
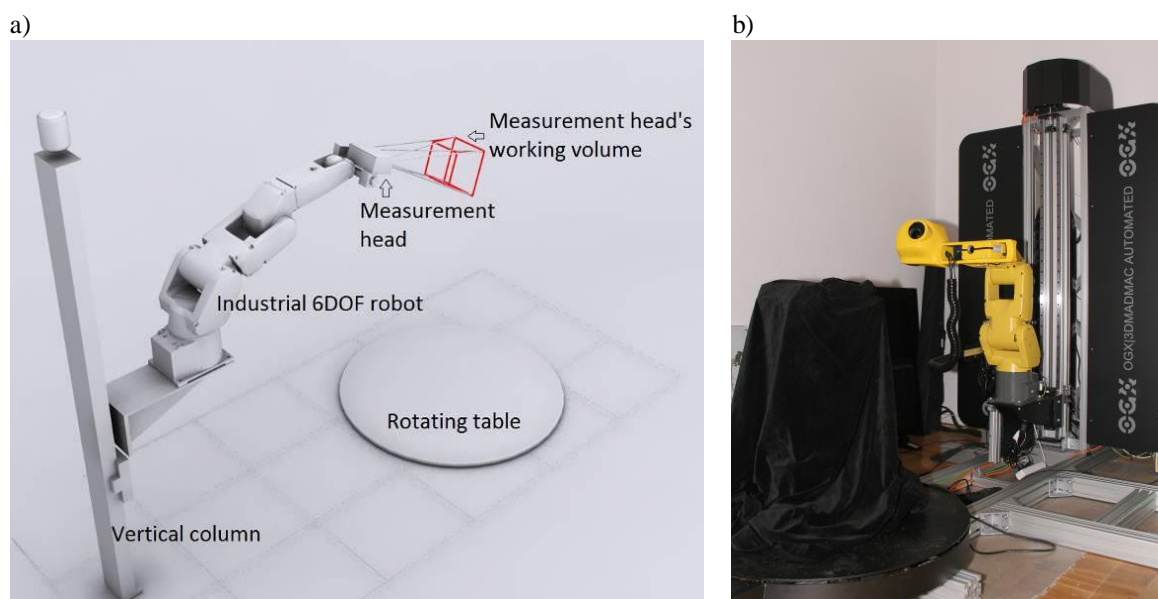
Figure 42. 3DMADMAC/AUTOMATED system: a) model, b) exemplary realization.
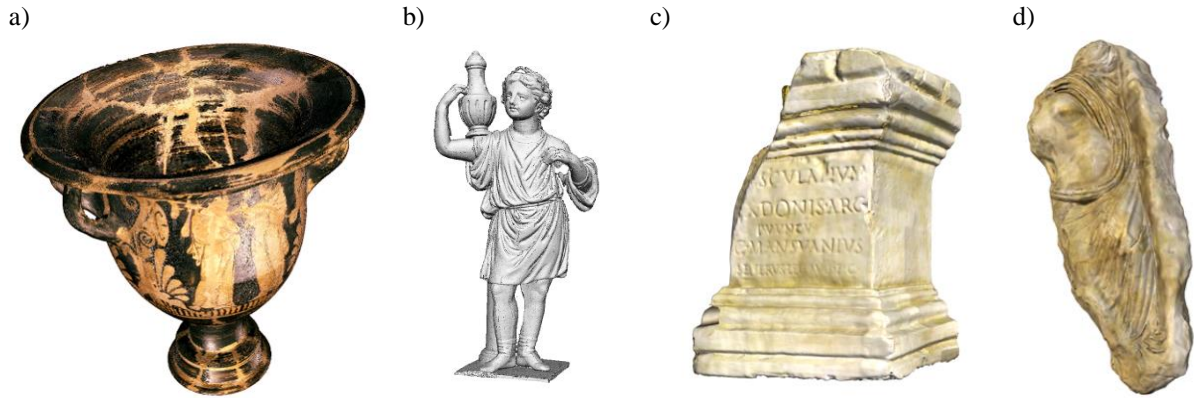
Figure 43. Typical objects digitized with 3DMADMAC}AUTOMATED system: a) greek vase (red-headed hydria from Museum of King Jan III's Palace in Wilanów); b) biscuit; c) Plaster-of-Paris copy of roman votive altar with latin inscription, dedicated to Esculapius and Hygieia, dated at 2nd century AD; d) Plaster-of-Paris copy of white marble statue decorating antique building in Novae, Lower Moesia (2nd century AD).
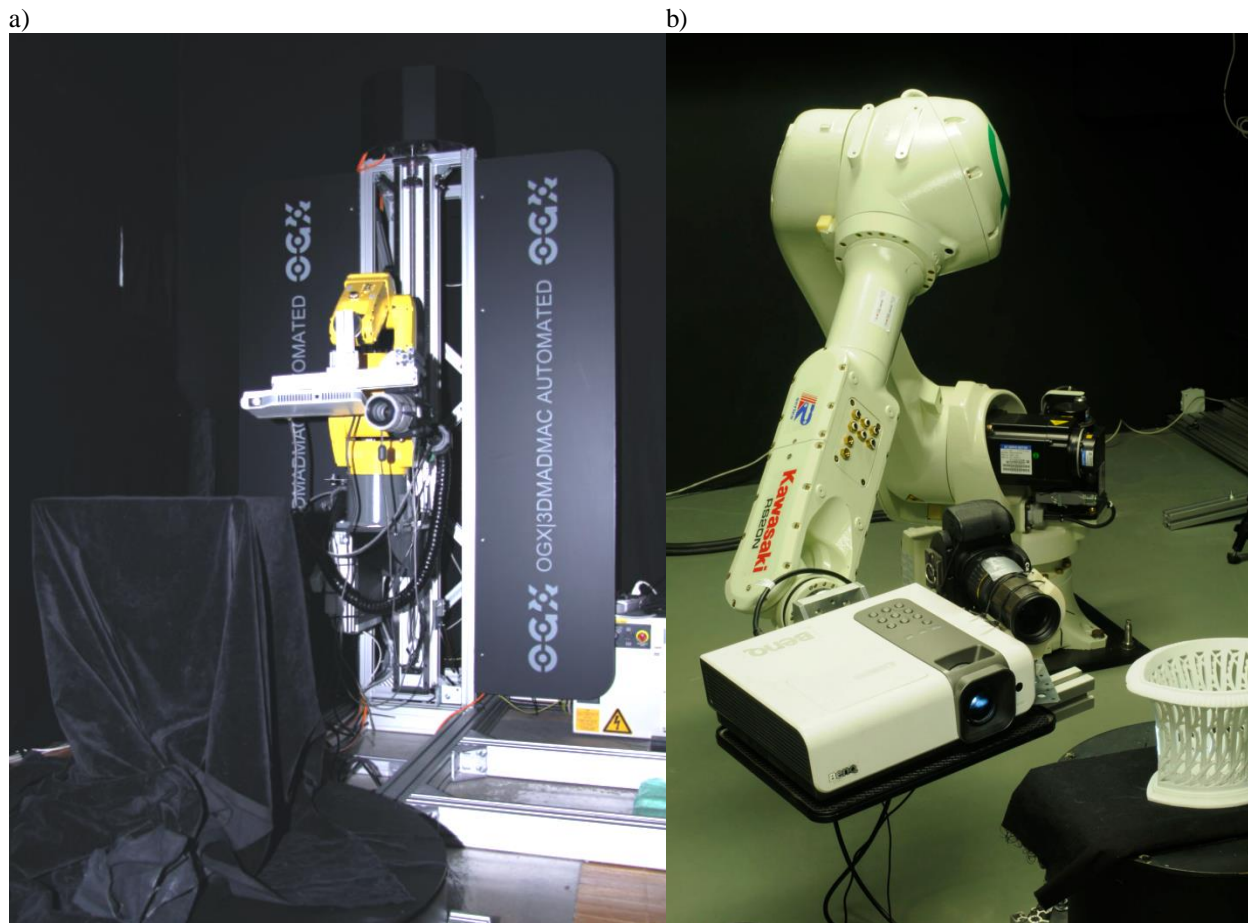
c)
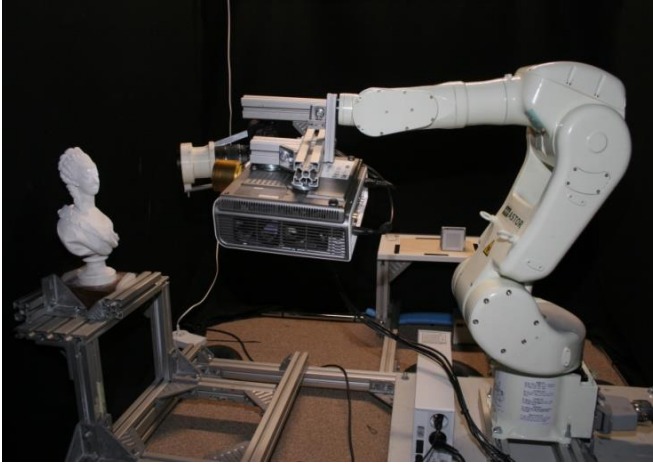
d)

Figure 44. Exemplary configurations of 3DMADMAC/AUTOMATED system.

For pilot project of digitization of outdoor placed objects (garden vases - Figure 45), another version of the system was constructed. It used large robot arm, Kawasaki RS020 which was placed on manually moveable platform. Each vase was semi-automatically scanned from four positions of this platform. The vase, robot and operator's control desk was placed in dark tent with climate control (humidity and temperature) (Karaszewski, et al., 2013).

a)

b)

c)
d)

Figure 45. Garden vases scanning: a) vase in the garden of Wilanow Museum; b) tent used to provide darkness and climate control; c) vase inside the tent; d) system during measurement.

Similar setup, but with small Fanuc LRMate 200i robot was used in pilot project of 3D digitization of paintings (Figure 46). Rotating table was not needed for this project as robot operating range was enough to scan whole surface of painting. In this case, 3D sensor movements were simple – due to the nature of the painting only planar movement was required without any changes of scanner orientation. The results of this pilot project allowed to build specialized system for paintings documentation – SAPO (Figure 46d) (Karaszewski, et al., 2013).

Recently, the same Fanuc robot arm placed on the vertically moving column was used in Museum of King Jan III's Palace in Wilanów for digitization of King's Chinese Room (Figure 47) (Muzeum Pałacu Króla Jana III w Wilanowie, 2016). During this project, over 100 m^2 of walls, ceiling and decorations of this famous lacquered room were digitized with 100 points / mm^2 resolution. For this purpose, robot and column were manually moved around the room; for each position, all measurements were collected automatically (Figure 47c).

All systems which were presented above, utilize the same set of software modules:

- Calibration of coordinate systems,
- Inverse kinematics,
- Trajectory calculation with collision detection,
- Next Best View.

The details of these modules are given in the next section of this document.

a) b)

c)

3D model (fragment) Detail – ripple of paint Surface structure

Photo Height map Local curvature map Height map of surface structure

Vincent's Chair
with His Pipe,
National Gallery,
London

Histogram of height map Histogram of curvature map Histogram of local height map
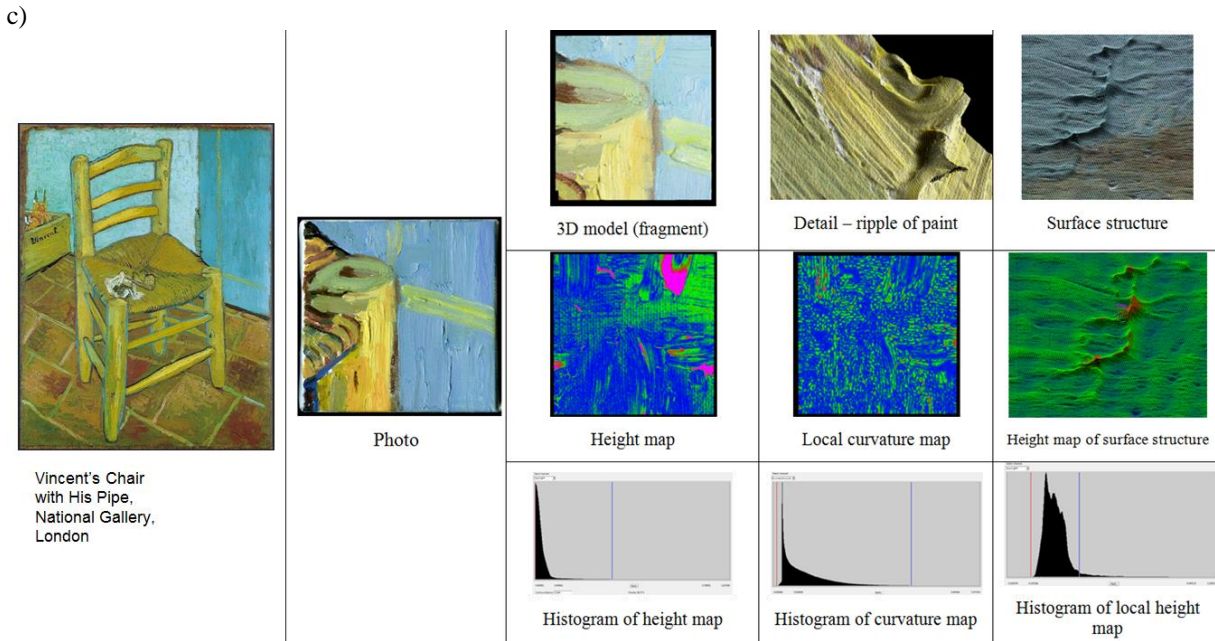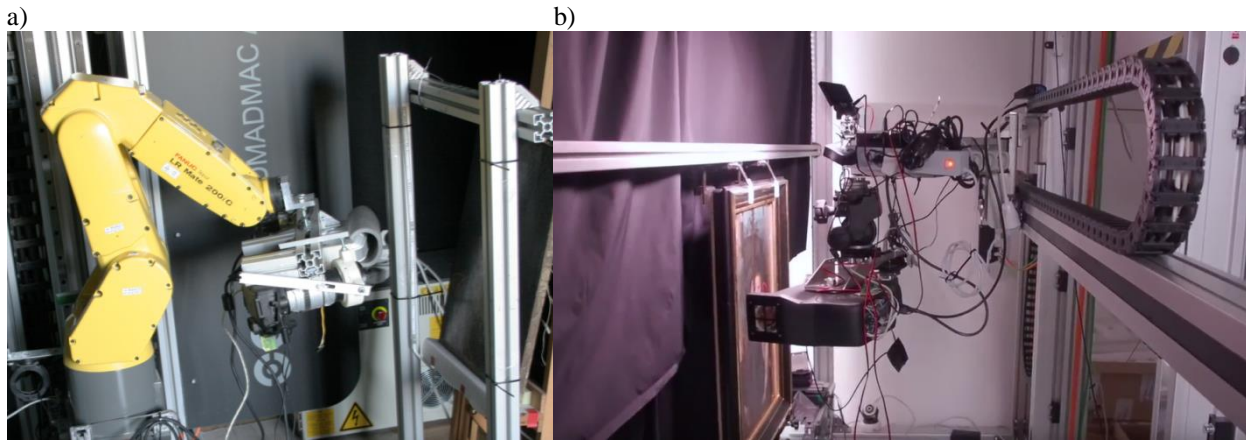
Figure 46. Painting scanning: a) robot-based system with painting, b) SAPO system, c) exemplary painting (copy of Van Gogh painting): photo, 3D model, 3D details.

a)
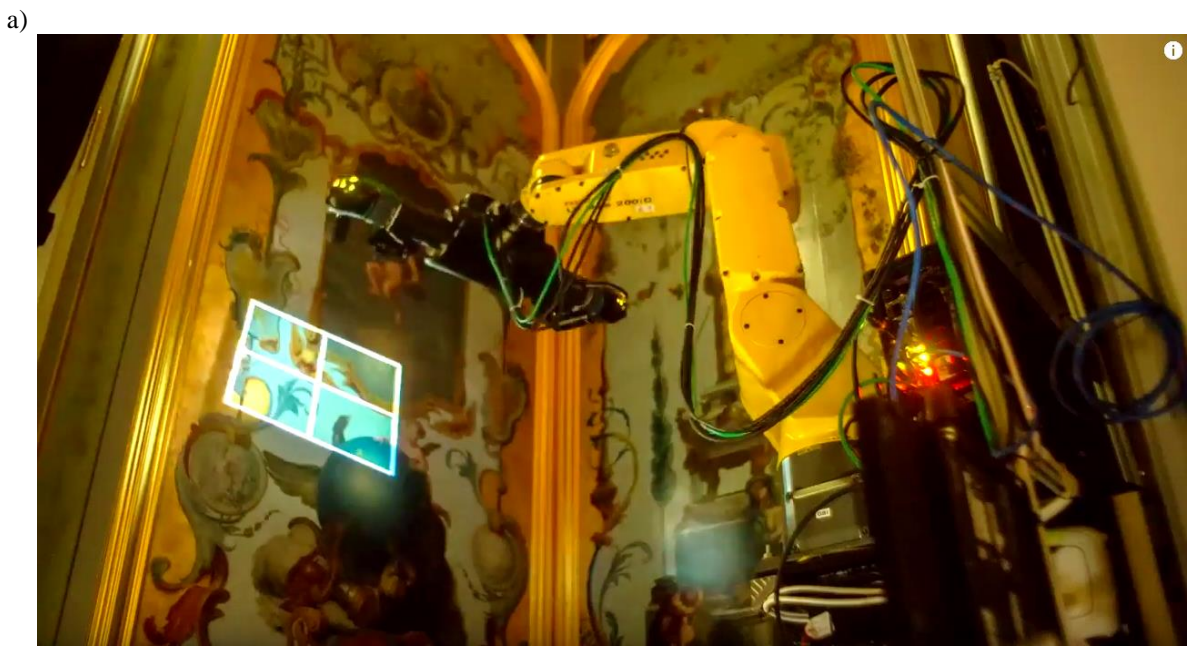
b)

c)

Figure 47. Chinese Room scanning: a) measurement system during scanning, b) fragment of 3D model, c) comparison between models from 2009 (before restoration) and 2015 (after restoration). Images source: Museum of King Jan III's Palace in Wilanów YouTube channel.

4.1.1 Calibration of coordinate systems

Typical 3D sensors return measurement data in fixed coordinate system. If such sensor is put on robot arm (or any other positioning system) or scanner is stationary but object is moved (for example on rotary stage), without knowing the transformation between sensor and positioners coordinate systems it is impossible to automatically build 3D model from directional measurements. Similarly, it is not possible to put sensor in vantage points calculated on the basis of partial 3D model. Therefore, it is crucial to identify transformation matrices which join all coordinate systems present in automated digitization station.

In 3DMADMAC|AUTOMATED systems, relation between two coordinate systems is found by comparing transformations given in those systems. For example, for scanner – robot arm relation, four pairs of transformations are required, obtained from five measurements of

calibration unit taken in different scanner positions (transformations are relative to the first measurement). In case of robot coordinate system, transformations are calculated from position and orientation of end effector. For 3D sensor, transformations are calculated during integration of directional measurements (Figure 48).

a)   b)   c)
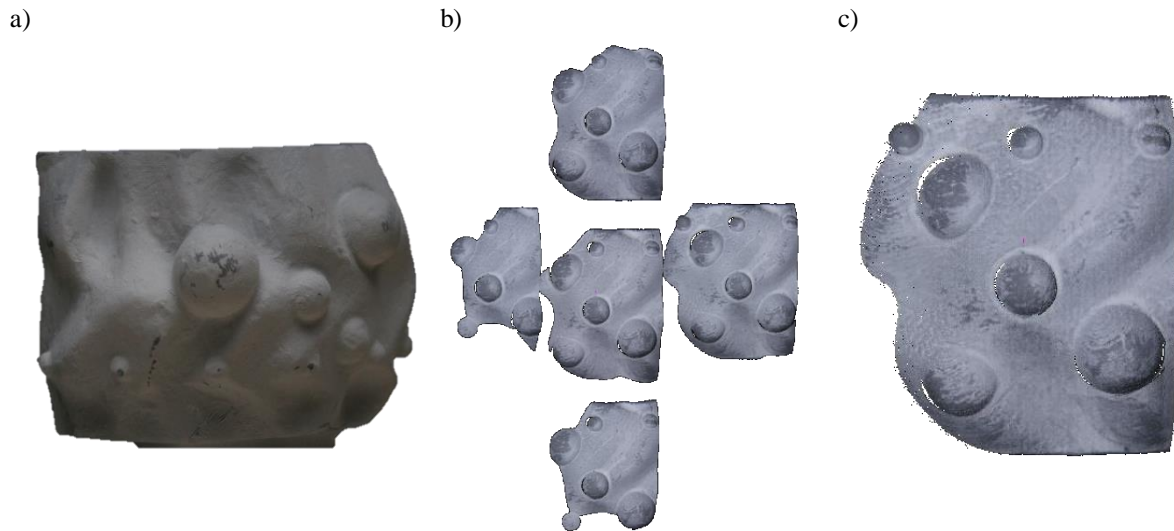
Figure 48. Five directional measurements taken from different vantage points: a) calibration unit, b) raw measurements, c) measurements after integration.

This schematic is repeated for all other positioners used in the system. Depending on the number of degrees of freedom and type (rotational, translational) of positioner, different number of directional measurements is required, however usually more than minimal number is taken to provide data redundancy which improves precision.

The crucial stage of above described process is integration of directional measurements. The more precise integration, the higher quality calibration is obtained. To achieve automatic, precise integration of measurements, special measurement object is used (Figure 48a). It was computer-modelled and 3D printed. Its surface contains high number of unique shaped features which can be automatically detected and used by integration algorithms. Nevertheless, due to measurement errors, nature of fitting algorithms etc. the integration is never ideal. Combined with limited precision of encoders used in positioners, these problems reduce accuracy of recovered transformation between coordinate systems.

Coordinate systems calibration has to be performed after each calibration of measurement head or any reconfiguration of the positioning system.

4.1.2   Inverse Kinematics

Assumptions which were accepted at the stage of 3DMADMAC|AUTOMATED system development, namely the universality of positioning system, collision avoidance etc. led to the necessity of implementing inverse kinematics algorithm. Inverse kinematics is a term used for a procedure of finding configuration of joints in multi-joint positioning system which leads to required position of this system end effector. This topic was widely researched in the years of rapid robotic systems development and numerous solutions were introduced. In 3DMADMAC|AUTOMATED system, two simple algorithms were implemented – one based on Newton optimization method (Bertsekas, 1999), the other – on Cyclic Coordinate Descent paradigm (CCDp) (Sciavicco & Siciliano, 1996). During tests, CCDp method proved to be much more effective as Newton optimization sometimes tended to converge to local minima of optimization function thus yielding incorrect kinematic chain configurations.

4.1.3   Trajectory calculation with collision detection

Trajectory calculation in 3DMADMAC|AUTOMATED was at first based on method in which the path between starting and ending point was divided into linear segments shot through empty voxels represented as connected graph (Figure 49). Path was selected using Dijkstra algorithm (Dijkstra, 1959). Unfortunately, this method proved to be ineffective and was discarded due to the requirement of linear movements of robot end-effector between subsequent nodes. Due to implementation of robot control algorithms, such movements were often impossible to perform (singularity points, joint rotation limits) (Dasgupta & Mruthyunjaya, 1998). This problem was present in Fanuc robots as well as Kawasaki ones. For this reason, the straight-line-segments trajectories method was discarded.
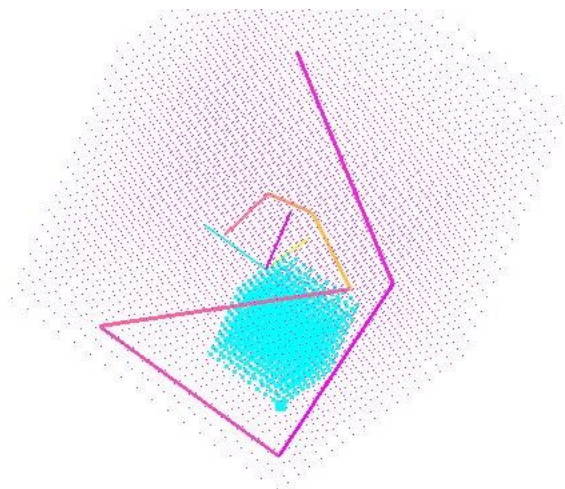
Figure 49. Visualization of positioning path coming through empty voxels (violet) omitting collision areas (blue).

87

In the second method, trajectory was simply an effect of simultaneous movement of all joints of positioning system. Such movement is easy to obtain when robot arm is controlled in joint-interpolated mode. For each joint, angular speed of rotation is calculated to provide required angular displacement in the same time. Using this assumption, it is easy to calculate the position of end effector (and 3D sensor) as well as each robot segment in any moment of positioning (Figure 50). Therefore, it is relatively easy to divide movement to small parts and check for collisions between 3D sensor, positioning system, object and environment.
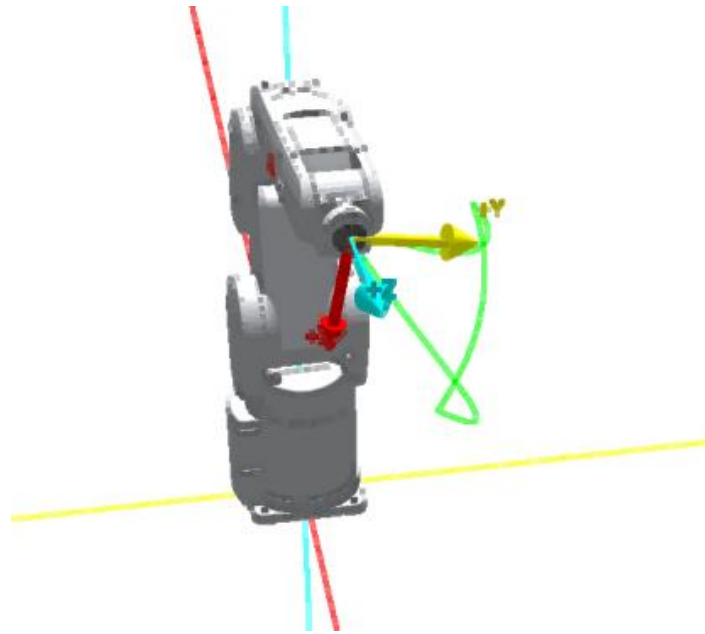
Figure 50. Exemplary trajectory of robot end effector (green) during movement between three positions defined in joint coordinates.

Collision detection is based on the analysis of triangle meshes which represent different elements of digitization station: environment (floor, walls, other not movable elements), positioning system (all segments), measurement head. For this purpose, those elements have to be modelled, but it is enough to represent them with approximate mesh built for example from bounding boxes (Figure 51). Similarly, object has to be modelled also. In this case, triangle mesh is built basing on voxels (marked as used and unknown) representing working space of the system.

For each trajectory, collision, position and orientation of meshes representing positioning system and measurement head is updated to reflect their displacement in each trajectory segment. Collisions are detected using ColDet 3D library (Photoneffect, 2016). If any collision is detected at any section of trajectory, this information is returned to the controlling module.
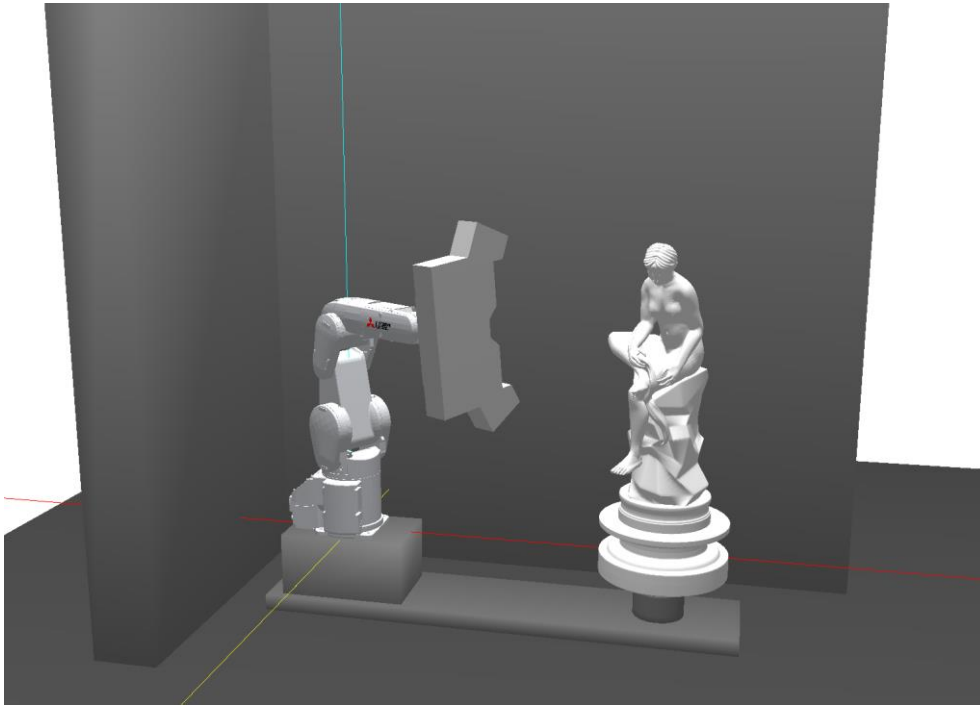
Figure 51. Exemplary simplified model of system environment, robot with scanner and object placed on rotating table.

4.1.4 Next Best View algorithm

3DMADMAC|AUTOMATED system is designed to obtain 3D models of unknown (i.e. having no digital model) objects. For this reason, digitization process starts with operator defining size of the object. To simplify this necessity, it is assumed that object fits into cylinder of given radius and height, centered on the rotating stage. At this moment, automated digitization process begins.

Implemented Next Best View algorithm can be divided into three stages: the first one is the discovery of unknown measurement space (in search of object surface), the second one – main digitization and the final stage – filling discontinuities. In following subsections, all three stages are presented.

4.1.4.1 Search for object surface

Surface of cylinder encompassing the object my lie far away from objects surface (because of the object shape - Figure 52 or inaccuracy of operator-entered parameters - Figure 53). Therefore, it is necessary for the system to locate any part of the surface starting from surface of the cylinder and moving closer to its symmetry axis. To locate surface, a scan is performed. If there are no points present in the data (after noise filtering), the part of system volume is

considered as empty. In case when point groups appear in the scan result, it is assumed that object is located.
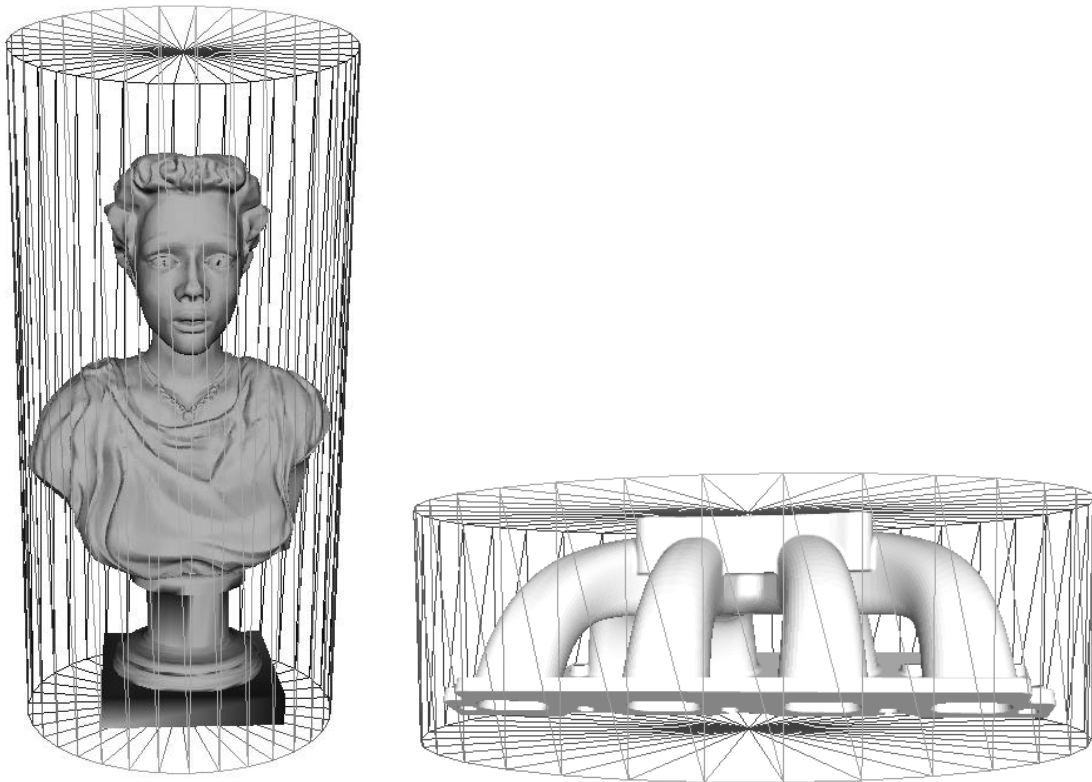
Figure 52. Different shaped objects in their encompassing cylinders.

a)   b)   c)
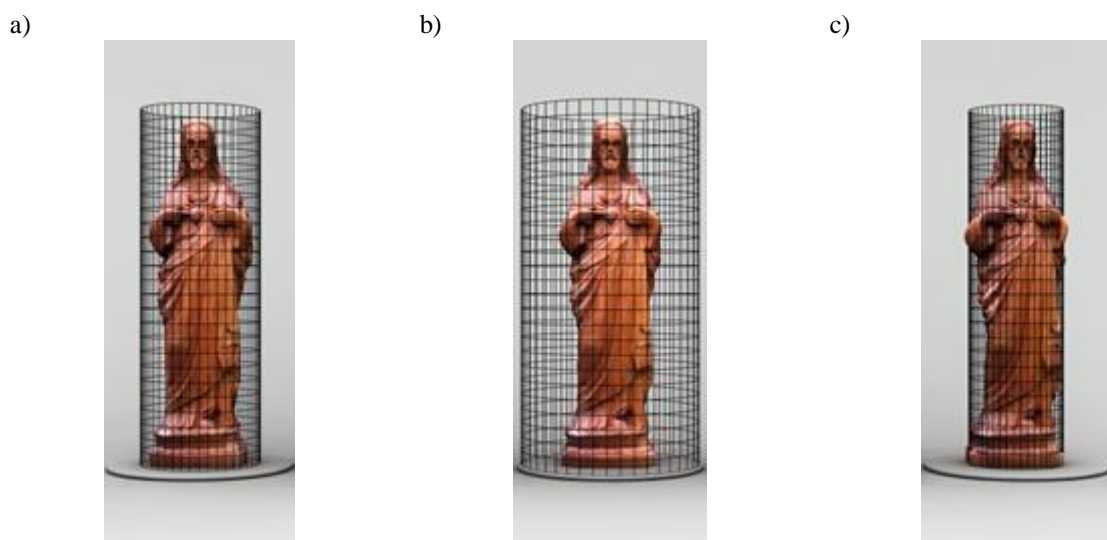
Figure 53. Virtual cylinder representing the measurement volume: a) correct, b) of too big radius, c) of too small radius.

The surface localization process is similar to Papadopoulos-Orfanos digitization by carving (Papadopoulos-Orfanos & Schmitt, 1997). In this case, the scanner aims at the surface of encompassing cylinder, at half of its height (Figure 54a). If no surface is located, it is moved

in four directions (each time scan is performed), like illustrated in Figure 54b. If still no surface is located, scanning head is moved towards encompassing cylinder axis (Figure 54c). This process is repeated until surface is located (Figure 54d).

a)

b)

c)

d)
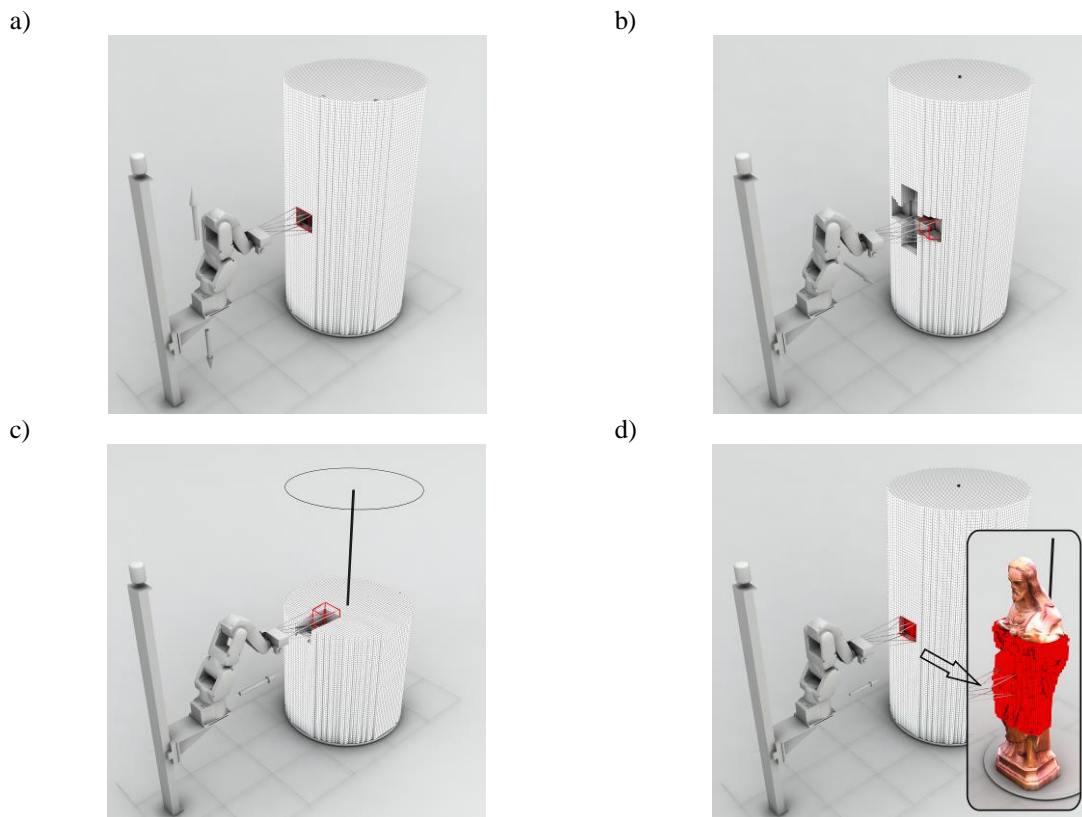
Figure 54. Localization of object in encompassing cylinder: a) first scan (empty measurement); b) four scans in up/down/left/right directions (empty measurements); c) next scan, closer to cylinder axis; d) part of surface localized.

When any part of object surface is found, the discovery algorithm terminates and main digitization stage begins.

4.1.4.2 Main digitization

The Next Best View algorithm implemented in the 3DMADMAC|AUTOMATED system is based on the assumption that by aiming the scanner at the boundary of partially obtained 3D model, its further parts can be measured. This assumption is fulfilled best when small gradients of shape are present. In fact, those gradients do not necessarily be close to zero, it is enough if the slope of the surface in the place of partial model boundary is not larger than scanner observation angle. However, sharp edges and corners are problematic and may not be measured correctly at this stage of the process.

As the NBV algorithm is based on the analysis of the partially obtained model (which is supplemented with each directional measurement), it is run after every successful scan (i.e.

the one which contains new data). To shorten the time of analysis, each time, the partial digital model is homogenously simplified and all further calculations are performed on its simplified representation. Radius of filtering (R_{simpl}) is described by Equation (1). Other parameters calculated in this procedure are minimal (R_{min}) and maximal (R_{max}) radiuses used in selection of boundary points. Scaling factors in these equations were determined experimentally to reach a compromise between time of calculations and scanning quality.

$$R_{simpl} = \frac{D_{op\,max}}{100}, \ R_{min} = \frac{D_{op\,max}}{25}, \ R_{max} = \frac{D_{op\,max}}{10} \tag{1}$$

Where D_{opmax} – maximum dimension of scanning head's measurement volume.

Knowing average distance between points in simplified model, number of points found in spherical neighborhood of radius R_{min} (C_{min}) and R_{max} (C_{max}) can be described by Equation (2).

$$C_{min} = \pi \left(\frac{R_{min}}{R_{simpl}} \right)^2 = 16\pi, \ C_{max} = \pi \left(\frac{R_{max}}{R_{simpl}} \right)^2 = 100\pi \tag{2}$$

C_{min} and C_{max} parameters do not depend on any parameter of the system (distance between points, working volume etc.) so they do not change regardless of the 3D sensor used. Radiuses of neighborhoods for point selection are bound to the D_{opmax} parameter which reflects sensor working volume. This means that they are adjusted automatically with the change of 3D sensor.

After calculation of control parameters, the set of proposed sensor positions in next measurement is calculated. This procedure starts with calculation of number of points in neighborhoods of radius R_{min} and R_{max}, yielding c_{pmin} and c_{pmax} parameters for every point in point cloud. Points with values of those parameters fulfilling Equation (3) are marked for further processing. They represent part of the model which is close to its boundary (Figure 55). Points on the actual boundary are ignored because usually they are measured with lower accuracy (Sitnik & Karaszewski, 2010).

$$\left(c_{p\,min} > \frac{1}{2} C_{min} \right) \text{ and } \left(c_{p\,max} < \frac{3}{4} C_{max} \right) \tag{3}$$
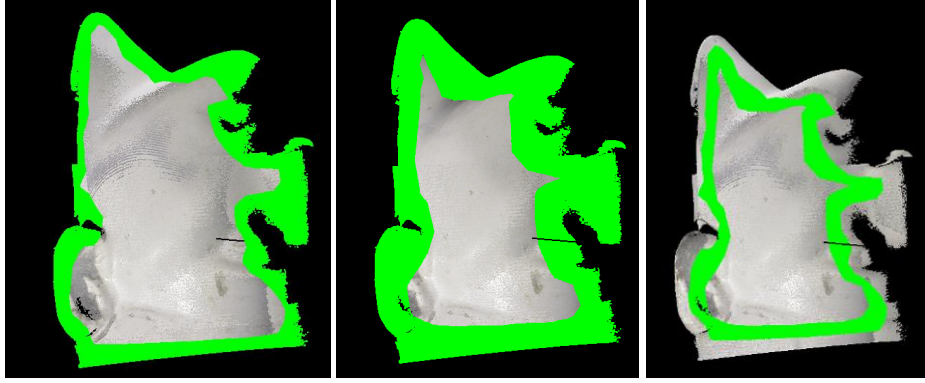
Figure 55. Border points selected with: a) R_{min}, b) R_{max}, c) R_{max}-R_{min}.

For each of marked points, best fit plane is calculated. Its normal vector, oriented towards the object is the viewing vector for measurement head. The point itself is a center of head working volume. Such view candidate, defined by point and vector is remembered if its weight factor (w) is big enough. This weight factor defines how different is the proposed observation vector (n_{new}) from looking direction used in current measurement ($n_{current}$) – Equation (4).

$$w = \sin\left(\angle(n_{current}, n_{new})\right) \tag{4}$$

After this procedure, a set of proposed sensor poses is calculated. It is then filtered according to the distance between centers of scanner working volume for each pose. The remaining pose set is sent to Inverse Kinematics module. Pose, which is reachable and have largest weight (w) value is selected as vantage point for sensor in next measurement.

The NBV algorithm continues until all sparse regions are congested or no suggested view can be reached by the positioning system.

Because of the C_{min} and C_{max} thresholds used in Equation (3), 3D model obtained with above described algorithm may contain discontinuities of size smaller than 10% of D_{opmax}. For such places, borders are not detected and therefore no sensor pose is calculated to fill them (Figure 56). Of course, during digitization process they can be filled by other, nearby directed scans, nevertheless some holes in the model remain. For this reason, another stage of NBV algorithm is required, namely filling of discontinuities.

a)   b)
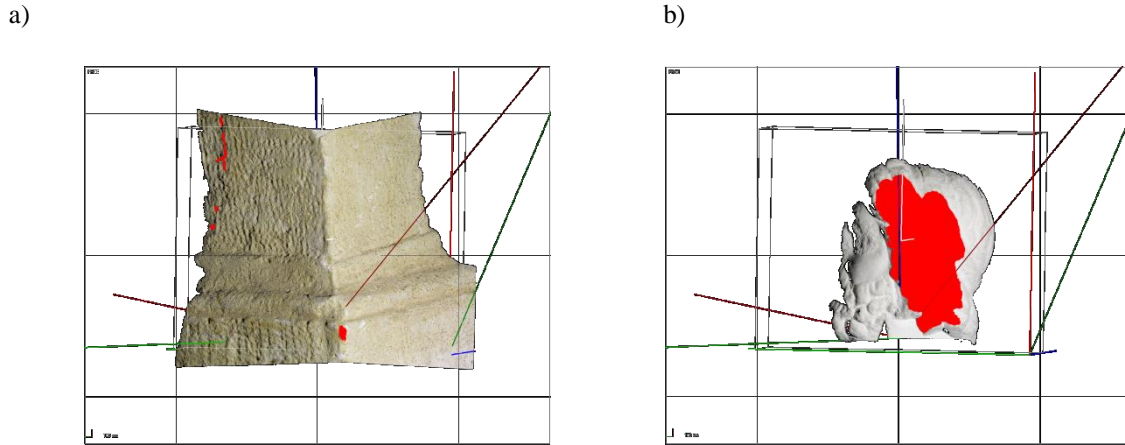
Figure 56. Discontinuities detected in the model; a) smaller than 10% of measurement head working volume (acceptable) b) larger than 10 %, – not acceptable.

4.1.4.3 Filling discontinuities

Procedure aimed at filling holes detected in 3D model is run at the end of the digitization process. Its main part is the detection of areas with low point density which appear in places where discontinuities are present. For this purpose, for each point of the 3D model, number of points (C_n) in its neighborhood is calculated. Radius of neighborhood (R_n) is crucial in this operation; in the course of system development it was found that the good compromise between time of calculations and obtained results is achieved for radius value equal to three times the average distance between points (R_{av}). If C_n value is smaller than C_{thresh}, (Equation (5)) analyzed point neighborhood is assumed to be measured correctly, otherwise it is marked as potential discontinuity.

$$C_{thresh} = \left(\frac{\pi \cdot R_n}{\pi \cdot R_{av}}\right)^2 = \frac{9R_{av}}{R_{av}} = 9 \qquad (5)$$

Figure 57a illustrates local point density for exemplary object. Areas marked red have density higher than C_{thresh}. Lower density is marked in other colors. After binarization (Figure 57b), areas marked with blue color are grouped (analysis is performed within R_{min} neighborhood) according to distance. Six largest groups are selected as targets for 3D sensor during measurement (areas marked green in Figure 57c will be filled during next measurements). If new measurements provide additional information, it is added to 3D model. Otherwise, areas which were targets for 3D sensor and were not filled with new data are marked as impossible to measure. The analysis and measurements are performed until discontinuities are detected in parts of the model which are not marked as unmeasurable.

94

a)   b)   c)
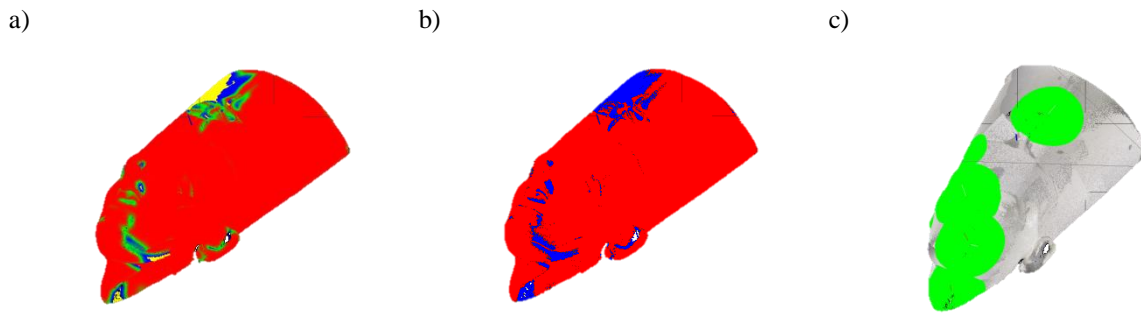
Figure 57. Areas of low density: a) local point count; b) local point count after binarization c) areas which will be measured again.

4.1.5   Discussion

3DMADMAC|AUTOMATED digitization system was developed during project realized in cooperation with Museum of King Jan III's Palace in Wilanów 3D Documentation Laboratory. In the prototype system, all modules (excluding measurement head) were designed from the beginning. As such, they are burdened by some disadvantages which were identified during digitization projects run by Museum of King Jan III's Palace in Wilanów 3D Documentation Laboratory. Those problems usually lead to obtaining 3D models of not satisfying quality (low surface coverage) after time-consuming digitization. The most important problems of 3DMADMAC|AUTOMATED system are:

1. Very long digitization time.
2. Low surface coverage for complicated objects, especially with self-occlusions and cavities.
3. Low quality of initial measurements fitting.
4. Difficult calibration of coordinate systems.
5. Fitting error propagation.

Ad 1. The suboptimal digitization time is caused by two deficiencies of used NBV algorithm. The first one is the necessary to scan some portion of system working volume for collision detection purposes. As scans are performed using high resolution measurement head (of small working volume), their number is significant. The second problem is caused by simplicity of measurement plan generation – NBV algorithm does not analyze potential self-occlusions and for complicated objects generates sensor poses which do not add much data to the model (due to occlusions). This way, some discontinuities are measured several times until they are marked as unmeasurable.

Ad 2. Low surface coverage obtained for complicated objects is also a result of simplicity of NBV algorithm. One can observe that it generates proposed sensor poses which do not provide data due to occlusions. In many cases, slight modification of the observation angle would allow to reduce or mitigate occlusions. Additionally, the NBV calculations which are based on fitting surface to the edge of the current model are not efficient when digitized object has large shape gradients. Sensor poses generated for such places usually do not allow for obtaining good datasets as they are calculated basing on wrong surface trend prediction.

Ad 3. Low quality of initial measurement fitting is a problem caused by few factors. One of them is a limited accuracy of positioning systems and it cannot be eliminated without using, for example, external tracking system for measurement head localization. This factor is related to used hardware, its stiffness and general quality and results in discrepancy between reported and actual positions of positioning devices. Using imprecise information, position of 3D sensor during measurement is calculated with some error, thus initial fitting of directional data is burdened by error. Another factor, contributing to initial fitting quality is the accuracy of calculations of relations between coordinate systems (of scanner and positioning devices). Many tests performed by specialists from Laboratory of 3D documentation confirmed that the procedure of calibration is the main cause of low quality initial integration. In extreme situations, where measurement head weight was comparable with maximum load of used robot arm, the initial integration was so poor, that fine registration with Iterative closest point algorithm could not be used.

Ad 4. Calibration method, implemented in 3DMADMAC|AUTOMATED system turned out to be very sensitive to the quality of calibration measurements integration. This led to the construction of special calibration body with unique geometrical features. Nevertheless, even using this unit, the results of calculations were unstable. It was hard to define a procedure which led to high quality calibration with high level of certainty.

Ad 5. Regardless of quality of initial measurement fitting (as long as it is good enough to allow for ICP application), after fine registration stage, some fitting error between subsequent measurements remain. This is caused by ICP iterative nature, inaccuracy of 3D sensor etc. If 3D model is built from multiple directional measurements, this error propagates which leads to the deformation of obtained model. This problem is very hard to mitigate at data processing stage as there is no additional information about the shape of scanned object. Some methods for correcting the final model have been developed (Hołowko, et al., 2014), but generally

their efficiency depends on the characteristics of an object, thus their applicability in universal digitization system is discussable.

In spite of all above mentioned problem, 3DMADMAC|AUTOMATED system is used in Museum of King Jan III's Palace in Wilanów 3D Documentation Laboratory and up to now more than one hundred objects were digitized. Operators in the 3D Documentation Laboratory devised methods of conducting digitization projects which allow them to obtain very high quality, high resolution 3D models. However, those methods require significant operator contribution and what is more important – his or her experience. Therefore, system deficiencies have to be eliminated to allow for completely automated digitization.

4.2 HD3D|AUTO

The experience gained during development of 3DMADMAC|AUTOMATED systems and especially the feedback from their operators from Museum of King Jan III's Palace in Wilanów 3D Documentation Laboratory led author of this dissertation to the construction of next version of the system, possibly free of original system's disadvantages. The new system, named HD3D|AUTO includes modifications of all crucial modules of automated 3D digitization station and new, two-staged Next Best View algorithm. All modifications are presented in the following sections of this dissertation.

4.2.1   Measurement head

With the improvement and lower prices of professional cameras, DSLRs used in 3DMADMAC scanners were gradually replaced by CCD/CMOS cameras. This was caused mainly by disadvantages of DSLRs in measurement systems – slowness of image acquisition and transfer (via USB 2.0 interface), vibrations caused by opening and closing internal mirror and shutter, shutter wear (which causes uneven exposure times which result in measurement errors) and weight. Contrary, modern cameras provide images of quality similar to DSLR (especially with high-quality lenses), are fast and use efficient interfaces (USB 3.0 or gigabit Ethernet) (Basler, 2017), (IDS Imaging Development Systems GmbH, 2017). Moreover, they are significantly lighter, causing less wear in positioning system and reduces fitting errors caused by limited stiffness of robot. Also, small weight means that more than one detector can be used in systems built for small robots (which usually have maximum load of 5 kg (Kawasaki Robotics, 2016), (Fanuc Ltd., 2016)). Such measurement head has two CCD cameras placed symmetrically on both sides of projector (Figure 58). This configuration gives much flexibility – thanks to different observation angle, more surface can be captured from one scanner position, especially in situations when occlusions occur. Also, it is possible to calibrate cameras for different working volumes in effect providing two scanners in one chassis.

It is worth noting that HD3D|AUTO NBV method is developed with two 3D sensors of different working volumes in mind. It is still possible to use it without above described measurement head – classic, one-volume sensors can be used; they just have to be exchanged or readjusted between digitization stages.

Figure 58. Measurement head with two CCD cameras.

4.2.2 Calibration of coordinate systems

In the course of my work on automated digitization system, I have improved the coordinate system calibration method. New procedure uses special calibration unit composed of three spheres which are distinguishable by color (for scanners capable of capturing color information - Figure 59) or by radius. Size of the calibration unit is matched to working volume of used sensor. For each directional measurement, data is segmented into three groups representing spheres. For points in each group best-fit sphere equation is calculated. As a result, for each directional measurement, three points (centers of spheres) are returned. Transformations are calculated by finding relations between identical triangles (of each directional measurement). Results obtained with this procedure are significantly more precise due to high accuracy of calculating sphere centers (dataset used for such calculation contains from thousands to millions of points, depending on scanner resolution). Moreover, finding transformation between almost identical triangles is also very precise, simple to implement and fast to compute. Finally, new procedure is completely automatic. Overall, the improvement of calibration quality is at least fivefold, limited mainly by stiffness of positioners.
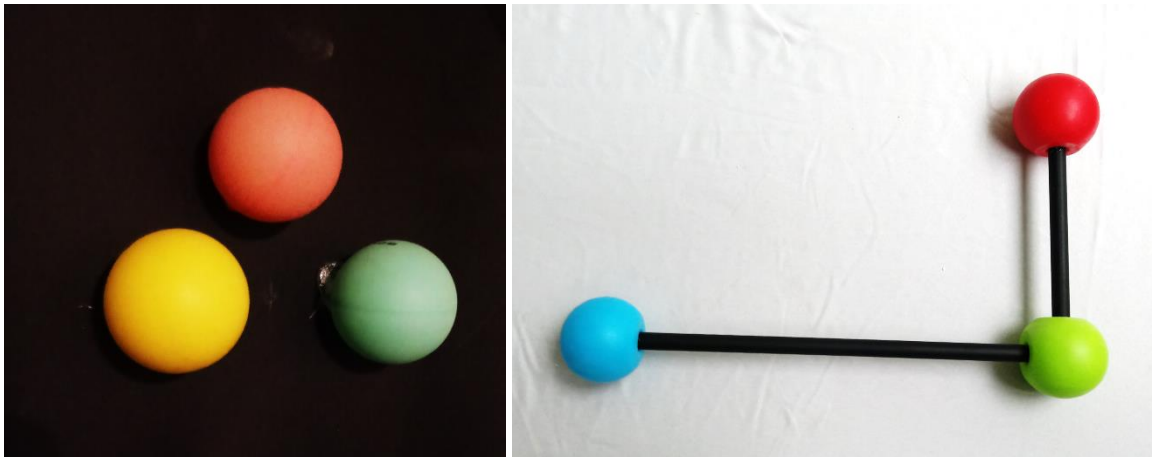
Figure 59. Calibration unit with three colored spheres: a) prototype, b) final version.

4.2.3 Inverse kinematics

Original inverse kinematics module was generalized as much as possible, allowing for unconstrained configuration of positioners and their kinematic chain. Therefore, all joints of the chain were treated evenly. After initial testing of 3DMADMAC|AUTOMATED prototype, the possibility of adding weights to each node was added, to make it possible to indicate joints which are more favorable (for example more precise or better calibrated) than others. During numerous digitization processes in Museum of King Jan III's Palace in Wilanów 3D Documentation Laboratory, three observations were made:

- Regardless of the weights given to joints, positioners configurations are sometimes strange, leading to complicated trajectories of 3D sensors which are collision-prone.

- For most objects, best configuration of positioners is a classic one, with object placed on rotary stage and 3D sensor fixed to robot arm.

- In robot-table configuration, sensor positions are often calculated on the both sides from table axis (Figure 60), which cause excessive robot movements with 3D sensor travelling close to scanned object.

The analysis of above presented observations led me to the significant modification of inverse kinematics module. This modification traded flexibility of kinematic chain configuration in exchange for better positioning of classic, robot-table setup. Namely, it is assumed that HD3D system contains rotating stage, on which object is placed. Table rotation is considered as main positioning operation, while robot arm is used only for small adjustments of scanner position. This is illustrated in Figure 61.

100
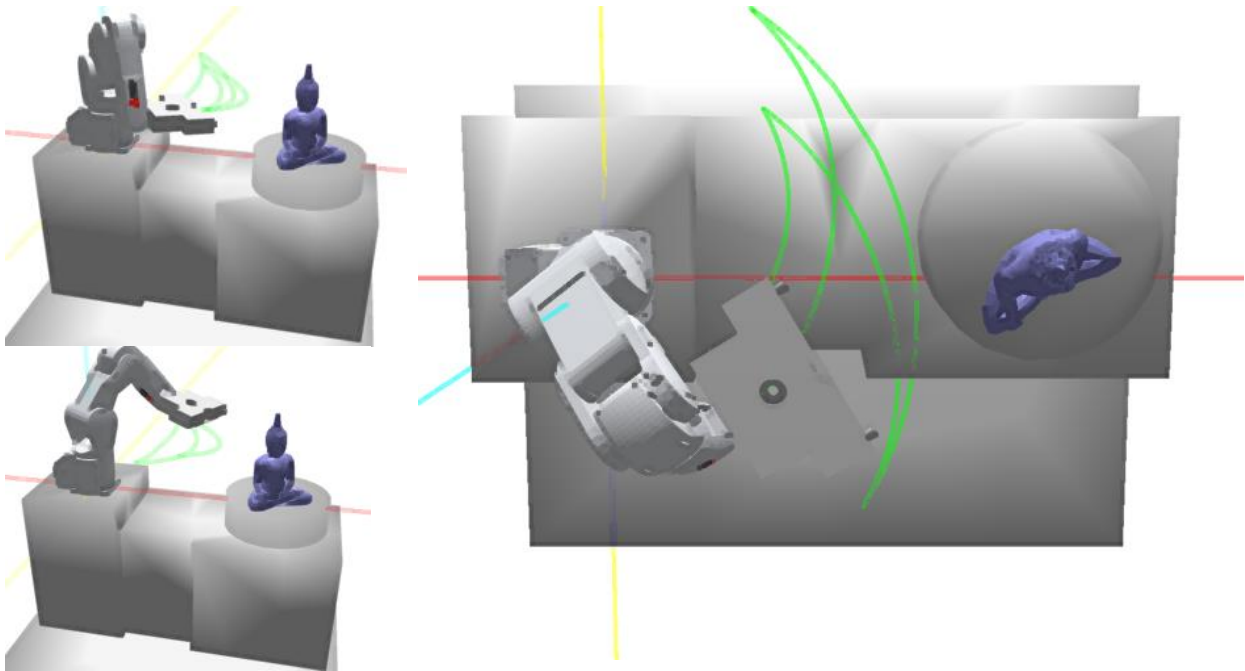
Figure 60. Excessive robot movements in the robot-table configuration of positioning system in 3DMADMAC/AUTOMATED station.
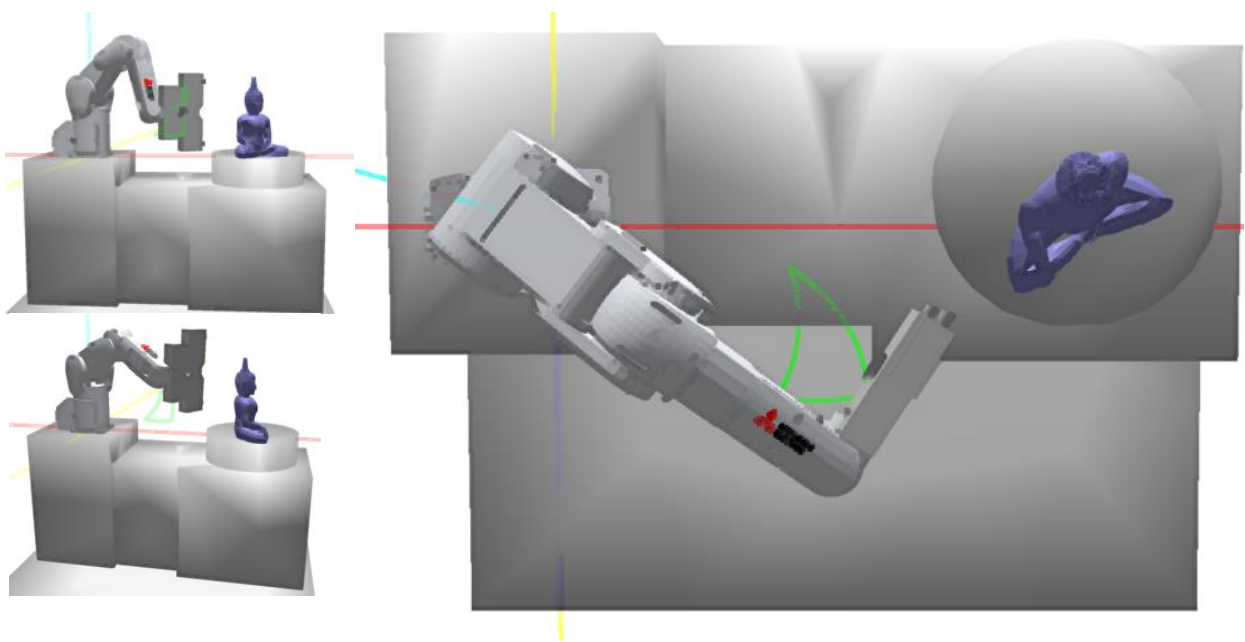
Figure 61. Robot movements in HD3D system (green path shows end-effector trajectory).

When new sensor pose is received by the module, calculations start with transformation of pose parameters (position - P, observation - O and rotation – R vectors) to coordinate system of kinematic chain. After this step, angle α between projection of vector O on table plane P_{table} and fixed observation vector O_{fixed} (lying on P_{table}) is calculated (Figure 62). This angle is an angle of table rotation needed to orient object surface in relation defined by sensor pose. Position P of sensor as well as observation and rotation vectors O and R, are then rotated virtually around table axis by angle α producing $P_{rotated}$, $O_{rotated}$ and $R_{rotated}$ respectively.

101

Input data:
- Measurement pose observation vector (P, O, R);
- Best observation vector for digitization station (B)

Calculate projection of O on rotating table plane (O_{pn})

Calculate projection of B on rotating table plane (O_{fixed})

Calculate angle α betwen O_{pn} and O_{fixed} in XY plane (2D)

Output data:
- Angle of table rotation (α)
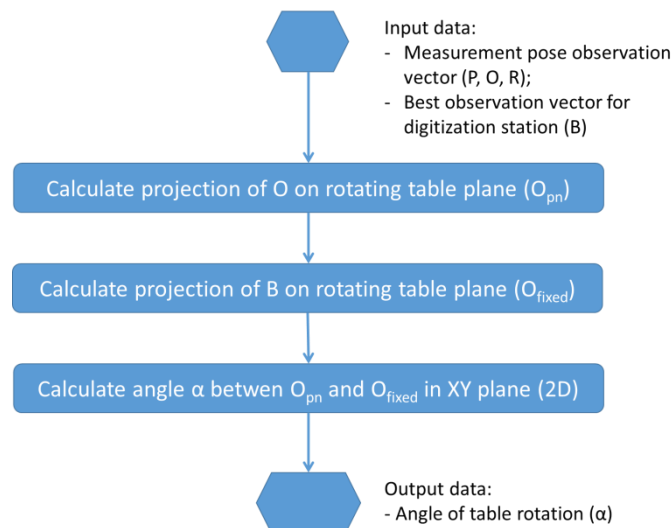
Figure 62. Calculation of table rotation angle.

Rotated sensor pose becomes a configuration for inverse kinematics calculations performed for the robot arm only. Due to the fact of using table rotation for initial targeting, the movements of robot are small, in fact closed within small box of size related to digitized object size (Figure 61).

Constraining robot movements to small box instead of large volume like in the original 3DMADMAC|AUTOMATED system has multiple advantages. The first and the most important one is that it significantly reduces the possibility of collisions which occur in the original system, when the head is moved from one side of the table to the other. Moreover, as distances travelled by measurement head are shorter, positioning is faster and robot wear is reduced, as well as energy consumption. Also, space requirements for the system are smaller because robot moves only on one side of the table. Up to now only one possible problem of such configuration was identified – non even wear of the robot as it works in limited operated range (especially joints 1 and 2). However, considering the fact that after thousands of hours of operation no observable robot wear was observed in any 3DMADMAC|AUTOMATED system, this problem is rather theoretical.

4.2.4 Trajectory calculation with collision detection

The main disadvantage of original trajectory analysis method used in 3DMADMAC|AUTOMATED system was the lack of any procedure to pass over colliding point. When collision was detected, the whole trajectory was returned as not valid rendering whole measurement direction invalid. For this reason, in HD3D|AUTO system, I have implemented mechanism allowing to find route around colliding point. It works by adding points to positioning path. Those points are created on the basis of collision point, by shifting

it along normal vector of the surface by distance specified in system configuration (Figure 63).

a)   b)
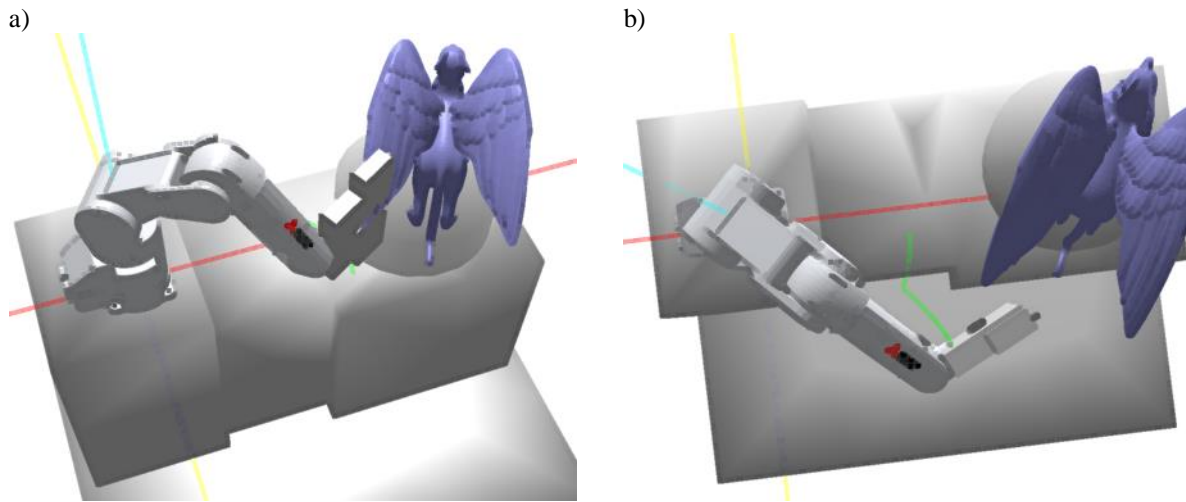
Figure 63. Inserting additional point in the trajectory to pass over collision: a) collision with object; b) right – no collision after trajectory modification.

This procedure is performed each time collision is detected, but no more than five times for trajectory. This limit is a compromise between time of calculations and obtained collision-free trajectories.

On the final note, it is worth mentioning that changed positioning method (i.e. making rotating table most important node and using robot arm for fine scanner pose adjustment) significantly decreased frequency of collisions during digitization processes. This is caused by limited movement of robot arm in comparison to the movement range in 3DMADMAC|AUTOMATED system.

4.2.5   Next Best View

To address disadvantages of original Next Best View algorithm which was implemented in software for 3DMADMAC|AUTOMATED system, new, two stage method was developed. In the first stage, rough and incomplete model of an object is obtained. For this purpose, low resolution, large working volume 3D sensor is used. Having rough 3D model of an object, Poisson-equation based triangulation method is used to extrapolate shape data over discontinuities. Obtained triangle mesh is then used to calculate set of poses for high resolution scanner. This set is afterwards sorted to minimize positioning time. Then precise digitization process is run. When it completes, one-pass hole detection procedure is run. For any detected hole, re-measuring is performed. Pose of scanner for this purpose is calculated using Loriot method (Loriot, et al., 2007). After all measurements are completed, the 3D

model is globally optimized using the method presented in Hołowko's paper (Hołowko, et al., 2014).

In subsequent sections of this chapter, all phases of new Next Best View algorithm are presented in detail.

4.2.5.1 Initial digitization

For many semi complicated objects, it is enough to make few directional measurements using large working volume 3D scanner, to obtain its rough model. Depending on surface complexity, this model will be more or less complete and most certainly will contain discontinuities. Due to this fact it cannot be treated as final model, but after processing it can be used for planning measurements with high resolution, small working volume 3D sensor.

While Poisson equation based method used for extrapolating data is extremely efficient, the closeness of extrapolated surface to real one is related to the completeness of cloud of points used for triangulation. As it was said before, this completeness depends on the number of directional measurements and complexity of object surface. From my experience, typical scanning objects can be initially digitized using predefined poses of 3D sensor, like the ones presented in Figure 64.

Figure 64. Predefined set of poses. For each robot configuration, table is rotated n times, by a 2π/n angle.

There are some cases though when scanning from such predefined set of poses does not allow to obtain model of required quality. This happens for example for objects which are heavily non symmetrical (for example concave). In this case, more advanced measurement planning has to be used. In HD3D|AUTO system, for this purpose, 3DMADMAC|AUTOMATED method is used albeit without the stage of hole filling. The only change which was made to the method is the selection of scanner working volume's center. In the original method, it was always chosen from border points of partial model (Figure 65a). Currently, there is possibility to shift it towards the unknown measurement space (Figure 65b) by specified distance. This allows to reduce size of overlaps, which in the original method were close to 50%, thus

reducing number of measurements and time of digitization. For large-volume sensors, this does not affect the results of fine data integration with ICP algorithm.

a)
b)
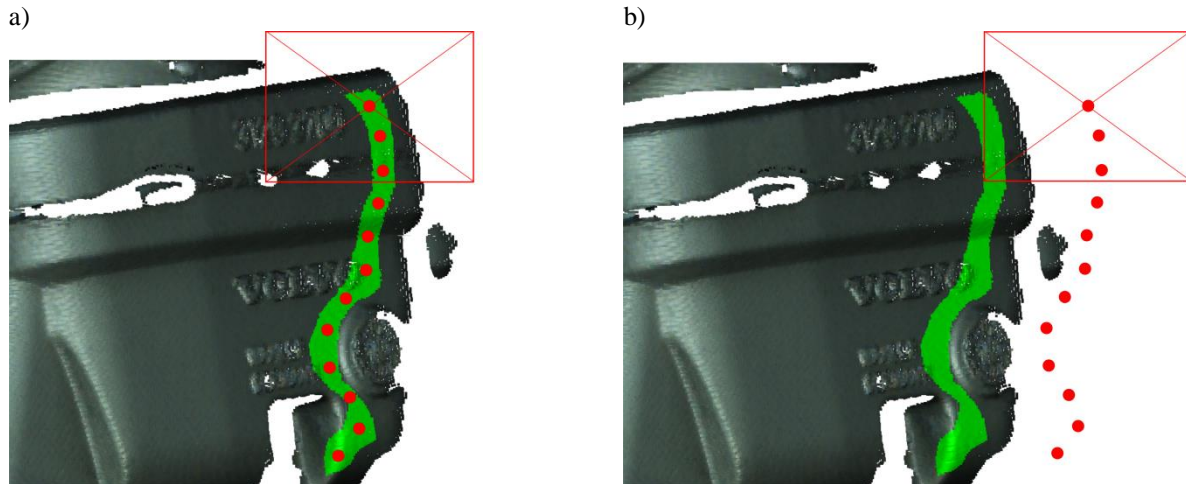
Figure 65. Selection of viewpoint center: a) 3DMADMAC|AUTOMATED; b) HD3D|AUTO. Red points are centers of candidate viewpoints. Red rectangle shows the area measured in next measurement.

Using Next Best View algorithm instead of predefined set of poses allows to obtain more complete models of complicated objects. However, it also extends the time required for initial digitization. For this reason, I have chosen to include both methods in HD3D|AUTO system and allow operator choose which method should be used for specific objects.

Regardless of the method used for initial scanning, data processing chain is the same (Figure 66) – raw cloud of points obtained from 3D scanner is filtered (to reduce noise and other measurement errors), initially integrated (using information from the positioning system) and fine integrated using ICP (Besl & McKay, 1992) algorithm. This last stage is required to limit positioning system errors influence on obtained 3D model.

After the measurements with low resolution sensors are completed, the model is processed to obtain input data for high resolution digitization stage (Figure 68). This process starts with global model optimization procedure (Hołowko, et al., 2014). This operation allows to redistribute any residual fitting error evenly over all clouds of points which form 3D model. In other case, small errors from ICP fitting accumulate causing significant deviations of shape for last fitted clouds. Distributing errors evenly allows to obtain model geometry which is not burdened by this problem.
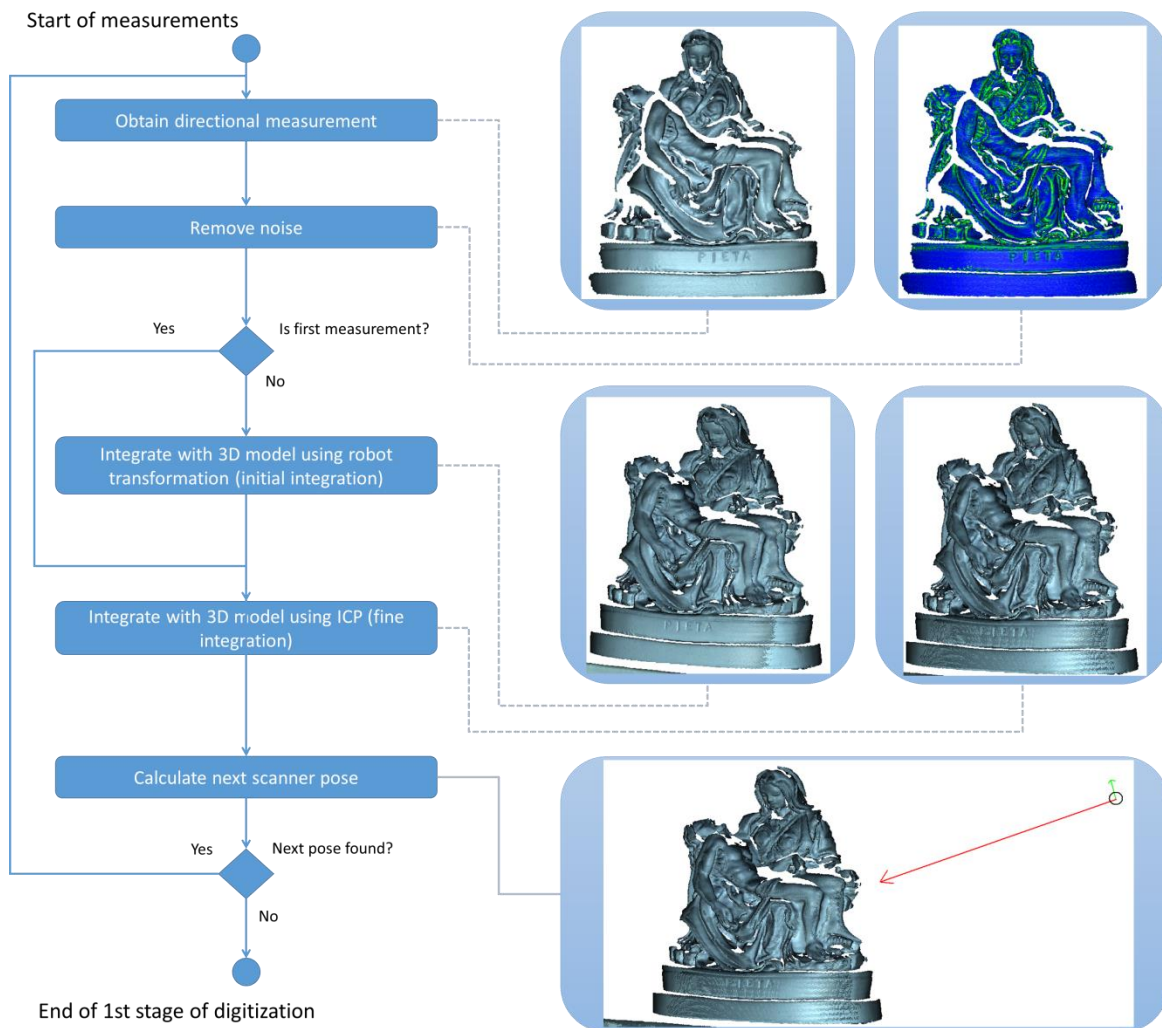
Figure 66. The schematics of the first digitization stage.

After data integration, 3D model is smoothed using coordinates averaging filter. This filter operates on point coordinates and normal vectors. Its purpose is to reduce measurement noise, which is especially present in normal vectors if measured surface is reflective or is not smooth (for example has some textured relief). After smoothing operation, those errors are reduced. It is extremely important procedure because Poisson-equation-based triangulation method results heavily depend on the quality of normal vectors (Kazhdan & Hoppe, 2013). Triangulation itself is done using implementation from Point Cloud Library suite (Rusu & Cousins, 2011). Poisson surface reconstruction filter always produce watertight mesh in which holes in source point clouds are extrapolated basing on normal vectors. The quality of extrapolation is extremely good even in cavities and other places of complicated shape (Figure 67). Owing to this, the measurement plan for high resolution 3D sensor can be calculated with high accuracy.

106
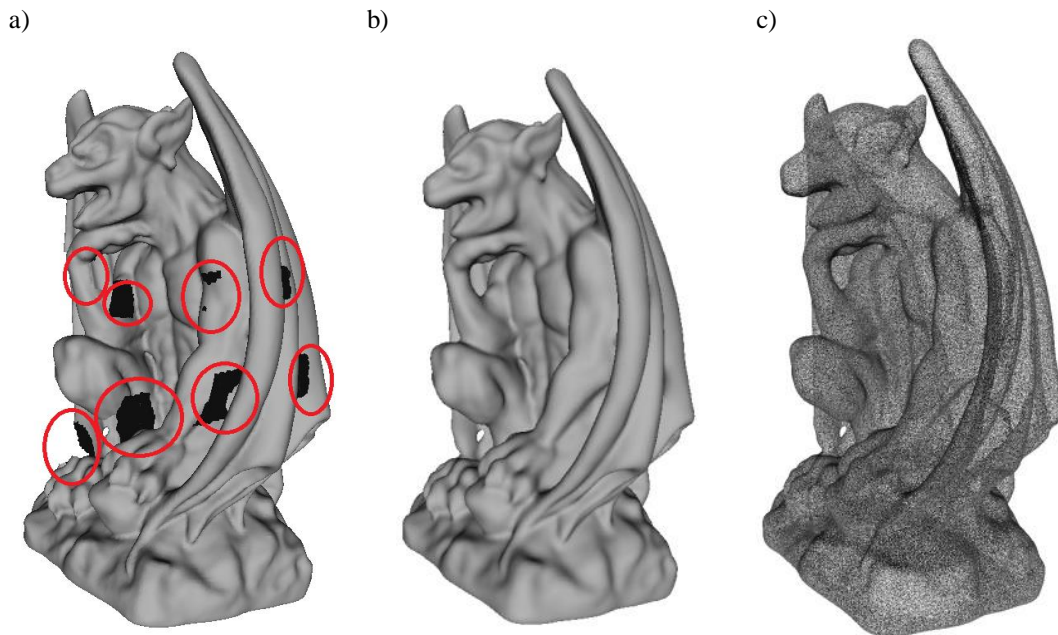
Figure 67. Poisson surface reconstruction as method for extrapolating shape data: a) incomplete model, b) reconstructed surface, c) point cloud from sampling of Poisson mesh.

Triangle mesh obtained from rough model is resampled to produce homogenous cloud of points (Figure 67d), a base for calculation of measurement plan for digitization with high resolution 3D sensor.
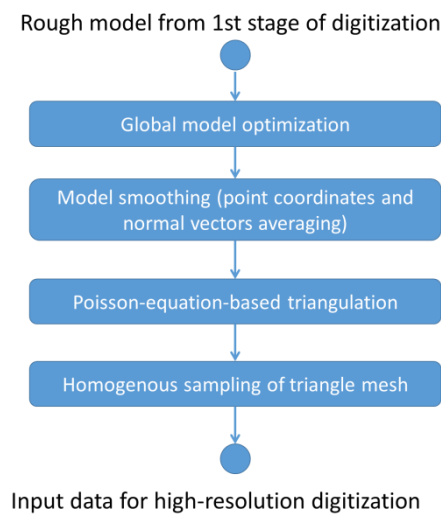
Figure 68. Preparation of rough model data for high-resolution digitization stage.

4.2.5.2 High-resolution digitization

High resolution digitization is problematic mostly due to very limited working volume of high resolution 3D sensors. Because of this, practically all known Next Best View algorithms do not allow to obtain high efficiency of scanning process. This is not in fact caused by deficiencies of those algorithms, but by need of collision detection (CultLab3D, 2016), (Bunsch, 2010), (Karaszewski, et al., 2012). To allow for safe, unsupervised digitization

process, collision detection and avoidance is a must. Therefore, to analyze possible collisions of positioning system, 3D sensor and object, their shape and positions in space have to be known. Of course rough models can be used for this purpose, but in case of complicated objects of varied shape, this becomes a significant limitation which sometimes leads to poor quality 3D models. The digitization of unknown objects and the need of 3D models of objects for collision detection are mutually exclusive. My concept of obtaining rough 3D model of an object which is then digitized with target 3D sensor is a solution which allows for binding those contradictory paradigms.

Calculation of set of Next Best Views basing on rough 3D model of an object is very similar in principle to the problem of digitizing objects with CAD models. Many algorithms were developed for this purpose; they are however not very well suited for the data obtained from measurement (which represents free-surfaces not parametric ones or geometrical primitives). Moreover, those algorithms were designed with industrial 3D sensors (i.e. having large working volume) in mind. There is no doubt that some of those algorithms can be adapted for high resolution digitization of cultural heritage objects. I have decided however to design and implement my own algorithm which could be tuned to all requirements of precise, professional 3D digitization (like maintaining correct observation angle, overlaps, handling occlusions etc.).

4.2.5.2.1 Surface observation angle

Depending on the type of 3D sensor used, the optimal angle of surface observation may vary. The main difference is of course between one-optical-path sensors (like time of flight detectors) and multiple-optical-paths devices (triangulation, structured light or photogrammetry sensors). The general rule, which is usually mentioned in literature is that to obtain best accuracy of measurement, the surface should be observed at normal angle (90 degrees between surface and system optical path which equals to 180 degrees between surface normal and system optical path). While it is simple to achieve for one-optical-path systems, it is not clear which angle should be treated as observation one in multi-optical-paths devices. Most researchers state that all paths are equally important, therefore they usually calculate observation angle in regard to average optical axis of the system (Callieri, et al., 2004), (Pito, 1999). On the contrary, Tarbox (Tarbox & Gottschlich, 1995) states that when digitization sensor use some kind of projector, it is more important to keep it perpendicular to the surface than detector devices (Tarbox & Gottschlich, 1995). On the other hand, experts from Museum of King Jan III's Palace in Wilanów 3D Documentation Laboratory state that for structured

light scanners with one detector, the best accuracy is obtained when detector axis is perpendicular to the measured surface. This is of course impossible to obtain in systems using two detectors (like the one shown in Figure 58). Considering all above stated observations I have chosen to design NBV algorithm in a way which allows for observation angle tuning (Figure 69). This feature makes my method universal and capable of be used with various 3D sensors.

Under normal conditions, all sensor poses are calculated to keep observation vector perpendicular to the object surface. In case of occlusions or collisions, when optimal sensor placement does not allow for making measurements, observation angle is modified within acceptable limit. This procedure permits to obtain 3D data but at slightly worse accuracy. The method of modifying observation angle under special conditions is described in further part of this chapter.

a)   b)   c)
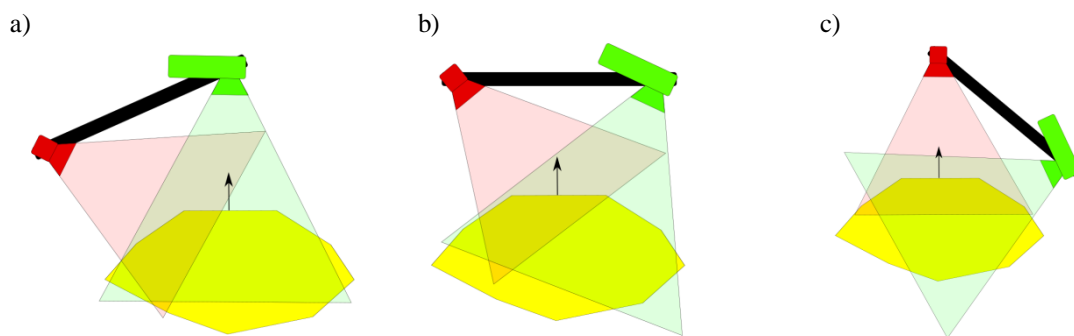
Figure 69. Position of 3D scanner in regard to object with different settings of observation angle: a) aiming with projector, b) aiming with average observation vector, c) aiming with detector.

4.2.5.2.2   Occlusion detection

When digitizing objects of complicated shape, especially ones with protruding elements or concave areas, working volume of 3D sensor becomes occluded. This phenomenon occurs when any part of object is situated between sensor and the surface which is selected for digitization (Figure 70). As a result, incomplete measurement is received.

The problem of occlusions is more pronounced in systems with multiple optical paths like structured light scanners or laser triangulation ones.

To check for occlusions, digital model of object is required. It does not need to be very precise, nevertheless the more accurate it is, the better occlusion detection can be achieved. In case of HD3D|AUTO system, detection is performed with raytracing. For each optical path of used detector, a projection truncated pyramid is constructed. Parameters of this pyramid (height, size of base) are calculated using parameters of device it simulates (camera,

109

projector). Its position and orientation results from current position of the scanner and relation between scanner's coordinate system center and the device. For each pyramid, distance from the base is also described. It represents device operating range (Figure 71) using planes P_{near} and P_{far}.

Figure 70. Occlusion during digitization process. Areas which cannot be digitized due to occlusion are marked with red ellipses.
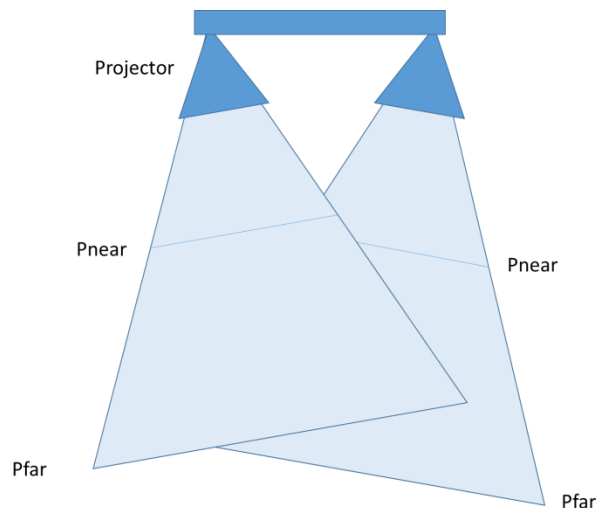
Figure 71. Simulation of optical device by projection / observation pyramid (view from the top).

The pyramid is divided into sectors which represents pixels of detector / projector. While it is possible to represent each pixel with different sector, it causes significant rise of calculations time without any rise of detection quality. Therefore, for detector / projector with 4:3 aspect ratio, usually the number of pixels is set to 20 x 15 (width x height), a good compromise

between detection accuracy and calculation time. Using these parameters, observation pyramid is divided into 300 sectors (Figure 72).
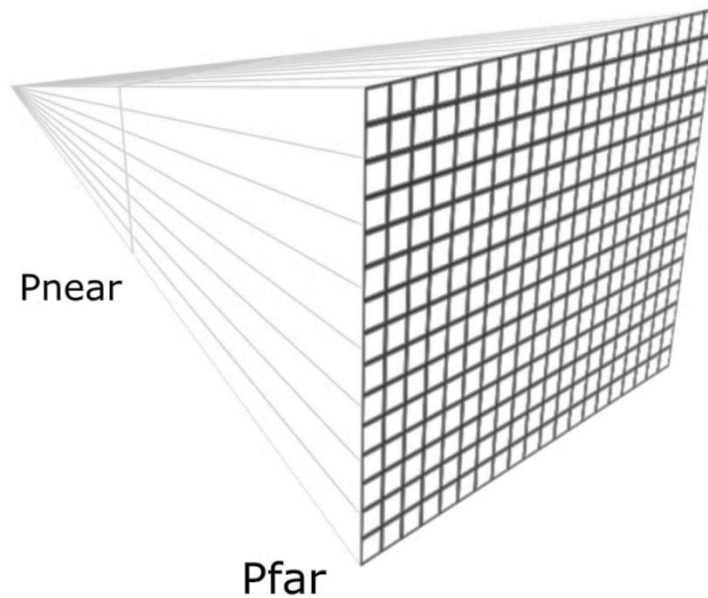
Figure 72. Observation pyramid divided into 20 x 15 sectors.

For each sector, all points contained within it are identified. If any point is detected between sector apex and the plane P_{near}, it means that it occludes working volume for this sector which is located between P_{near} and P_{far} planes (Figure 72). Therefore, points which lie between P_{near} and P_{far} planes in analyzed sector are marked as occluded. Iterating over all sectors, whole device is analyzed. The same operations are performed for all devices which are used in the 3D sensor. Afterwards, all points which were marked as occluded at any stage of the analysis are counted. If their number is higher than user defined threshold (usually equal to 0), the proposed sensor pose is reported as occluded.

4.2.5.2.3 Modification of observation vector

All sensor poses which are calculated during Next Best View calculations are checked whether they can be reached by positioning system and if no occlusion occurs. If not, proposed pose is modified iteratively within accepted limits. This procedure allows to obtain good quality measurements taken from pose similar to the optimal one which from some reason is invalid. This is an important feature of the algorithm, allowing to obtain better surface coverage with smaller number of directional measurements.

The modification of proposed pose is straightforward. The center of measurement volume is not modified at all while observation vector is being slightly changed. Due to significant standoff distance of the scanner (typically at least 400mm (Artec, 2016), (Creaform3D, 2016),

(GOM2, 2016)), even small changes of observation vector cause large sensor displacements. This is the easiest way to "move" scanner out of collision or occlusion situation.

Observation vector is modified iteratively, starting with very small change. This change is introduced in local, cylindrical coordinate system of the vector (Figure 73).
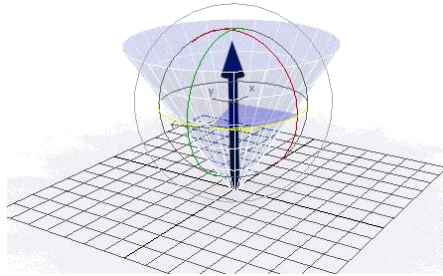
Figure 73. Observation vector in its local coordinate system along with angles (drawn with red and green circles) which are modified during the process of occlusion / collision mitigation.

Starting with the modification of angle a by 0.1 rad (roughly 6$^\text{o}$), the observation vector is rotated and scanner position and orientation is calculated. For obtained pose, occlusion and collision checks are performed. If both checks are negative, which means that no collision and no occlusion occur, the iteration procedure is terminated and valid sensor pose is returned. If any check is positive, the iteration angle is increased. While angle α, which represents rotation of sensor around observation vector is usually not limited (i.e. it is iterated in range from 0 to 2π rad), angle β which represents deviation of observation angle from optimal one is only modified within range permitted by user specified parameters. It is usually set to 50% of sensor acceptance angle.

Using above described procedure, it is usually possible to perform about 70% of measurements which are at first identified as invalid due to collisions or occlusion. This factor depends on digitized object's complexity and its size to robot operating range ratio.

All control parameters (modification angle, acceptance angle etc.) are configurable by user. Values which are given above were selected as best compromise between accuracy and time required for computations.

4.2.5.2.4 Calculation of measurement directions

The idea which lies behind measurement direction calculation is directly related to the task of perpendicular observation of surface which allows for best accuracy digitization. Therefore, object surface is divided into patches which have similar (i.e. changing within acceptable

limits) surface orientation. For this purpose, normal vectors of points are converted to cylindrical coordinate system and used to construct two-dimensional histogram (Figure 74). The size of histogram buckets is set according to acceptable deviation of surface orientation which can be measured by sensor from given observation angle with acceptable accuracy. This parameter should be set in accordance to used 3D sensor capabilities. It is important not to set it at maximum acceptable value as it limits the ability of the system to deal with occlusions and collision avoidance (described above).
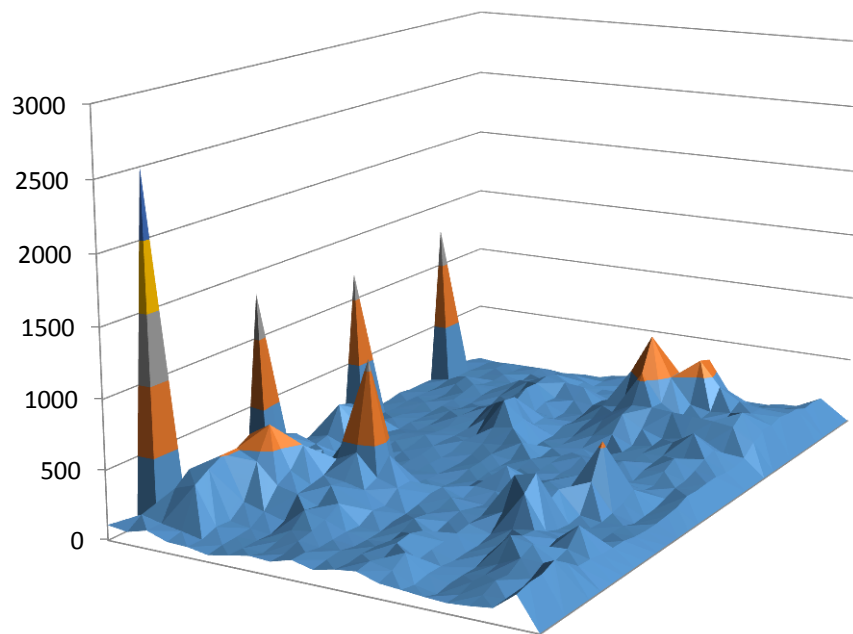
Figure 74. Histogram presenting object surface orientation.

Histogram of normal vectors directions represents object surface orientation. Most popular directions are identified and used for next stage of calculations. Extensive testing shown that selecting histogram peaks which represent about 90% of total number of points in source cloud is a good compromise between obtained results of digitization and time of calculations. Points contained in each of selected histogram buckets can be measured with same sensor orientation, albeit not necessarily from the same position (due to limited working volume).

In the next stage of NBV algorithm (presented in Figure 77), patches of similarly oriented points are analyzed. For each patch, points are divided into groups which can be fit in sensor working volume (Figure 76). For each of these groups, sensor pose is calculated. Afterwards, it is checked if positioning sensor at this pose is possible (due to range of positioning system and collisions) and whether there are no occlusions. If any of those conditions is not met, sensor pose is modified by iteratively modifying observation angle. If this procedure cancels

occlusion and positioning problems, calculated sensor pose is added to NBV list. Otherwise, analyzed group of points is marked as not possible to measure.

a)   b)
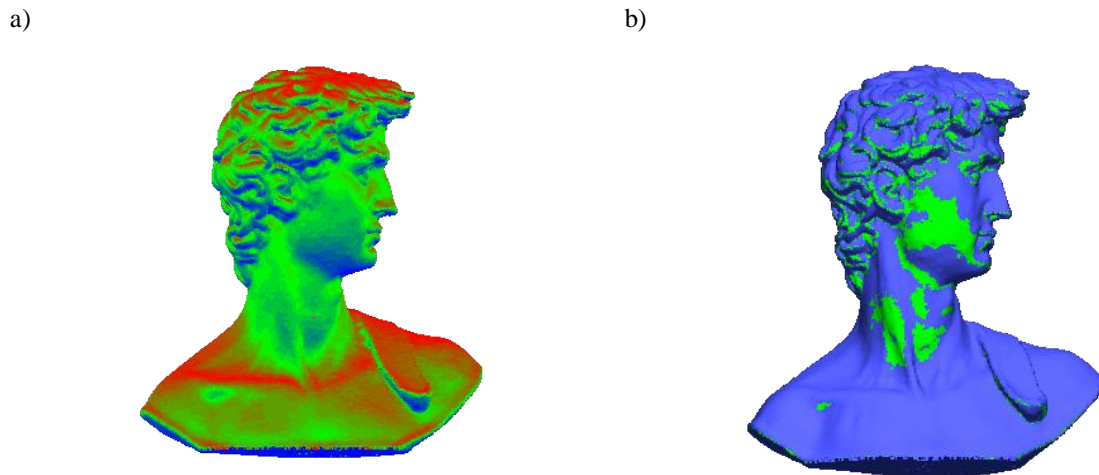
Figure 75. Visualization of points grouped by normal vector orientation: a) groups shown in pseudocolor, b) points belonging to one histogram bucket.

a)   b)
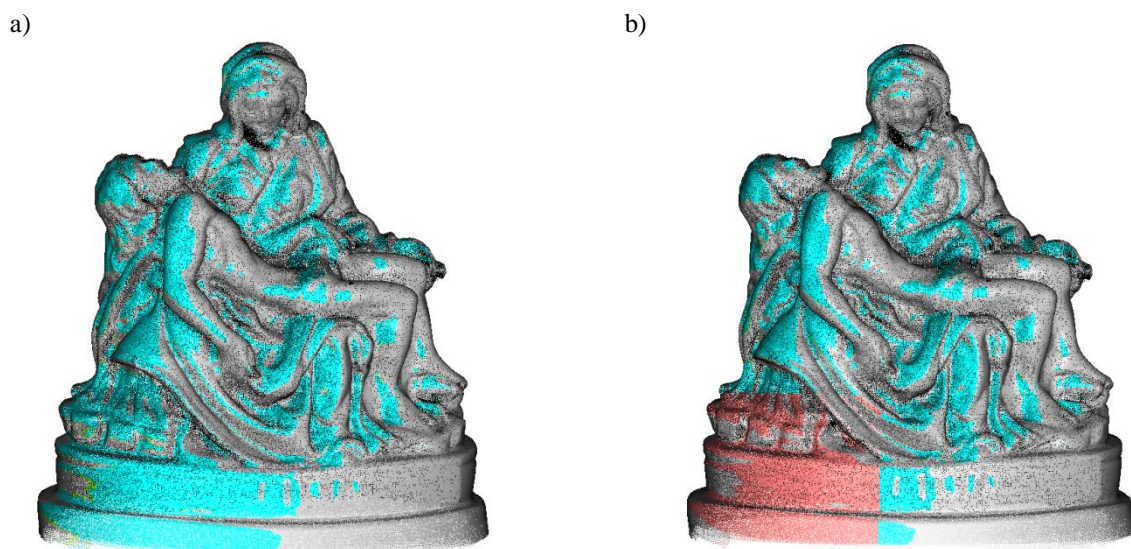
Figure 76. Patch of similarly oriented areas (a), area which can be measured from one sensor position (b).

When all groups of points, which were identified for digitized object's model are analyzed, the set of measurement directions is sorted. In fact, sorting function is exchangeable, which allows for adapting system to operator's requirements. Currently, three sorting functions are implemented:

- Sort by table rotation angle,
- Sort with travelling salesman paradigm,
- Sort by collision free trajectories.

Sorting by table rotation angle is the simplest method. Measurements are ordered in a way which is dictated by required angle of table rotation, without any consideration about robot

arm movements. As an effect, table movements are usually very small, while robot trajectories tend to be long. Nevertheless, this method allows for significant shortening of the digitization process when compared to unordered set of sensor poses.
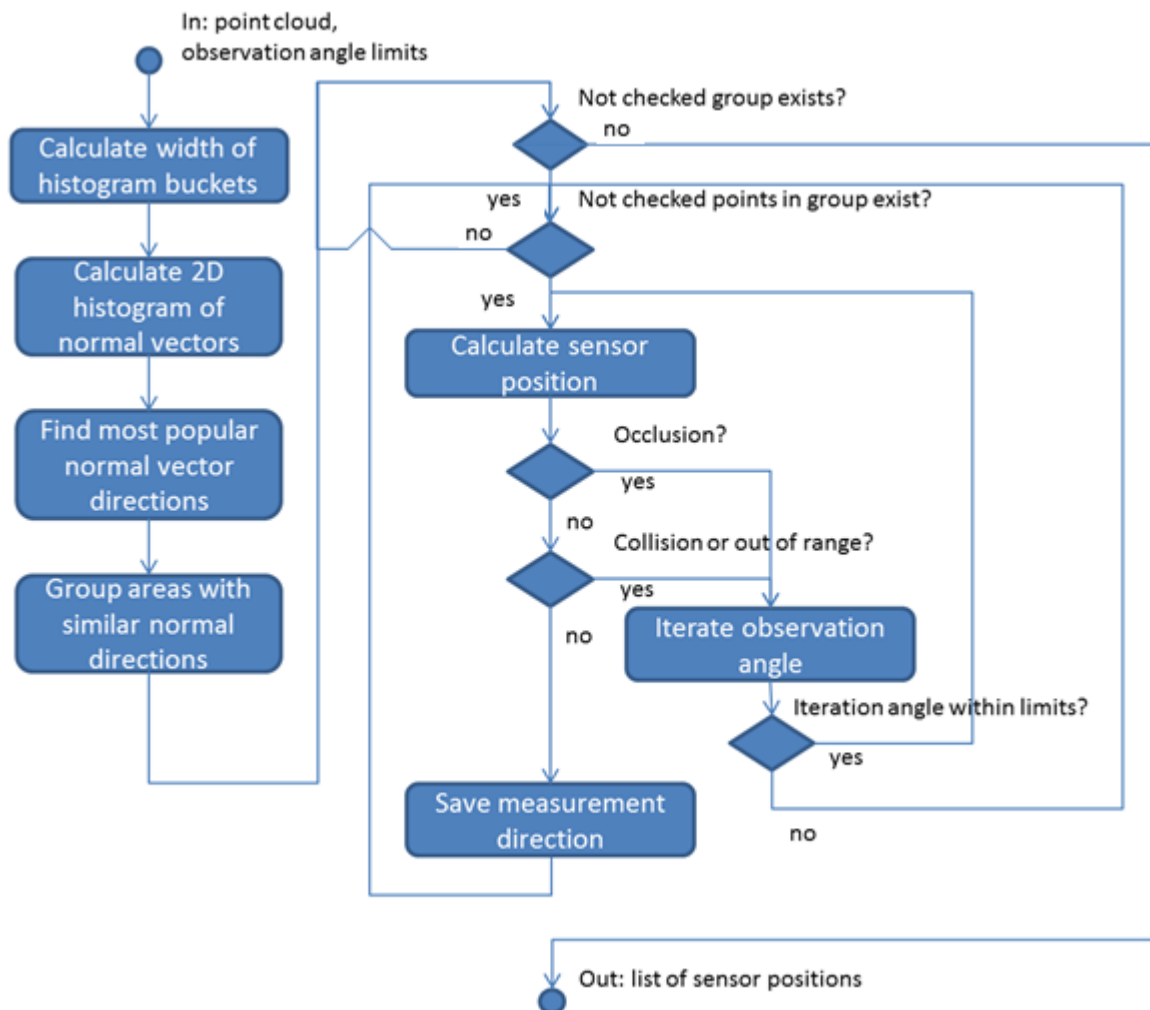
Figure 77. Schematic of NBV algorithm for high-resolution measurements.

Travelling salesman paradigm is a well-known method of finding shortest path which connects many locations, without visiting any of them more than once (Lenstra, et al., 1985). Implementation of this method allows for further shortening of digitization time, albeit the improvement over previous method is not very significant. In fact, usually the order of measurements is similar to the one obtained when sorting by table rotation angle method is used.

The third method, sorting by collision free trajectories is the improved version of table rotation angle sorting. In contrast to the original method, in this algorithm, trajectories between subsequent points are analyzed. If collision is detected, endpoint of the trajectory is moved further in the set of sensor poses. Usually, for such points no collision free trajectory

can be found from any of proposed sensor poses, therefore they tend to gather at the end of sorted measurement poses. This allows for performing all measurements for which sensor can be easily put in required pose at first, while difficult poses are left till the end of digitization process. Trajectories which lead to those poses are then modified with the procedure described in "Trajectory calculation with collision detection" section of this document. Sorting measurement poses with this method allows to obtain short time of digitization (similar to the first sorting method), while pushing difficult trajectories to end of the process. They are performed within short period of time, which makes them easily observable and controllable by the operator.

Visualization of exemplary list of measurement poses, sorted with travelling salesman paradigm is presented in Figure 78. Order of poses is shown by color scale, where blue points represent firstly measured ones and red points – poses from the end of the set.
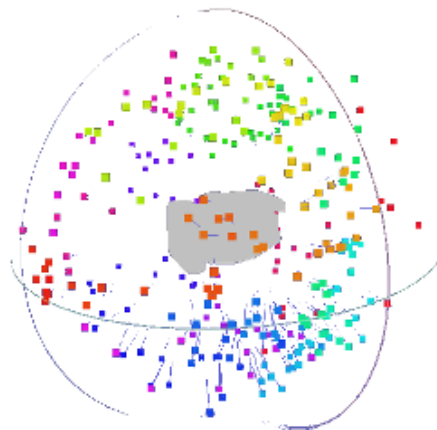
Figure 78. Set of sensor poses calculated for exemplary object.

When sensor poses are sorted, the digitization process can be started. Two modes are available – dry and normal run. Dry run procedure allows to perform all positioning moves without taking measurements. This allows for operator-assisted checking trajectories for collisions which were not detected during measurement process planning. Because no measurements are taken, the process can be performed within several minutes. When dry-run is completed, digitization process can be run without any supervision as the positioning devices will move along exactly the same trajectories as during dry run.

Digitization process takes much more time than dry run due to taking of measurements and processing of data. In case of complicated objects, it can take up to several hours. After all measurements are performed, global optimization of the model is performed using Hołowko's algorithm.

The output 3D model is analyzed for completeness. If any discontinuities are found, the re-measuring procedure is started.

4.2.5.2.5 *Detecting and filling of discontinuities*

Due to various factors, mainly object's shape details and the difference between real 3D sensor and its model used in calculations, obtained 3D model may contain discontinuities. Those areas are detected by calculating local density of the model. At first, obtained model is homogenously simplified (radius of simplification r_{hs} is directly related to the size of discontinuities to be detected). Then, for each point number of points in close neighborhood ($1.5 \times r_{hs}$) is calculated. Points, for which this number is smaller than 5, are selected as probably belonging to the edge of a hole (Figure 79).

a)   b)
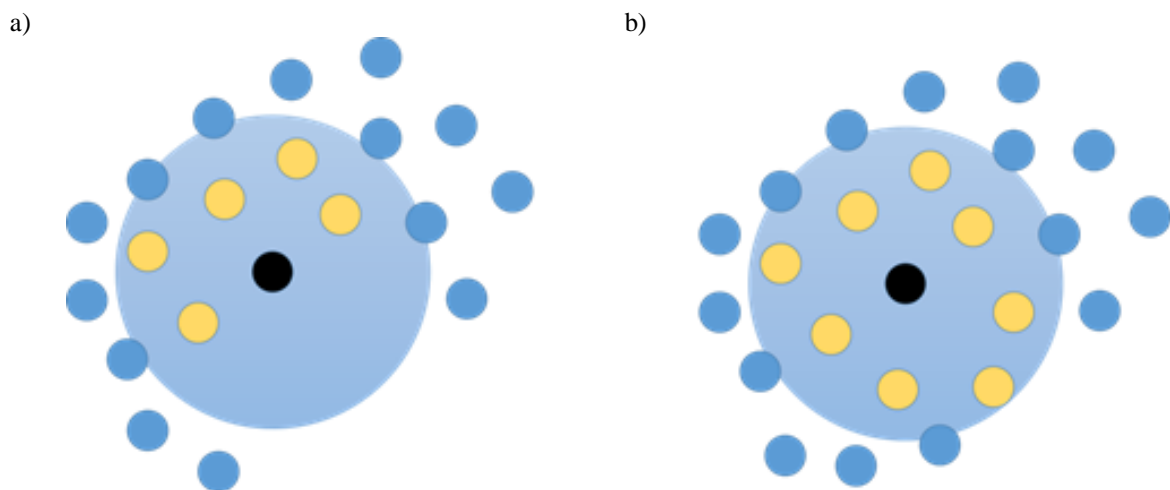
Figure 79. Analysis of point neighborhood: a) with, b) without discontinuity.

After analysis of each point in the model, selected points are grouped. For groups larger than 10 elements, sensor pose which is used for re-measuring is calculated using Loriot algorithm (Loriot, et al., 2007). This pose is analyzed in regard to possible collisions and occlusion. If any of those problem is present, observation angle is modified according to previously described method. After successful calculation of sensor position and orientation, directional measurement is made and data is integrated with existing model. After all areas with discontinuities are analyzed, digitization process is completed.

4.3 Summary

The HD3D|AUTO system for high resolution, automatic 3D shape digitization is the improved version of the original 3DMADMAC|AUTOMATED system which has been used in Laboratory of 3D digitization in Museum of King Jan III's Palace in Wilanów 3D Documentation Laboratory. Regardless of its many deficiencies, it was used for creating professional 3D documentation of more than hundred cultural heritage objects. The improvements implemented in HD3D|AUTO system attempted to fix most of the problems raised by professionals from the Museum Laboratory. Starting from the modification of measurement head itself, through selection of the most popular and universal positioning system configuration, ending at completely modified controlling algorithms (two-staged Next Best View, collision and occlusion detection, trajectory calculation), improvements were designed, implemented and integrated.

To assess new system capabilities, especially with regard to the original 3DMADMAC|AUTOMATED station, numerous digitization processes were performed. For all of those processes, test station was built. Its characteristics are given in Table 5.

Module name	Parameters	Device used
Positioning system – robot arm	6 axes, 500mm operating range radius, 5 kg load capacity.	Kawasaki RS005L with Kawasaki E controller. TCP/IP-based control.
Positioning system – rotating stage	250 mm radius, 0.05^o angular resolution, 100 kg load capacity.	Labster NO250. TCP/IP control using Wiznet WIZ110SR converter.
Station frame	2000 mm x 500 mm x 400 mm stiff frame integrating robot arm and table.	Bosch Rexroth aluminum profiles.
Measurement heads	Structured light system with two cameras and projector. Built in PC computer.	1. Custom-built head with two 2Mpix PointGrey Flea USB 3.0 greyscale cameras, Toshiba TDP-FF1A projector, Intel NUC with Intel Core i7 processor, 32GB RAM). Steel / aluminum frame. 2. PragmaVision SLScan5Mx2C scanner (two 5Mpix Basler ace USB 3.0 color cameras, Optoma ML750E projector, Intel NUC with Intel Core i5 processor, 16GB RAM).

		Carbon fiber frame with FDM printed elements.
Data processing unit	PC with Intel Xeon 8core processor, 96GB RAM, nVidia GeForce GTX980 graphic card, 10TB disk space. Microsoft Windows Server 2012 R2.	Supermicro X9-DRi-F based workstation.

Table 5. Parameters of digitization station used for testing.

Two measurement heads were used for testing. Low-resolution one, custom-built head with 2Mpix cameras was calibrated for large working volume. The other, with high resolution cameras was calibrated for spatial resolution of 2500 points per mm^2. Parameters of those measurement head are given in Table 6.

Sensor used in digitization stage	Resolution		Working volume (width [mm] x height [mm] x depth [mm])	Point count in full field measurement (approximate)
	points per mm^2	average distance between points [mm]		
Custom-built	100	0.1	180 x 110 x 100	2 million
PragmaVision SLScan5Mx2C	2500	0.02	50 x 50 x 25	6.25 million

Table 6. Parameters of measurement heads.

For initial testing, geometrical primitives were chosen: cylinder (50 mm radius, 150 mm height), cone (50 mm radius, 150 mm height) and cube (100 mm x 100 mm x 100 mm). Their 3D models were created in Autodesk Inventor (Autodesk, 2017) and printed using Dynamake Trinity 3D printer (Dynamake, 2015). 3D printed models were smoothed with acetone and covered with Heeling TiO$_2$ antireflective powder (Helling, 2015). Those objects were digitized with 3DMADMAC|AUTOMATED and HD3D|AUTO systems. Results are presented in Table 7.

Digitization processes conducted for such simple objects as cylinder, cone and cube were completed successfully by both methods. Obtained surface coverage is very good in all cases (Surface coverage was calculated by comparison with 3D model used for printing. Bases of objects are excluded from the calculations). In fact, in case of cylinder 3DMADMAC|AUTOMATED performs better (requires less measurements) due to the lack of initial scanning stage. With rising complexity of object, HD3D|AUTO system performance overtakes performance of 3DMADMAC|AUTOMATED, both in terms of digitization time and surface coverage.
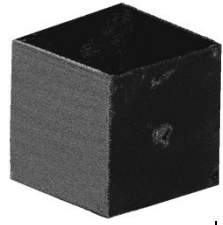
Statistics		3DMADMAC|AUTOMATED			HD3D|AUTO			
		Main digitization	Hole filling	**Total**	Initial digitization	Precise digitization	Hole filling	**Total**
	Number of single measurements	32	0	**32**	4	32	0	**32**
	Number of empty measurements	0	0	**0**	0	0	0	**0**
	Surface coverage [%]	100	100	**100**	100	100	100	**100**
	Digitization time [min]	12.5	0	**12.5**	1.8	12.6	0	**14.4**
	Number of measurements	58	0	**58**	4	41	0	**44**
	Number of empty measurements	9	0	**9**	0	0	0	**0**
	Surface coverage [%]	100	100	**100**	100	100	100	**100**
	Digitization time [min]	23.2	0	**23.2**	2.1	17.5	0	**19.6**
	Number of measurements	38	8	**46**	4	34	2	**40**
	Number of empty measurements	8	0	**8**	0	0	0	**0**
	Surface coverage [%]	74	95	**95**	95	92	99	**99**
	Digitization time [min]	15.9	5.3	**21.2**	1.6	15.2	2.2	**19.0**

Table 7. Comparison of simple objects digitization with 3DMADMAC|AUTOMATED and HD3D|AUTO systems.

After successful completion of evaluation procedure on simple objects, more complicated tests were conducted. Objects used for those tests were the same as the ones used in

evaluation of Next Best View algorithms performance described in previous section of this dissertation. Their results are presented in Table 8.

Object name	Number of measurements				Surface coverage [%]			Digitization time [min]			
	HD3D|AUTO			3DM ADM AC	HD3D|AUTO		3DM AD MA C	HD3D|AUTO			3D MA DM AC
	Initial stage	High resolution stage	Total	Total	Initial stage	High resoluti on stage		Initial stage	High resoluti on stage	Total	Total
David's Bust	10	68	78	92	95	99	94	3.2	23.5	26.7	37.0
Corinthian column	12	88	100	110	82	96	94	4.7	30.2	34.9	44.2
Luisville Public Library downspout	12	57	69	80	92	99	92	4.8	21.2	26.0	32.2
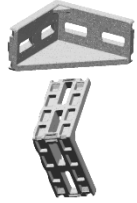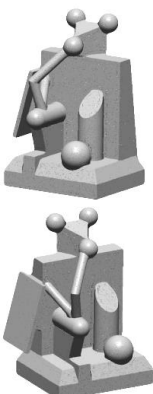
Aluminum profile gusset	8	21	29	42	84,	94	93	3.1	8.5	11.6	17.0
Artificial object for measurement testing	15	62	77	89	82	95	94	5.9	28.2	34.1	35.8

Table 8. Digitization of test objects with HD3D system compared with digitization performed using 3DMADMAC|AUTOMATED. Given time values does not include robot and table movement, data transmission, saving and processing.

The comparison between digitization processes which were performed by original 3DMADMAC|AUTOMATED system and newly proposed HD3D|AUTO (presented in Table 7 and Table 8) confirms that the new system performance rises with the complexity of the object. While for simple geometrical primitives, the overhead of initial scanning in HD3D|AUTO system is significant, it becomes negligible even for moderately complicated geometry. For objects with occlusions and significant shape gradients, the advantage of HD3D|AUTO systems are undisputable.

5. Evaluation of the novel digitization system capabilities in cultural heritage and technical parts documentation

Success of initial evaluation of HD3D|AUTO system capabilities, presented in previous chapter of this dissertation, allowed to perform tests of system applicability for cultural heritage as well as technical parts documentation. To be used for this purpose, scanning has to be performed with resolution of 2500 points per mm^2 (Bunsch, et al., 2011), (MacDonald, 2010). Data should also contain color information. Moreover, the surface coverage should be as high as possible, comparable with obtained by skilled operator. For typical digitization targets, coverage seldom reaches 100% due to occlusions and deep cavities. Number of directional measurements taken by automated system and by skilled operator should be similar.

To sum up, for digitization system, which is aimed to be used in massive, high-resolution digitization projects, the most important performance aspects are:

1. Spatial resolution and uncertainty of measurements.
2. Number of directional measurements required in the scanning process.
3. Obtained surface coverage.
4. Occurrence of collisions.
5. Duration of scanning process.

All of those performance criterions were evaluated using procedures described in the following sections of this dissertation. Spatial resolution and inaccuracy of measurements were measured using special objects which were measured using Coordinate Measuring Machine (CMM). Parameters 2-5 were assessed during digitization processes.

5.1 Spatial resolution and inaccuracy of measurements

Measurement head, used for high-resolution digitization, was commercially available device (SLScan5Mx2C - Table 6) from PragmaVision Sp. z o. o. company (PragmaVision Sp. z o. o., 2017). Spatial resolution, declared by manufacturer is 2500 points per mm^2. This parameter was verified by measuring a flat, non-reflective surface (with area of 65 mm x 60 mm from which 50 mm x 50 mm fragment was analyzed) situated perpendicularly to the head's projector optical axis. The result of measurement is shown in Figure 80. For obtained

data, local points density histogram was calculated. The center value was 2704.83 points per mm^2, better than declared 2500 points per mm^2.

Accuracy of measurements was calculated according to VDI/VDE 2634 norm (VDI/VDE, 2008) which is often used for such purposes. The evaluation procedure described in this norm consists of conducting multiple measurements of test unit, built from two spheres (Figure 81). Radiuses and distance between spheres are known with high precision (usually those values are obtained using CMM). VDI/VDE 2634 norm described how the test unit should be placed within scanner working volume. Data from measurements is segmented into parts representing the spheres. The distance between calculated centers of those spheres is compared to nominal one (Młynarska, 2017). The result of the validation is called Maximum Permissible Error.

Results of the test measurements confirmed that inaccuracy of SLScan5Mx2C scanner is within 25 um (3 sigma). This value is acceptable for spatial resolution of 2500 points per mm^2.
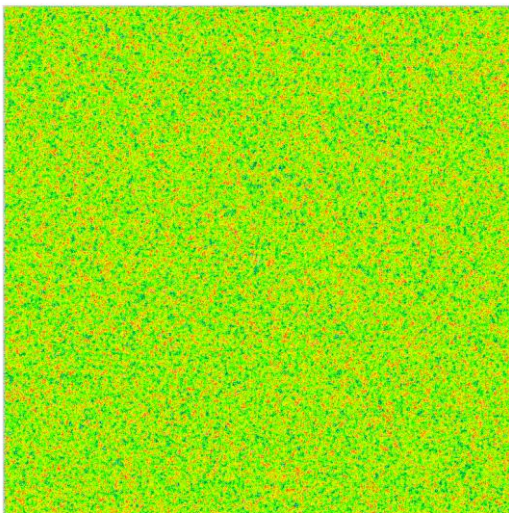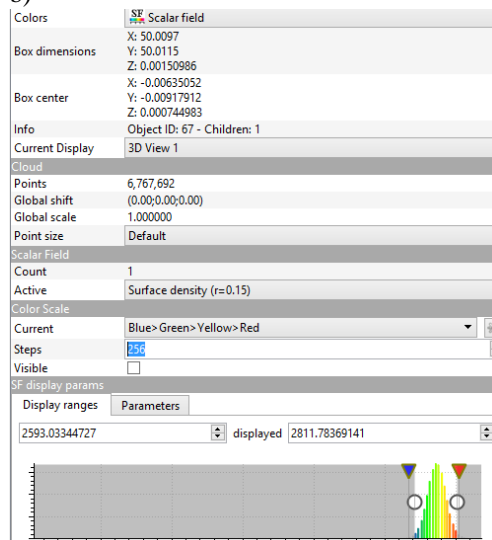
Figure 80. Spatial resolution measurement result: a) cloud of points with density represented by colors; b) cloud statistics with histogram of local points density.

Figure 81. Test object (ball bar) used for assessing 3D sensor accuracy up to VDI/VDE standard.

5.2 General remarks on the digitization station and software

The digitization station used for the assessment of HD3D|AUTO performance was built around Kawasaki RS005L robot arm (Kawasaki Robotics, 2016), custom-made 3D scanner for rough scanning and PragmaVision SLScan5Mx2C measurement head. Robot arm was fixed to one end of station frame. On the other end of the frame Labster NO250 rotary table was fixed. The digitization station is presented in Figure 82. The maximum speed of robot movement was overridden to 2% of its nominal value (roughly 1mm/s) because of the delicate nature of measurement head. Due to this limited travel speed, the time required for positioning measurement head is not negligible.

Figure 82. The digitization station used in the evaluation process. Custom-made 3D scanner for rough 3D scanning is fixed to robot arm.

The station was controlled by set of software modules. Almost all modules were implemented in Virtual Reality Techniques Division at Warsaw University of Technology (VRTD, 2017). Below, the list of all modules is presented with author participation percentage given in brackets.

1. Measurement head control (calibration & measurement) – VRTD / PragmaVision Sp. z o. o. (90%).

2. Robot and table communication – VRTD (100%).

3. Collision detection and avoidance, trajectory calculations – VRTD (100%). Contains Coldet library (Photoneffect, 2016) (0%).

4. Point cloud processing – VRTD (20%).

5. Poisson surface reconstruction (triangulation) – PointCloud Library (Rusu & Cousins, 2011).

6. Next Best View – VRTD (90%).

7. Visualization – CloudCompare (CloudCompare, 2017) (0%).

Whole software collection was implemented in C++ language (Henricson & Nyquist, 1997), using QT5 libraries (Qt Company, 2017) and Microsoft Visual Studio 2015 (Microsoft, 2016) as compiler.
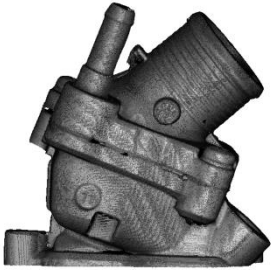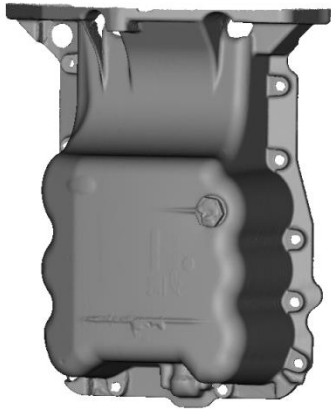
Measurement head control application was run on the computer built into the measurement head. In case of both heads, it was Intel NUC minicomputer with Intel Core i5 2.4GHz processor, 16GB of DDR3 RAM memory and M2 solid state disk.

Data processing, Next Best View, collision analysis, triangulation and visualization was run on a PC computer with Intel Xeon 8core processor, 96GB RAM, nVidia GeForce GTX980 graphic card, 10TB disk space. Microsoft Windows Server 2012 R2.

5.3 Performance assessment during digitization processes

To assess HD3D|AUTO performance during digitization of various objects, six artifacts were chosen. They have been digitized numerous times by 3D digitization experts from WUT using measurement heads of various resolutions and working volumes. Three of those objects represent class of cultural heritage objects, while other three ones – technical parts. Those objects have different characteristics than cultural heritage ones – contain many sharp edges, nearly ideal cylinders, flat surfaces etc. Due to the material they are built from (aluminum), such elements have to be covered with reflection-reducing powder (Helling, 2015).Test objects are presented in Table 9.

Object	Description	Photo	3D model (obtained at WUT)
Roman votive altar	Copy of roman votive altar with Latin inscription, 2nd century. The copy is made from plaster. Size of the object: 286 mm x 168 mm x 168 mm.		
Kybele sculpture	Copy of Kybele figurine from 2nd century BC (Greece). The copy was 3D printed with ZCorp plaster-powder color printing machine. Size of the object: 390 mm x 160 mm x 110 mm.		

Gargoyle	Copy of Gargoyle sculpture from Mont Saint Michel abbey (France). The copy is made from plaster and covered with creamy-grey polychrome. Size of the object: 362 mm x 266 mm x 179 mm.		
Automotive part (thermostat housing)	Thermostat housing used in various models of Volvo cars. It is made from aluminum (except brass pipe). The part comes from dismantled engine. Object size: 96 mm x 79 mm x 88 mm.		
Automotive part (oil sump)	Oil sump used in Opel/Vauxhall Corsa cars. It is made from aluminum. The part comes from dismantled engine. Object size: 340 mm x 152 mm x 287 mm.		

Automotive part (water pump)	Water pump used in various Volkswagen cars. It is almost entirely from aluminum (rotor is made from ABS). Object size: 95 mm x 106 mm x 111 mm.		

Table 9. Objects previously digitized at WUT, used for HD3D performance evaluation. Digitization procedure

For all objects, full digitization procedure was performed. Its outline is presented below:

1. Placing the object on rotating table. To allow for measurements with 3D sensor below object base, measured element was placed on stick or pedestal protruding from the table (depending on the object). All objects were digitized in one placement pose (to simplify the process), therefore some parts of their surfaces were not digitized.

2. Initial measurement of object using 3D sensor with large working volume (further referred to as **LWV**). Measurement poses were calculated using Next Best View algorithm presented in *Initial digitization* section of previous chapter of this document.

3. Data processing (noise removal, fine integration with ICP algorithm, global relaxation).

4. Triangulation with Poisson surface reconstruction algorithm.

5. Resampling of triangle mesh to obtain homogenous cloud of points.

6. Calculation of set of measurement directions for high resolution scanning with SLScan5Mx2C head.

7. Dry-run of digitization procedure.

8. High resolution measurements, using 3D sensor with small working volume (further referred to as **SWV**).

9. Data processing (noise removal, fine integration, global relaxation).

5.3.1   Roman votive altar digitization

The altar was placed on the small pedestal fixed to rotating table. Due to weight and shape of altar, no additional fixing tools were necessary.

The relation between object size and LWV working volume and high percentage of quasi-planar surfaces caused small number of directional measurements in the initial stage of digitization (28). After this process, obtained model was cleaned, fine-integrated and globally-relaxed. Those operations yielded 3D model which is shown in Figure 83. The model presented below was heavily simplified to speed-up further calculations. The color of 3D model presented in Figure 83 differs significantly from real color of the object due to the problems with setting proper color balance for cameras used in the scanner.

Figure 83. Rough 3D model of roman votive altar composed of 28 directional measurements.

Using rough 3D model of the altar, triangle mesh was created using Poisson surface reconstruction algorithm. This mesh, presented in Figure 84, was then sampled to provide homogenous cloud of points used in Next Best View calculations. The artifacts visible on the lower part of 3D model are a result of poor integration of directional measurements caused by the nature of the measured object (planar surfaces and small number of distinct geometrical features). After considerations the model was left as presented to check if the presence of such errors causes problems at Next Best View calculations stage.

Figure 84. Triangle mesh created from rough 3D model of roman votive altar.

Next Best View calculations completed yielding 321 directional measurements for SWV 3D sensor. Figure 85 Presents altar model with distinguished similarly-oriented regions (Figure 85a) as well as proposed measurement directions (Figure 85b). The system did not report any collisions or unreachable measurements directions.

For safety reasons, the measurement plan was launched in dry-run mode. No collisions or other problems were reported during this operation.

After dry-run, normal scanning with SWV were started. The whole process took 6 hours, 52 minutes. After collection of measurement results, the subsequent scans were processed with noise-removal algorithm, fine integrated using ICP algorithm. Afterwards, global relaxation algorithm was run. Finally, algorithm for detecting discontinuities was started. It did not report any holes in 3D model apart from lacking basis of the altar (which cannot be digitized as it is occluded by table pedestal). Result of digitization is presented in Figure 86. Statistics for the whole process are given in Table 10. No apparent problems which could be caused by poor integration of clouds (at rough scanning stage) were observed during scanning process. Probably the total number of measurements would be a little lower if the initial model was error-free.

a)   b)
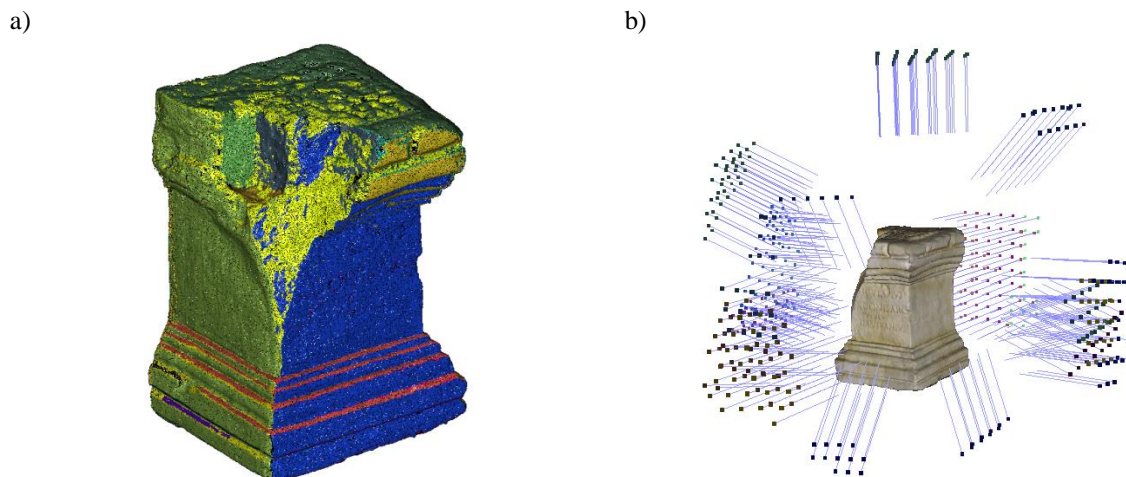
Figure 85. Results of NBV calculations for roman votive altar: a) similarly oriented areas; b) calculated scanner poses.

Figure 86. Final, high resolution model of roman votive altar.

Parameter	Value / description
Number of measurements (LWV)	28
Time of rough scanning	0.3 h
Data processing of rough model	0.2 h
Points count (rough model)	10.5 M
Triangle mesh creation	0.03 h
Triangle mesh sampling to point cloud (average distance 0.5 mm)	0.01 h
NBV calculations	0.2 h
Number of measurements (SWV)	321
Dry-run time	1.25 h
Time of high-resolution scanning	6.87 h
Data processing of high-resolution model	5.51 h
Number of discontinuities excluding object base (detected / measureable)	0 / 0
Time of discontinuities filling	0 h
Points count (high-resolution model)	2694 M
Total digitization time	14.37 h

Table 10. Statistics for roman votive altar digitization process.

5.3.2 Kybele figurine digitization

The 3D printed figurine of goddess Kybele was placed on the small pedestal fixed to rotary table. Due to weight and shape of the figurine, no additional fixing tools were necessary.

The complexity of the object required high number of directional measurements in the initial stage of digitization (45). After this process, obtained model was cleaned, fine-integrated and globally-relaxed. Those operations yielded 3D model which is shown in Figure 87.

The figurine is of much more complicated shape than the altar which was previously presented, therefore the data integration process was more successful. However, as the color of the surface appears different depending on the angle of measurement (due to different lighting angle), borders of measurements are clearly visible. This is not an geometrical integration error, only the unevenness of the lighting conditions.

Using rough 3D model of the figurine, triangle mesh was created using Poisson surface reconstruction algorithm. This mesh, presented in Figure 88, was then sampled to provide homogenous cloud of points used in Next Best View calculations

Next Best View calculations completed yielding 171 directional measurements for SWV 3D sensor. Figure 89 presents goddess figurine model with distinguished similarly-oriented regions (Figure 89a) as well as proposed measurement directions (Figure 89b). The system reported 21 collisions or occlusions in original set of proposed directions. 15 of them were mitigated using method presented in "Modification of observation vector" section of this dissertation. The remaining 6 directions remained unreachable.


Figure 87. Rough 3D model of Kybele figurine composed of 45 directional measurements.

.
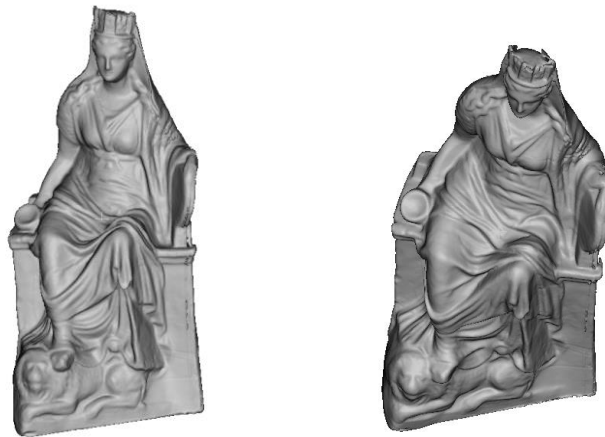
Figure 88. Triangle mesh created from rough 3D model of Kybele figurine.

a)

b)
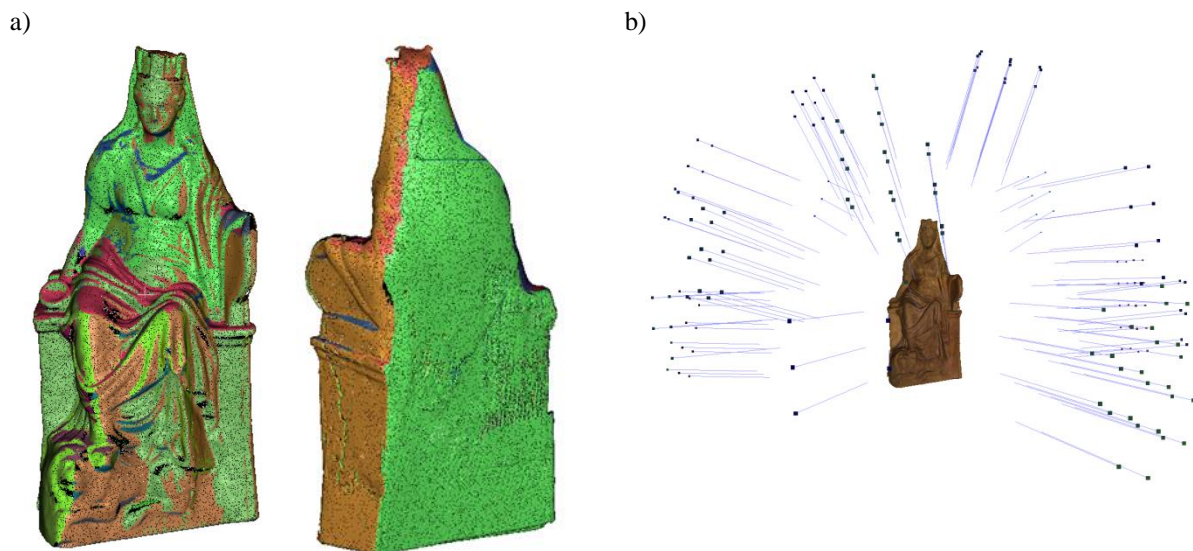
Figure 89. Results of NBV calculations for Kybele figurine: a) similarly oriented areas; b) calculated scanner poses.

For safety reasons, the measurement plan was launched in dry-run mode. No collisions or other problems were reported during this operation.
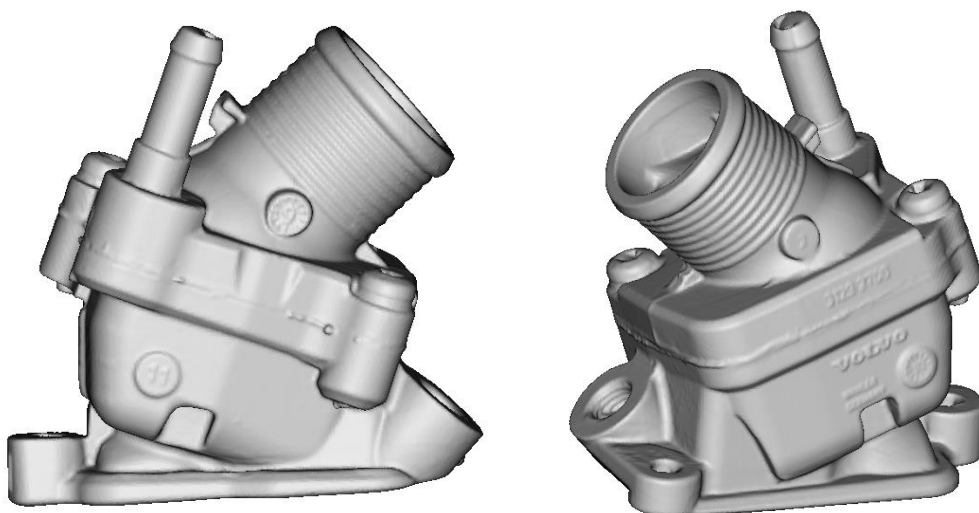
After dry-run, normal scanning with SWV were started. The whole process took 3 hours, 46 minutes. After collection of measurement results, the subsequent scans were processed with noise-removal algorithm, fine integrated using ICP algorithm. Afterwards, global relaxation algorithm was run. Finally, algorithm for detecting discontinuities was started. It reported 4 holes in 3D model apart from lacking basis of the figurine (which cannot be digitized as it is occluded by table pedestal). Unfortunately, those holes could not be filled as two of them appear in deep cavities and the other two required to put the scanner below floor of the digitization station. Result of digitization is presented in Figure 90. Statistics for the whole

process are given in Table 11. For the high-resolution model, the color information was corrected (Karaszewski, et al., 2014) leading to better quality of the final model.

Figure 90 presents the close-ups of the model surface. It is worth emphasizing that the scanned object was not an original Kybele sculpture but its copy, printed on Z-Corp powder printer. Therefore, on the surface of the object, features like distinct layers which are typical for 3D print can be observed. Also, the surface is smooth thanks to acetone-based preservative treatment of the print.
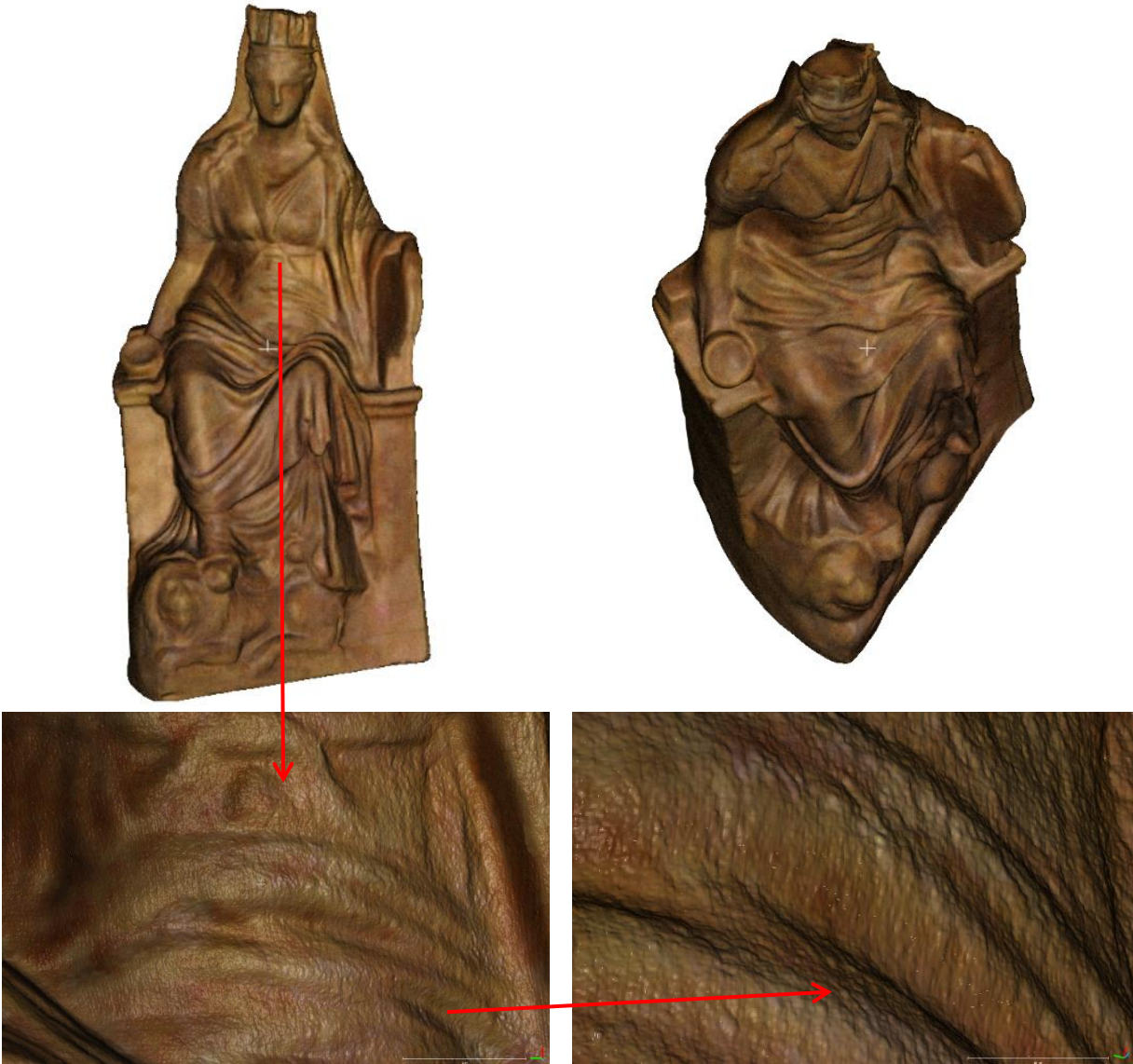
Figure 90. Final, high resolution model of Kybele figurine.

Parameter	Value / description
Number of measurements (LWV)	45
Time of rough scanning	0.8 h
Data processing of rough model	0.4 h
Points count (rough model)	21.2 M
Triangle mesh creation	0.06 h
Triangle mesh sampling to point cloud (average distance 0.5 mm)	0.02 h
NBV calculations	0.3 h
Number of measurements (SWV)	171
Dry-run time	0.35 h
Time of high-resolution scanning	3.76 h
Data processing of high-resolution model	1.27 h
Number of discontinuities excluding object base (detected / measureable)	4 / 0
Time of discontinuities filling	0 h
Points count (high-resolution model)	1238 M
Total digitization time	6.96 h

Table 11. Statistics for digitization process of Kybele figurine.

5.3.3 Gargoyle sculpture digitization

The polychrome-covered sculpture of Gargoyle was placed on the small pedestal fixed to rotating table. Due to weight and shape of the object, no additional fixing tools were necessary.

The complexity and size of the object required high number of directional measurements in the initial stage of digitization (57). After this process, obtained model was cleaned, fine-integrated and globally-relaxed. Those operations yielded 3D model which is shown in Figure 91. While geometrical complexity of the model is high, the integration phase was completed quickly. Rough 3D model was not treated with color correction procedure, therefore borders of measurements and other effects of uneven lighting are clearly visible.

Using rough 3D model of the Gargoyle, triangle mesh was created using Poisson surface reconstruction algorithm. This mesh, presented in Figure 92, was then sampled to provide homogenous cloud of points used in Next Best View calculations.

Next Best View calculations completed yielding 313 directional measurements for SWV 3D sensor. Figure 93 presents 3D model of sculpture with distinguished similarly-oriented regions (Figure 93a) as well as proposed measurement directions (Figure 93b). The system reported 29 collisions or occlusions in original set of proposed directions. 25 of them were mitigated using method presented in "Modification of observation vector" section of this dissertation. The remaining 4 directions remained unreachable.

Figure 91. Rough 3D model of Gargoyle composed of 57 directional measurements.
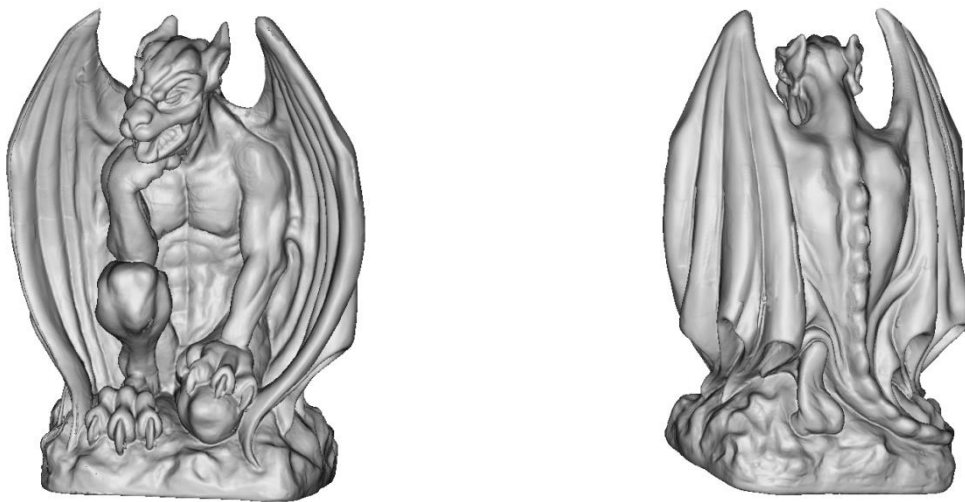
Figure 92. Triangle mesh created from rough 3D model of Gargoyle sculpture.

a)

b)
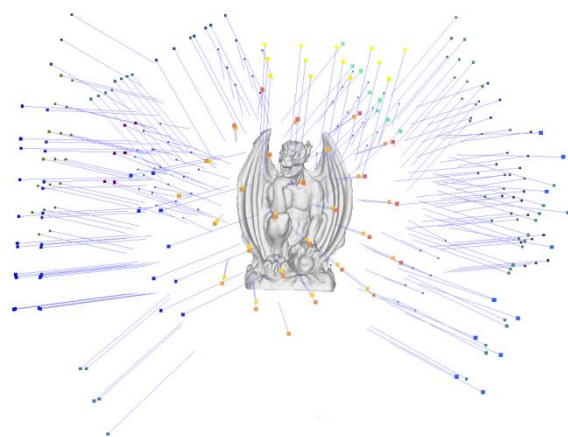
Figure 93. Results of NBV calculations for Gargoyle sculpture: a) similarly oriented areas; b) calculated scanner poses.

For safety reasons, the measurement plan was launched in dry-run mode. No collisions or other problems were reported during this operation.
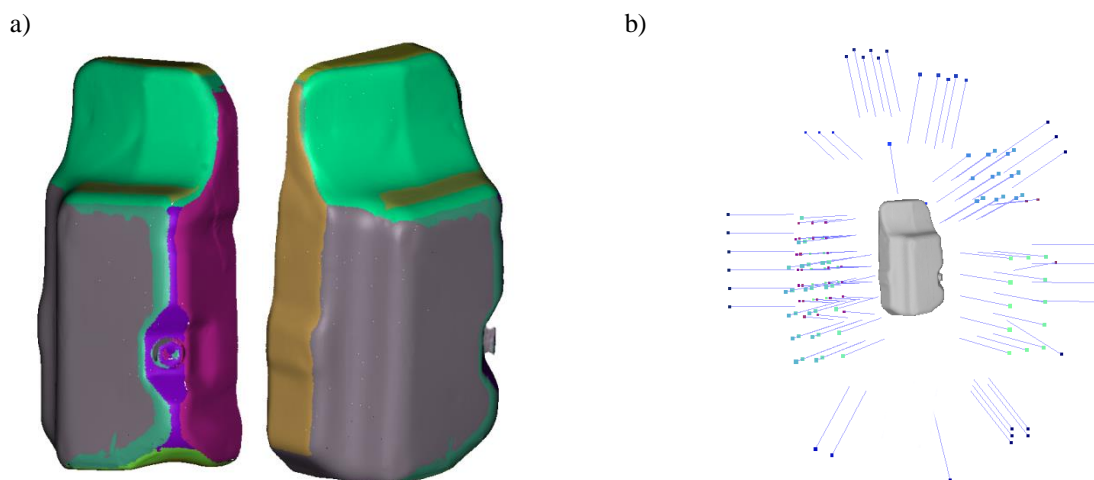
After dry-run, normal scanning with SWV were started. The whole process took 6 hours 42 minutes. After collection of measurement results, the subsequent scans were processed with noise-removal algorithm, fine integrated using ICP algorithm. Afterwards, global relaxation algorithm was run. Finally, algorithm for detecting discontinuities was started. It reported 7 holes in 3D model apart from lacking basis of the figurine (which cannot be digitized as it is occluded by table pedestal). One of the holes could be re-measured while other are placed in deep cavities which cannot be simultaneously seen by projector and detector of used 3D scanner. Result of digitization is presented in Figure 94. Statistics for the whole process are given in Table 12. The final model was processed with color-evening procedure. On the close-ups of the result point cloud, the smoothness of the surface can be observed. This is a result of the polychromic treatment of the scanned object which closed the pores in plaster and made the statue resistant to water and dirt.
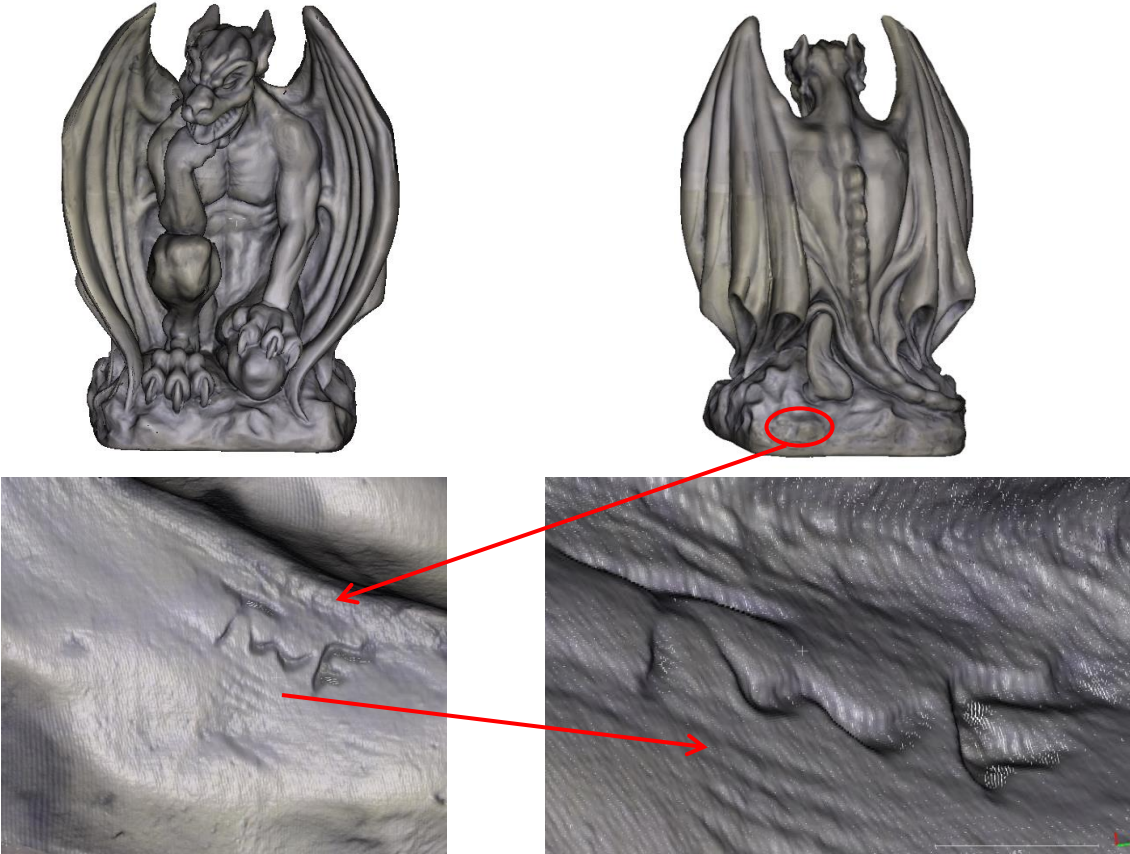
Figure 94. Final, high resolution model of Gargoyle figurine.

Parameter	Value / description
Number of measurements (LWV)	57
Time of rough scanning	0.9 h
Data processing of rough model	0.6 h
Points count (rough model)	29.3 M
Triangle mesh creation	0.1 h
Triangle mesh sampling to point cloud (average distance 0.5 mm)	0.05 h
NBV calculations	0.5 h
Number of measurements (SWV)	313
Dry-run time	1.1 h
Time of high-resolution scanning	6.7 h
Data processing of high-resolution model	5.4 h
Number of discontinuities excluding object base (detected / measureable)	7 / 1
Time of discontinuities filling	0.2 h
Points count (high-resolution model)	2541 M
Total digitization time	15.55 h

Table 12. Statistics for digitization process of Gargoyle sculpture.

5.3.4 Thermostat housing digitization

The aluminum thermostat housing was fixed in a vice which was in turn fixed a pedestal mounted on rotating table. The use of vice was necessary because the center of gravity of digitized object is far from its center, therefore the housing tends to shake or even fall over during table movements.

The size of the object and its moderate complexity reduced the number of required directional measurements in the initial stage of digitization (12), especially when compared to Gargoyle sculpture. After performing those measurements, obtained model was cleaned, fine-integrated and globally-relaxed. Those operations yielded 3D model which is shown at Figure 95.

The color information was removed from presented images as such information is not usually used in technical parts 3D scans. Moreover, the thermostat housing was not new (i.e. it was removed from a car) and therefore its surface was not as in new parts.

Using rough 3D model of the housing, triangle mesh was created using Poisson surface reconstruction algorithm. This mesh, presented in Figure 96, was then sampled to provide homogenous cloud of points used in Next Best View calculations.

Next Best View calculations completed yielding 59 directional measurements for SWV 3D sensor. Figure 97 presents 3D model of sculpture with distinguished similarly-oriented regions (Figure 97a) as well as proposed measurement directions (Figure 97b). The system

reported 21 collisions or occlusions in original set of proposed directions. 18 of them were mitigated using method presented in "Modification of observation vector" section of this dissertation. The remaining 3 directions remained unreachable.
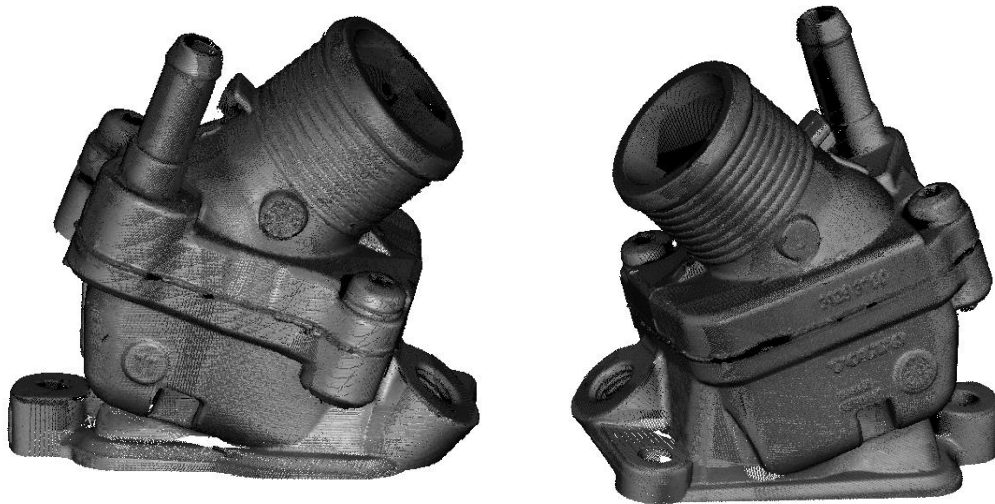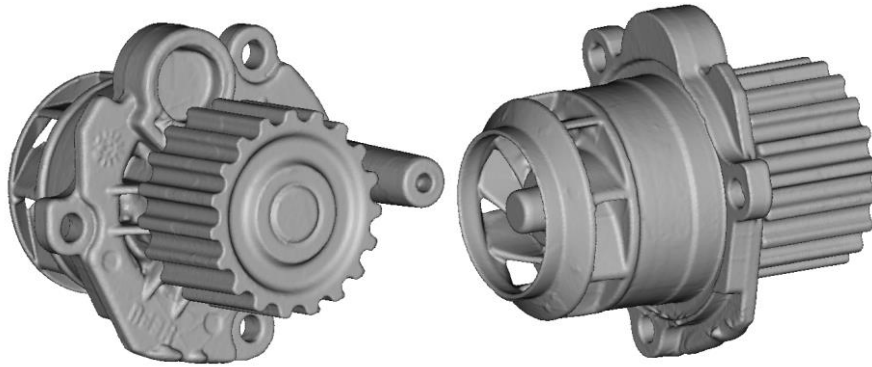

Figure 95. Rough 3D model of thermostat housing composed of 12 directional measurements.

For safety reasons, the measurement plan was launched in dry-run mode. No collisions or other problems were reported during this operation.

Figure 96. Triangle mesh created from rough 3D model of thermostat housing.

After dry-run, normal scanning with SWV were started. The whole process took 1 hour and 15minutes. After collection of measurement results, the subsequent scans were processed with noise-removal algorithm, fine integrated using ICP algorithm. Afterwards, global relaxation algorithm was run. Finally, algorithm for detecting discontinuities was started. It reported 3 holes in 3D model apart from areas occluded by vice and pedestal. None of the holes could be

re-measured due to multiple occlusions. Result of digitization is presented in Figure 98. Statistics for the whole process are given in Table 13. When looking at high resolution model using big magnification, the structure may be observed on the surface. It is probably the result of cleaning the part with sandpaper. This structure is not so well visible on the rough model. Dark areas on the 3D model represent places where shiny silicone seal was protruding.

a)

b)
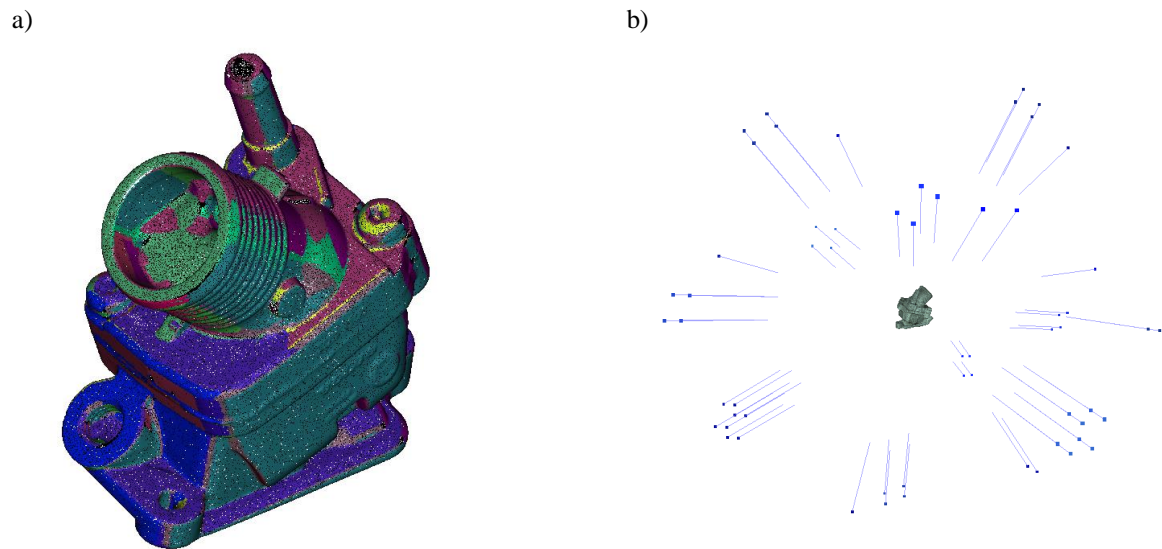
Figure 97. Results of NBV calculations for thermostat housing: a) similarly oriented areas; b) calculated scanner poses.
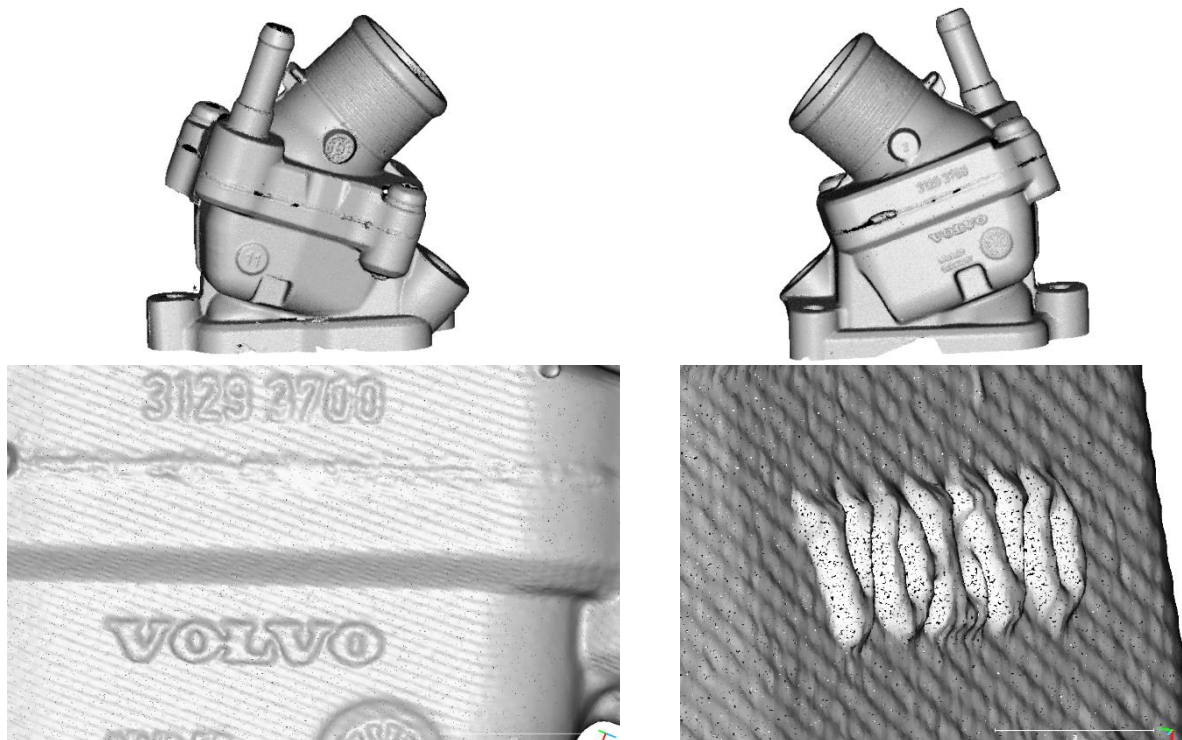
Figure 98. Final, high resolution model of thermostat housing.

Parameter	Value / description
Number of measurements (LWV)	12
Time of rough scanning	0.2 h
Data processing of rough model	0.1 h
Points count (rough model)	4.8 M
Triangle mesh creation	0.02 h
Triangle mesh sampling to point cloud (average distance 0.5 mm)	0.01 h
NBV calculations	0.1 h
Number of measurements (SWV)	59
Dry-run time	0.2 h
Time of high-resolution scanning	1.25 h
Data processing of high-resolution model	0.4 h
Number of discontinuities excluding object base (detected / measureable)	13 / 0
Time of discontinuities filling	0.0 h
Points count (high-resolution model)	384 M
Total digitization time	2.28 h

Table 13. Statistics for digitization process of thermostat housing.

5.3.5   Oil sump digitization

The aluminum oil sump was fixed pedestal mounted on rotating table with hot glue. The use glue was necessary because the center of gravity of digitized object (when it stands on its narrow wall) is far from its center, therefore the housing tends to shake or even fall over during table movements.

The complexity of the object is low, but the size is comparable to 3D sensor working volume. Because of this, initial digitization required 28 measurements. After performing those measurements, obtained model was cleaned, fine-integrated and globally-relaxed. Those operations yielded 3D model which is shown in Figure 99. The sump is not geometrically complicated, therefore integration of directional measurements took a long time. The model presented in Figure 99 is edited – the border of sump which connects to the engine was removed. This was caused by severe damage (spikes, splinters etc.) to this part of sump (the object comes from car scrapyard) which made the measurement of this section almost impossible. Color information was removed from the measurements.
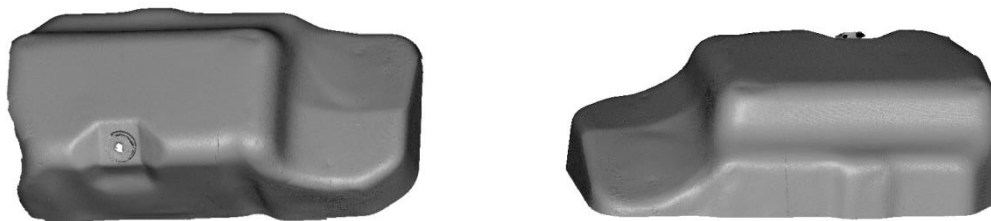
Figure 99. Rough 3D model of oil sump composed of 28 directional measurements.

143

Using rough 3D model of the sump, triangle mesh was created using Poisson surface reconstruction algorithm. This mesh, presented in Figure 100, was then sampled to provide homogenous cloud of points used in Next Best View calculations.
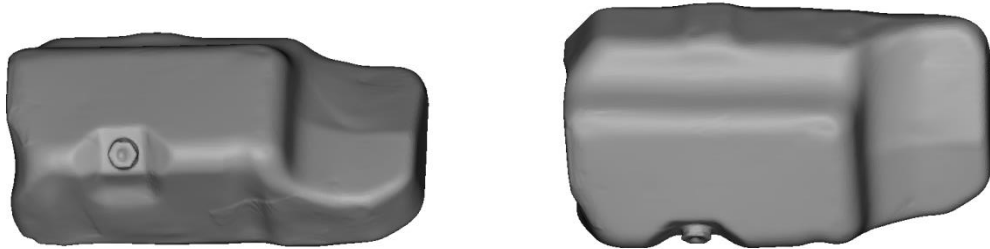
Figure 100. Triangle mesh created from rough 3D model of oil sump.

Next Best View calculations completed yielding 157 directional measurements for SWV 3D sensor. Figure 101Figure 85 presents 3D model of sculpture with distinguished similarly-oriented regions (Figure 101a) as well as proposed measurement directions (Figure 101b). The system reported 3 collisions or occlusions in original set of proposed directions. All of them were mitigated using method presented in "Modification of observation vector" section of this dissertation.

For safety reasons, the measurement plan was launched in dry-run mode. No collisions or other problems were reported during this operation.

a)   b)

Figure 101. Results of NBV calculations for oil sump: a) similarly oriented areas; b) calculated scanner poses.

After dry-run, normal scanning with SWV were started. The whole process took 3 hours 20 minutes. After collection of measurement results, the subsequent scans were processed with noise-removal algorithm, fine integrated using ICP algorithm. As the object is not complicated geometrically, integration of directional measurements posed a problem (surface lacked distinct features for ICP algorithm). Therefore, high-resolution measurements were

fitted to rough model from first stage of digitization). Afterwards, global relaxation algorithm was run. Finally, algorithm for detecting discontinuities was started. It reported no holes in 3D model apart from areas occluded by pedestal. Result of digitization is presented in Figure 102. Statistics for the whole process are given in Table 14. High resolution measurements allow to see little dents on the surface of the sump as well as not removed grease and dirt aggregations.
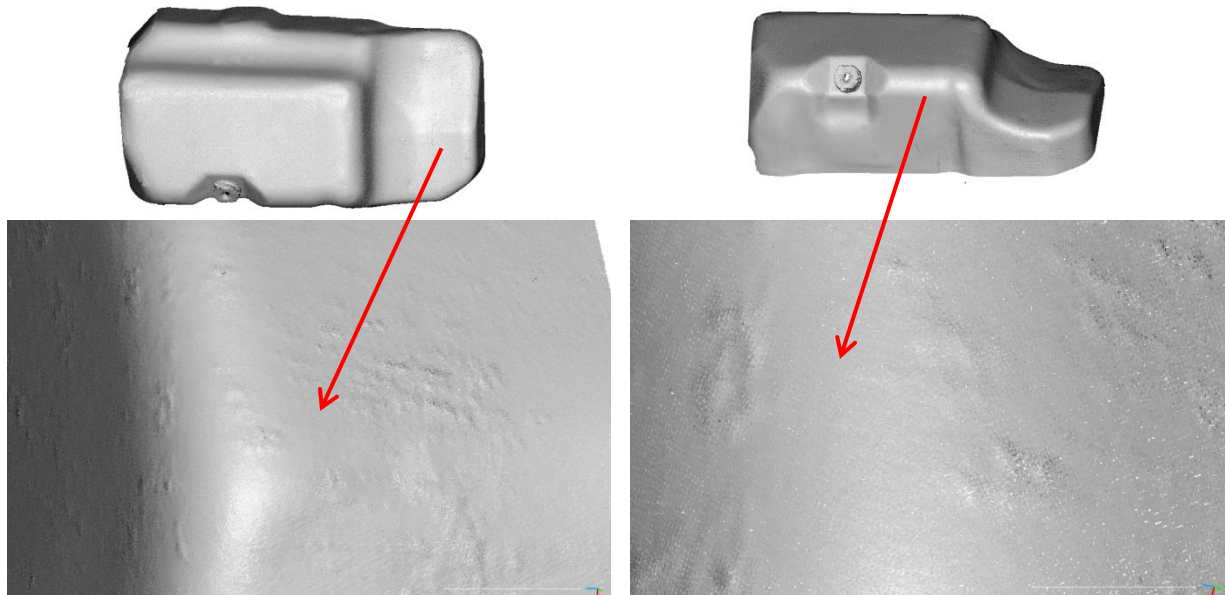
Figure 102. Final, high resolution model of oil sump.

Parameter	Value / description
Number of measurements (LWV)	28
Time of rough scanning	0.5 h
Data processing of rough model	0.3 h
Points count (rough model)	15.1 M
Triangle mesh creation	0.1 h
Triangle mesh sampling to point cloud (average distance 0.5 mm)	0.05 h
NBV calculations	0.2 h
Number of measurements (SWV)	157
Dry-run time	0.75 h
Time of high-resolution scanning	3.33 h
Data processing of high-resolution model	1.8 h
Number of discontinuities excluding object base (detected / measureable)	0 / 0
Time of discontinuities filling	0.0 h
Points count (high-resolution model)	1301 M
Total digitization time	7.03 h

Table 14. Statistics for digitization process of oil sump.

5.3.6 Water pump digitization

The aluminum water pump was fixed in a vice which was in turn fixed a pedestal mounted on rotating table. The use of vice was necessary because the object does not have flat base on which it could lie on.

High complexity of the object caused high number of required directional measurements in the initial stage of digitization (26), especially when size of the object is considered. After performing those measurements, obtained model was cleaned, fine-integrated and globally-relaxed. Those operations yielded 3D model which is shown in Figure 103. The water pump has very complicated shape and many occluded areas, especially in the part where pump rotor is present. Because of this reason it poses significant problem for scanning, even for experienced operator. The initial stage of automated digitization yielded a model which has several discontinuities. As such the model is far from perfect, but it is good enough for farther processing.
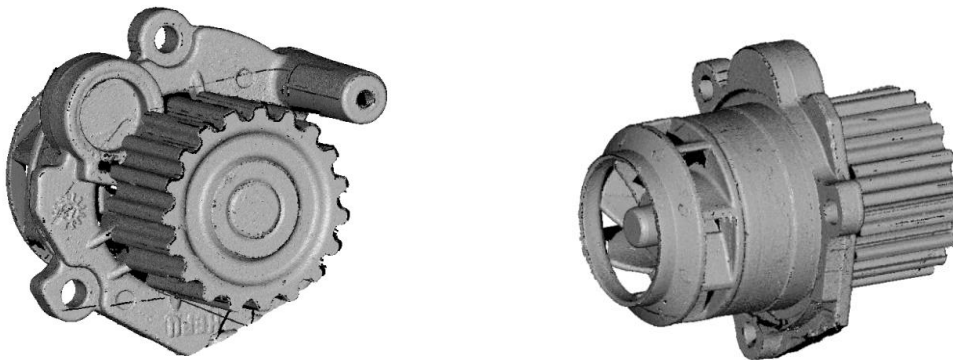
Figure 103. Rough 3D model of water pump composed of 26 directional measurements.

Using rough 3D model of the housing, triangle mesh was created using Poisson surface reconstruction algorithm. This mesh, presented in Figure 104, was then sampled to provide homogenous cloud of points used in Next Best View calculations. As it is clearly visible, the triangulation filled the areas with discontinuities, however sometimes the generated geometry was deviated from the original shape. This deviation causes suboptimal measurement direction calculations for high-resolution stage of digitization.

Next Best View calculations completed yielding 86 directional measurements for SWV 3D sensor. Figure 105 presents 3D model of sculpture with distinguished similarly-oriented regions (Figure 105a) as well as proposed measurement directions (Figure 105b). The system reported 14 collisions or occlusions in original set of proposed directions. 8 of them were

mitigated using method presented in "Modification of observation vector" section of this dissertation. The remaining 6 directions remained unreachable.

Figure 104. Triangle mesh created from rough 3D model of water pump.

a)   b)
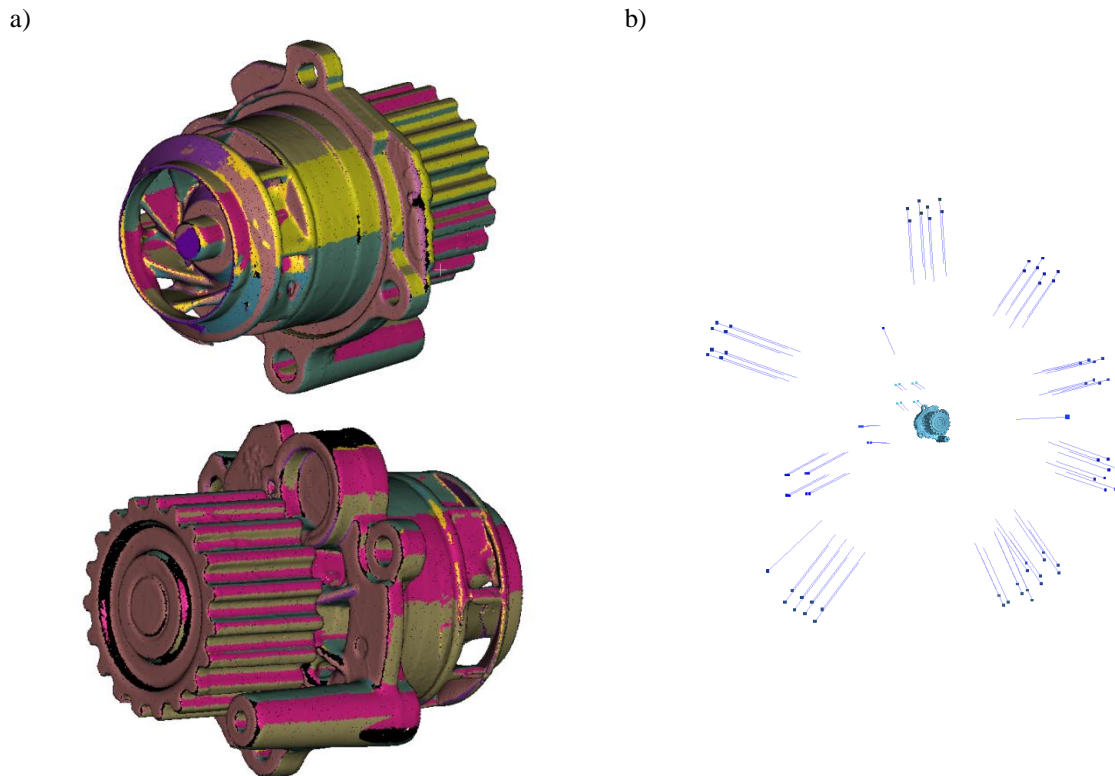
Figure 105. Results of NBV calculations for water pump: a) similarly oriented areas; b) calculated scanner poses.

For safety reasons, the measurement plan was launched in dry-run mode. No collisions or other problems were reported during this operation.

After dry-run, normal scanning with SWV were started. The whole process took 1 hour 45 minutes. After collection of measurement results, the subsequent scans were processed with noise-removal algorithm, fine integrated using ICP algorithm. Afterwards, global relaxation algorithm was run. Finally, algorithm for detecting discontinuities was started. It reported 7 holes in 3D model apart from areas occluded by vice and pedestal. None of the holes could be

re-measured due to multiple occlusions. Result of digitization is presented in Figure 86. Statistics for the whole process are given in Table 15. The pump, while being used element, shows very little signs of wear. However, when high resolution model is observed, slight damage to pulley gear teeth can be noticed.
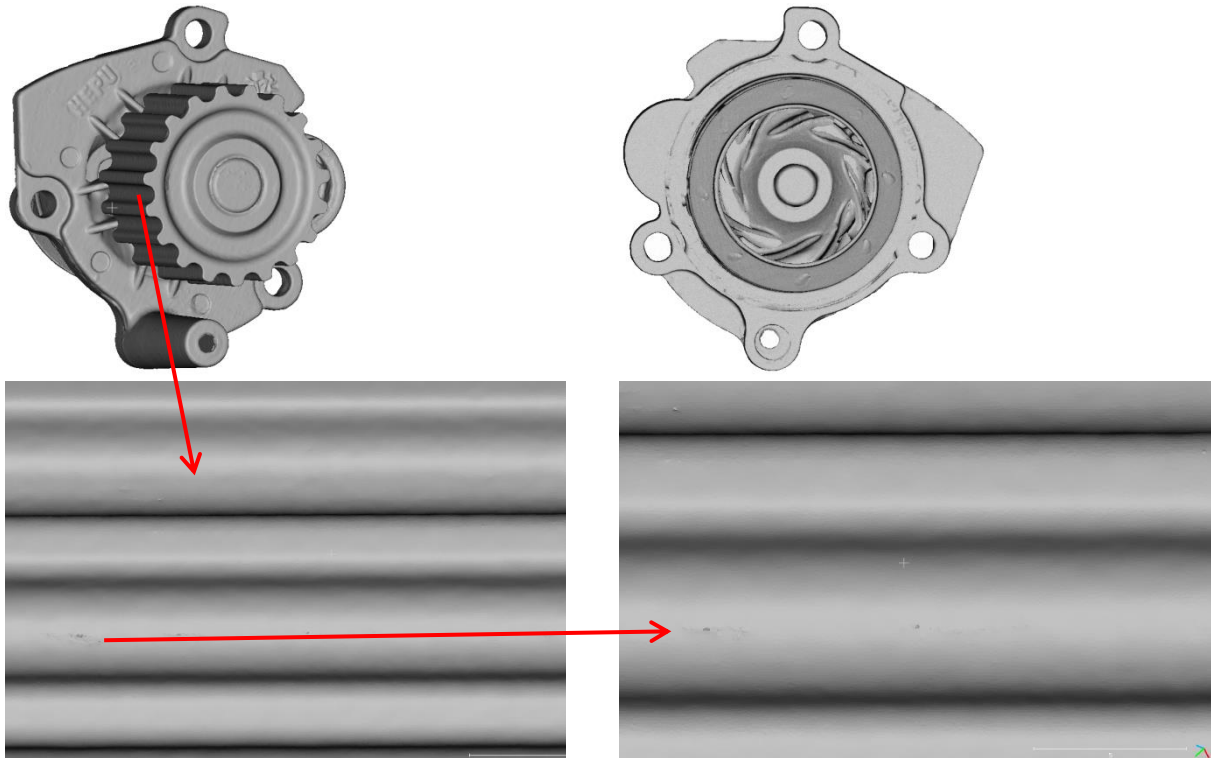
Figure 106. Final, high resolution model of water pump.

Parameter	Value / description
Number of measurements (LWV)	26
Time of rough scanning	0.5 h
Data processing of rough model	0.3 h
Points count (rough model)	6.2 M
Triangle mesh creation	0.1 h
Triangle mesh sampling to point cloud (average distance 0.5 mm)	0.05 h
NBV calculations	0.3 h
Number of measurements (SWV)	86
Dry-run time	0.3 h
Time of high-resolution scanning	1.75 h
Data processing of high-resolution model	0.95 h
Number of discontinuities excluding object base (detected / measureable)	17 / 0
Time of discontinuities filling	0.0 h
Points count (high-resolution model)	623 M
Total digitization time	4.25 h

Table 15. Statistics for digitization process of water pump.

5.3.7   Summary

The digitization of exemplary cultural heritage objects (votive altar, Kybele and Gargoyle sculptures) and mechanical parts (thermostat housing, oil sump, water pump) using HD3D|AUTO system was successful. Most importantly, for all objects, their high resolution 3D models with high surface coverage were obtained. Some discontinuities were present in the models (Figure 107), but they occurred in places which could not be at the same time visible for projector and camera of used scanner. Such areas are impossible to digitize even by experienced operator.
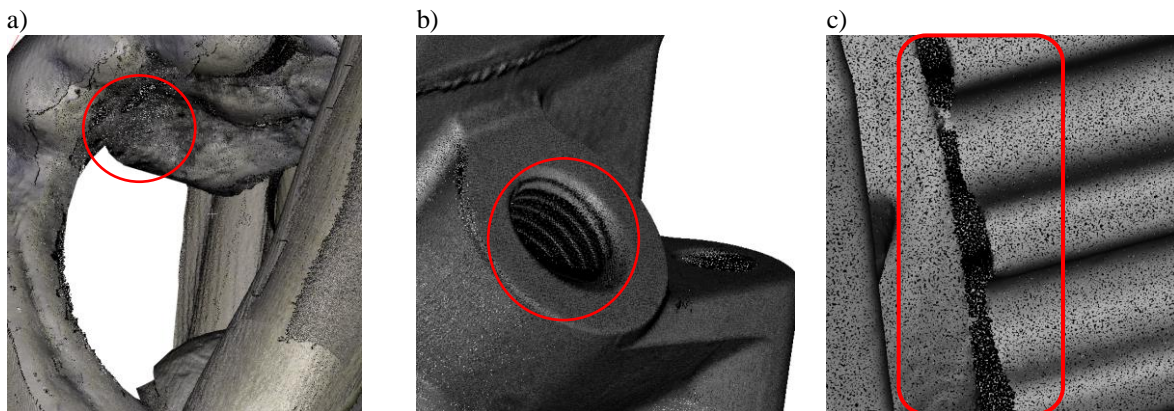
Figure 107. Examples of areas with discontinuities caused by occlusions: a) the inner part of Gargoyle's hand; b) inside of threaded hole in thermostat housing; c) cavity between the pulley and water pump chassis.

In all cases, the process did not require any operator assistance, apart from fixing the object to rotating stage. There were no collisions during scanner positioning nor any of measurements was empty (i.e. did not contain some part of surface measured object). Overall, it can be stated that the HD3D|AUTO system allows for autonomous, high quality, high-resolution 3D digitization of typical cultural heritage objects and mechanical parts.

5.4 Comparison of digitization with HD3D|AUTO to experienced operator

To assess performance of HD3D|AUTO system during digitization process in relation to semi-automated digitization performed by experienced operator, two models of objects (biscuits) from Museum of King Jan III's Palace in Wilanów 3D collection were chosen to represent typical digitization targets. For those objects, high resolution digitization was already performed in the Museum of King Jan III's Palace in Wilanów 3D Documentation Laboratory by highly skilled operators.
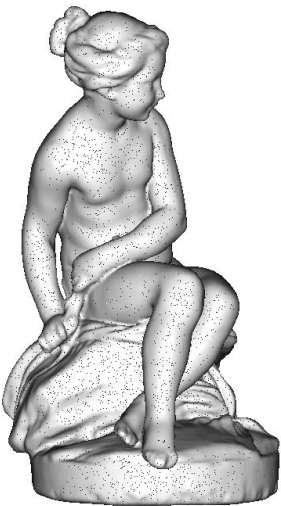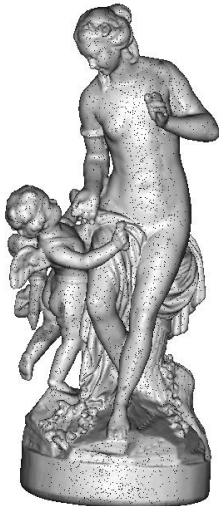
Object	Description	3D model (obtained from Museum of King Jan III's Palace in Wilanów 3D Documentation Laboratory)
Wil. 3739 "Psyche"	Psyche figurine was made by Etienne-Maurice Falconet in 1761 year in Sevres. The size of the object is: 235 mm x 130 mm x 117 mm. Geometrically it is not very complicated, however some cavities and self-occlusions are present. The object is moderately challenging for 3D scanning. Digitization performed in the 3D Documentation Laboratory required 139 directional measurements using 3D scanner with 50mm x 50mm x 25mm working volume.	
Wil. 4178 "Venus and Cupid"	The biscuit presenting Venus and Cupid was made in Paris at La Courtille manufactory, at the beginning of XIXth century. The size of the object is: 300 mm x 133 mm x 111 mm. Geometrically much more complicated than Psyche figurine, this object poses significant challenge for operator due to high number of occluded areas and deep cavities. Digitization performed in the 3D Documentation Laboratory required 182 directional measurements using 3D scanner with 50mm x 50mm x 25mm working volume.	

Table 16. Objects from Museum of King Jan III's Palace in Wilanów 3D which were used for performance evaluation of HD3D|AUTO system in relation to experienced operator.

5.4.1   Performance assessment

The assessment of HD3D|AUTO performance in comparison with skilled operator is performed by calculating directional measurements (using virtual measurement head with the same working volume and positioning system configuration as used in Laboratory for 3D digitization). Real measurements are not performed because of the problem with access to objects. However, digitization projects described in previous chapter (altar, Kybele, Gargoyle figurines, mechanical parts), proved that performing digitization using measurement poses calculated by HD3D|AUTO method allows to obtain 3D model of an object with surface coverage similar to the one calculated in occlusion/collision checking stage of HD3D algorithm. Basing on this assumption, the only two parameters which is used for comparing human operator and HD3D|AUTO system are the number of directional measurements and surface coverage. The time of digitization process with HD3D|AUTO is calculated by multiplying number of measurements by average time of positioning and measurement observed during digitization processes described in the previous section of this dissertation.

To allow for HD3D NBV calculations, 3D models of antique objects, provided by Museum of King Jan III's Palace in Wilanów 3D Documentation Laboratory as point clouds, were treated as rough models usually obtained in the first stage of HD3D|AUTO digitization process. Those models were then triangulated using Poisson surface reconstruction algorithm which filled all discontinuities in models. Point clouds with homogenous point-to-point distance were created by sampling those meshes. Those datasets were then used as input data for HD3D Next Best View module.

a)   b)
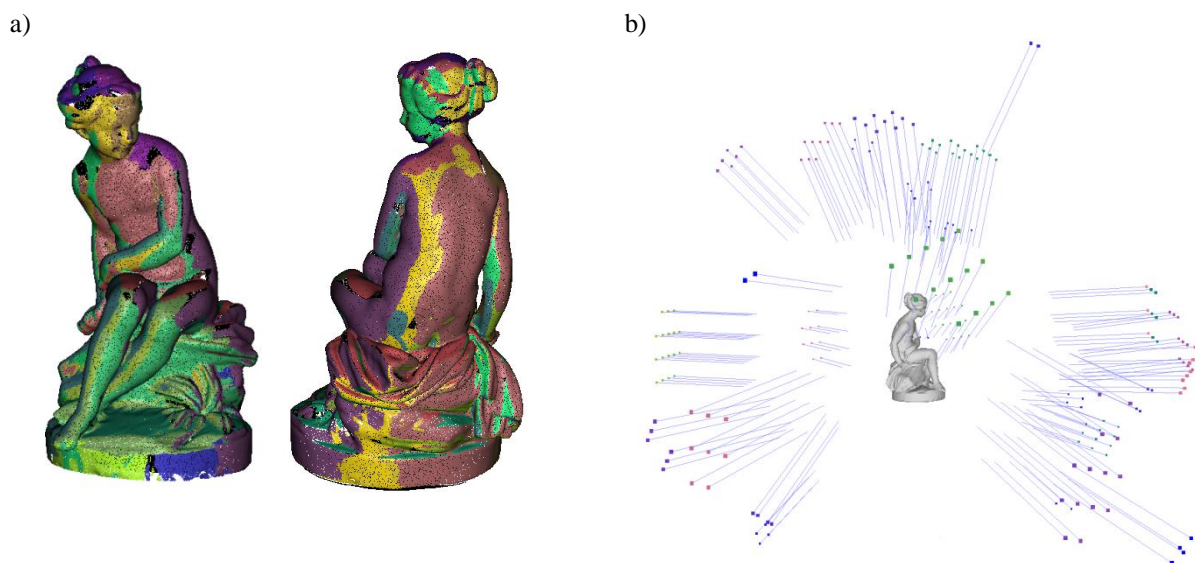
Figure 108. High-resolution Next Best View algorithm results for Wil. 3739 object: a) visualization of similarly-oriented surfaces, b) calculated measurement directions.

a)   b)
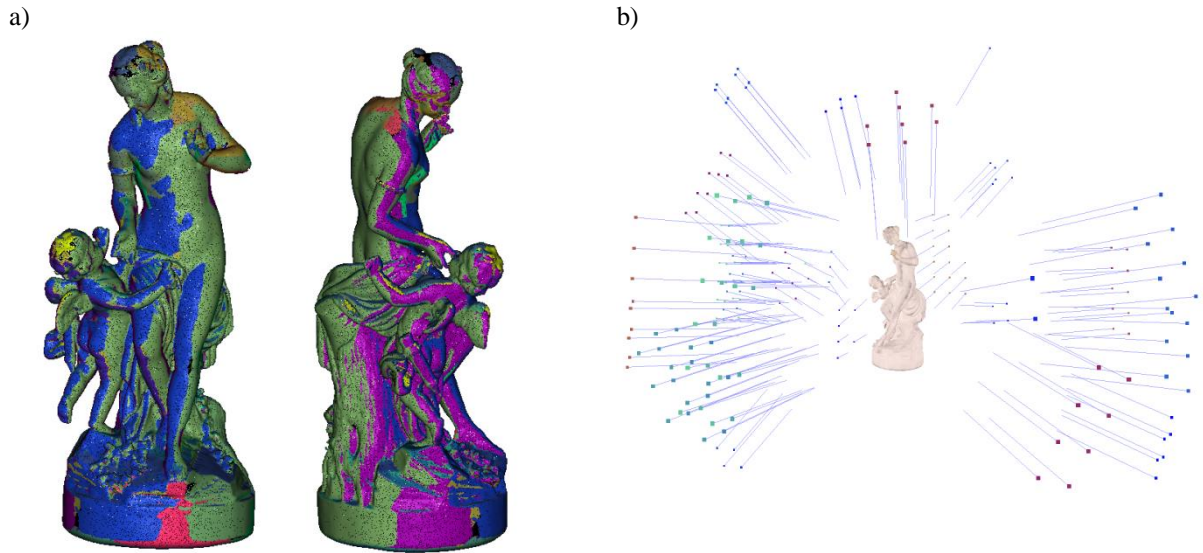
Figure 109. High-resolution Next Best View algorithm results for Wil. 4178 object: a) visualization of similarly-oriented surfaces, b) calculated measurement directions.

Statistics comparing operator-controlled and fully automated digitization processes for Wil. 3738 object are presented in Table 17. Similar comparison for Wil. 4178 object is given in Table 18. Surface coverage was calculated by comparing density of point cloud (from Museum or from HD3D calculations) to triangle mesh (obtained with Poisson-surface-reconstruction). Time of digitization process for HD3D|AUTO was calculated using average time of positioning and obtaining directional cloud of points for high-resolution measurement head from all previous digitization processes (about 74 seconds).

Parameter / system	Semi-automated, guided by Museum of King Jan III's Palace in Wilanów 3D Documentation Laboratory operator	Fully-automated (HD3D|AUTO)
Number of directional measurements (time of digitization process)	139 (8.5 hours)	169 (3.5 hours)
Surface coverage [%]	96 % 	95%

Table 17. Comparison of semi- and fully automated digitization processes for Wil. 3739 object. Histograms present density of point cloud related to triangle mesh. Histogram values lower than 9 are considered as not measured correctly.

152
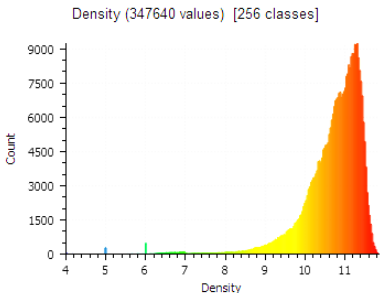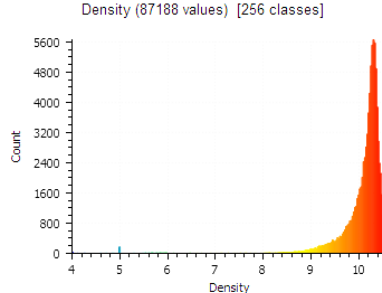
Parameter / system	Semi-automated, guided by operator from Museum of King Jan III's Palace in Wilanów 3D Documentation Laboratory	Fully-automated (HD3D|AUTO)
Number of directional measurements	182 (13 hours)	198 (4.1 hours)
Surface coverage [%]	85% Density (347640 values) [256 classes]	83% Density (87188 values) [256 classes]

Table 18. Comparison of semi- and fully automated digitization processes for Wil. 4178 object. Histograms present density of point cloud related to triangle mesh. Histogram values lower than 9 are considered as not measured correctly.

5.4.2 Summary

The comparison of performance between skilled human operator and HD3D|AUTO system was assessed using data from Museum of King Jan III's Palace in Wilanów 3D Documentation Laboratory. The objects (biscuit figurines) were digitized by robotized system controlled by experienced operators. This system automatically placed 3D measurement head in places indicated by the operator, so the set of measurement poses is a result of their skill and 3D imagination. Sometimes, those poses are not optimal, especially when occlusion happens. On the contrary, in HD3D|AUTO system, the set of poses is calculated using algorithm described in this dissertation. This algorithm includes analysis of possible robot collisions and scanner optical paths occlusions which allows for higher surface coverage measurements.

Results of comparison, presented in Table 17 and Table 18, confirm high performance of HD3D|AUTO system. The number of directional measurements which were required to digitize given objects is slightly higher than in case of operator-guided process, the surface coverage is comparable. While this at first may be considered as HD3D|AUTO mediocre performance, the skill of Museum of King Jan III's Palace in Wilanów 3D Documentation Laboratory operators has to be taken into account. In essence, the fully autonomous

digitization system performs similarly to highly skilled specialists. While the system can work in 24/7 operating mode, does not get tired nor have worse days and can work without any supervision, it may produce high quality 3D models much faster than trained operators – as indicated in Table 17 and Table 18.

6. Conclusions

The process of obtaining 3D digital models of real-world objects is a complicated process. The complexity rises significantly with spatial resolution of model because high resolution 3D sensors have small working volume and thus require more directional measurements to cover the whole surface of object. In professional 3D documentation, for example used in cultural heritage, the spatial resolution may reach 2500 points per mm^2 or even higher. Therefore, to obtain 3D model of typical digitization target, few hundred of directional measurements may be required. At this point, conducting the process manually becomes almost impossible or at least very time consuming and costly. Therefore automation of the process is well-founded.

In this dissertation, the automated 3D high-resolution digitization station is presented along with all of its hardware and software modules and results of its performance assessment. The successful development of the station and results of digitization processes (shown in Chapter 4) confirms achievement on the research claim. The claim, stated at the beginning of this work, is that automated 3D digitization system will allow make it possible to obtain high resolution 3D models of objects, simultaneously lowering cost, shortening time of such process and eliminating influence of operator on measurement result.

6.1 Fulfillment of research claim

Digitization processes conducted in order to assess HD3D|AUTO system performance involved various real-world objects. Cultural heritage objects (votive altar, Kybele and Gargoyle figurines) represented typical targets of professional 3D documentation created for conservators, art historians etc. Even moderately complicated object like Gargoyle figurine was digitized successfully by HD3D|AUTO system with resolution of 2500 points per mm^2. There was no need for operator intervention during all scanning projects. Even tough more than 300 directional measurements were required for Gargoyle digitization, the whole process (with data processing) took less than 16 hours. Similarly, technical parts were successfully digitized. 3D model of the most complicated object (water pump) was obtained in less than 4.5 hours with only 7 areas of surface discontinuity.

The comparison of HD3D|AUTO system performance with semi-automated system guided by experienced operator confirms high efficiency of fully automated digitization. While obtained surface coverage was slightly smaller than in semi-automated process, the shortening of the time of the process was significant. Moreover, as automated system may work 24 hours per day, the possibility of significant time gains for typical digitization processes is high. Eliminating the need of skilled-operator attendance during the process not only lowers its cost, but also eliminates influence of the operator on obtained 3D model.

Taking above stated facts, research claims may be acknowledged as fulfilled.

6.2 Research and application objectives

During realization of this work, following research fields were completed:

- development of the method allowing for calculation of a set of measurement directions to be used for obtaining high-resolution 3D model of unknown object with high surface coverage (Chapter 4);
- development of the method for collision and occlusion detection and avoidance for set of measurement directions (Chapter 4.2.4);
- evaluation of developed NBV method for various classes of objects (Chapter 5) and comparison to other NBV algorithms (Chapter 4.3).

The following application field objectives were completed:

- construction of the automated digitization system, with high-resolution, color 3D scanner, 6axis robot arm and rotary stage (Chapter 4.2);
- implementation of applications controlling robot and table movements as well as libraries for NBV calculations (Chapter 5.2);
- digitization of few representative cultural heritage objects as well as technical parts in order to test and prove the potential of the new NBV method in future applications (Chapter 5).

6.3 Future work directions

The HD3D|AUTO system is capable of obtaining high-quality high-resolution 3D model of real-world objects without using any a priori knowledge about their surface apart from general dimensions of the object. The time of digitization and complexity of the process is moderately reduced, when compared to operator-guided digitization. However, few elements of the system should be addressed to further improve its performance and quality: directional measurements fine integration and color correction.

6.3.1 Fine integration

During digitization of test objects, especially when the object is not very complicated, the problem of data integration occurs. When the measured surface has low number of distinct geometrical features, the ICP algorithm may introduce errors to the model. Those errors may usually be corrected by global relaxation algorithm, but nevertheless sometimes persist in the model. This problem should be dealt with using either extended version of ICP (for example utilizing color information) or other fine integration algorithm.

6.3.2 Color correction

The unevenness of color information which is caused by different lighting and observation conditions (direction) during subsequent measurements is a significant problem in cultural heritage documentation. The color correction method which was used for objects presented in Chapter 5 provides good results when the object is semi-flat. The more shape gradient occur, the more uneven color is recovered. It is probably inevitable to deal with this problem without additional, ideally shadow-less lighting. This kind of lighting is hard to introduce when there are moving objects (robot, scanner head) near the digitization target.

References

3D Systems, 2016. *Sense™.* [Online]
Available at: http://www.3dsystems.com/shop/sense
[Accessed 03 10 2016].

ABB, 2016. *ABB IRB4400.* [Online]
Available at:
http://www.abb.com/product/seitp327/7d5dc02dc2cf8db0c12575580006b119.aspx
[Accessed 09 09 2016].

Ahmadabadian, A. H., Robson, S., Boehm, J. & Shortis, M., 2014. Stereo-imaging network design for precise and dense 3d reconstruction. *The Photogrammetric Record*, pp. 317-336.

Aicon 3D Systems, 2016. *Aicon SmartScan.* [Online]
Available at: http://aicon3d.de/produkte/aicon-scanner/smartscan/auf-einen-blick.html
[Accessed 22 10 2016].

Ajmal, M., Bennamoun, M. & Owens, R., 2010. On the repeatability and quality of keypoints for local feature-based 3d object retrieval from cluttered scenes. *International Journal of Computer Vision*, pp. 348-361.

Altintas, Y., 2012. *anufacturing automation: metal cutting mechanics, machine tool vibrations, and CNC design.* s.l.:Cambridge University Press.

Artec, 2016. *Artec Spider.* [Online]
Available at: https://www.artec3d.com/3d-scanner/artec-spider
[Accessed 22 09 2016].

Autodesk, 2017. *Autodesk Inventor.* [Online]
Available at: https://www.autodesk.pl/products/inventor/overview
[Accessed 21 05 2017].

Bagci, E., 2009. Reverse engineering applications for recovery of broken or worn parts and re-manufacturing. *Advances in Engineering Software*, pp. 407-418.

Banks, S. A., 2008. *Radiographic medical imaging system using robot mounted source and sensor for dynamic image capture and tomography.* USA, Patent No. 7.

159

Banta, J., Wong, L. & Abidi, M., 2000. *A next-best-view system for autonomous 3-D object reconstruction.* s.l., s.n., p. 589−598.

Barrile, V., Bilotta, G., Lamari, D. & M. G. M., 2015. Comparison between techniques for generating 3D models of cultural heritage. *Recent Advances in Mechanics, Mechatronics and Civil, Chemical and Industrial Engineering, Mathematics and Computers in Science and Engineering Series*, pp. 140-145.

Basler, 2016. *Basler TOF.* [Online]
Available at: http://www.baslerweb.com/en/products/cameras/3d-cameras/time-of-flight-camera
[Accessed 29 09 2016].

Basler, 2017. *Basler - the power of sight.* [Online]
Available at: https://www.baslerweb.com/en/products/product-highlights/ace-10mp-14-mp-models/
[Accessed 22 05 2017].

Bathow, C. & Breuckmann, B., 2011. *High-definition 3D acquisition of archaeological objects: An overview of various challenging projects all over the world..* s.l., s.n., pp. 12-16.

Bay, H., Tuytelaars, T. & Van Gool, L., 2006. *Surf: Speeded up robust features.* s.l., Springer Berlin Heidelberg, pp. 404-417.

Benford, S. et al., 1998. Understanding and constructing shared spaces with mixed-reality boundaries. *ACM Transactions on Computer-Human Interaction*, pp. 185-223.

Beraldin, J. A. et al., 2003. *Active 3D sensing.* s.l.:National Research Council of Canada.

Beraldin, J. A. et al., 2007. *Traceable 3D imaging metrology: Evaluation of 3D digitizing techniques in a dedicated metrology laboratory.* s.l., s.n.

Bernardini, F. & Rushmeier, H., 2002. The 3D model acquisition pipeline. *Computer graphics forum*, pp. 149-172.

Bertsekas, D. P., 1999. *Nonlinear programming.* s.l.:Belmont: Athena scientific.

Besl, P. J. & McKay, N. D., 1992. Method for registration of 3-D shapes. *Robotics-DL tentative*, pp. 586-606.

Bianchi, S. D. et al., 2004. Evaluation of scanning parameters for a surface colour laser scanner. *International Congress Series*, pp. 1162-1167.

Bitner, J. R., Ehrlich, G. & Reingold, E. M., 1976. Efficient generation of the binary reflected Gray code and its applications. *Communications of the ACM*, pp. 517-512.

Borisov, K., 2015. *The Captain.* [Online]
Available at: http://www.thingiverse.com/thing:941025
[Accessed 2 9 2015].

Bottino, A. & Laurentini, A., 2008. A nearly optimal sensor placement algorithm for boundary coverage. *Pattern Recognition*, pp. 3343-3355.

Bresenham, J., 1965. Algorithm for computer control of a digital plotter. *IBM Systems Journal*, pp. 25-30.

Buller, G. S. et al., 2005. Multiple wavelength time-of-flight sensor based on time-correlated single-photon counting. *Review of Scientific Instruments*.

Bunsch, E., 2010. *Praktyczne aspekty digitalizacji zabytków* [Interview] (24 08 2010).

Bunsch, E., Sitnik, R. & Michoński, J., 2011. *Art documentation quality in function of 3D scanning resolution and precision.* s.l., International Society for Optics and Photonics, pp. 78690D-78690D-11.

Büttner, H., Janssen, D. & Rostan, M., 2003. EthetCAT- the Ethernet fieldbus. *PC Control Magazine*, pp. 14-19.

Calhoun, G. L. et al., 2005. *Synthetic Vision System for Improving Unmanned Aerial Vehicle Operator Situation Awareness.* s.l., SPIE.

Callieri, M. et al., 2004. *RoboScan: an automatic system for accurate and unattended 3D scanning.* s.l., IEEE, pp. 805-812.

Cheng, X. J. & Jin, W., 2006. Study on reverse engineering of historical architecture based on 3D laser scanner. *Journal of Physics: Conference Series*.

Chen, S. & Li, Y., 2005. Vision sensor planning for 3-D model acquisition. *IEEE Transactions on Systems, Man and Cybernetics*, pp. 894-904.

Chen, S., Li, Y. & Ngai, M. K., 2011. Active vision in robotic systems: A survey of recent developments. *The International Journal of Robotics Research*, pp. 1343-1377.

Cline, M. S., 2005. *Power, Madness, & Immortality: the Future of Virtual Reality.* s.l.:University Village Press.

CloudCompare, 2017. *CloudCompare - 3D point cloud and mesh processing software.* [Online]
Available at: http://www.danielgm.net/cc/
[Accessed 01 10 2017].

Coherent Inc., 2012. *Coherent 3D Machine Vision.* [Online]
Available at: https://www.coherent.com/assets/pdf/3D_Machine_Vision.pdf
[Accessed 20 11 2016].

Concheri, G., Cristofolini, I., Meneghello, R. & Wolf, G., 2001. *Geometric dimensioning and tolerancing (GD&T) versus geometrical product specification (GPS). In XII ADM International Conference, Grand Hotel, Rimini, Italy..* s.l., s.n.

Connoly, C., 1985. *The determination of next best views.* s.l., IEEE, pp. 432-435.

Creaform3D, 2016. *Creaform Handyscan.* [Online]
Available at: http://www.creaform3d.com/en/metrology-solutions/portable-3d-scanner-handyscan-3d
[Accessed 17 11 2016].

Creaform3D, 2016. *Creaform3D ScanMaster.* [Online]
Available at: http://www.creaform3d.com/en/metrology-solutions/truly-accurate-turnkey-3d-scanning-solution-automated-quality-control
[Accessed 11 11 2016].

Creaform3D2, 2016. *Creaform3D MetraSCAN 3D R.* [Online]
Available at: http://www.creaform3d.com/en/metrology-solutions/robot-mounted-optical-cmm-scanners-metrascan-r
[Accessed 11 11 2016].

CultLab3D, 2014. *CultLab3D flyer.* [Online]
Available at: http://cultlab3d.eu/files/2014-01-15_CHD3D_Flyer_EN_web.pdf
[Accessed 18 11 2016].

CultLab3D, 2016. *CultLab3D.* [Online]
Available at: http://www.cultlab3d.de/
[Accessed 18 11 2016].

CultLab3D, 2016. *CultLab3D - results.* [Online]
Available at: http://www.cultlab3d.de/results.html
[Accessed 18 11 2016].

CultLab3D, 2016. *CultLab3D pipeline.* [Online]
Available at: https://www.youtube.com/watch?v=sRLyEuzuF2A
[Accessed 18 11 2016].

Curless, B. & Levoy, M., 1995. *Better optical triangulation through spacetime analysis.* s.l.,
IEEE, pp. 987-994.

Dasgupta, B. & Mruthyunjaya, T. J., 1998. Force redundancy in parallel manipulators:
theoretical and practical issues. *Mechanism and Machine Theory,* 33(6), pp. 727-741.

Davis, N., 2016. Project Anywhere: digital route to an out-of-body experience. *The Guardian*,
09.

De Luca, L., Véron, P. & Florenzano, M., 2006. Reverse engineering of architectural
buildings based on a hybrid modeling approach. *Computers & Graphics*, pp. 160-176.

De Reu, J. et al., 2013. De Reu, J., Plets, G., Verhoeven, G., De Smedt, P., Bats, M.,
Cherretté, B., ... & Van Meirvenne, M. (2013). Towards a three-dimensional cost-effective
registration of the archaeological heritage. Journal of Archaeological Science, 40(2), 1108-
1121.. *Journal of Archaeological Science*, pp. 1108-1121.

Dijkstra, E. W., 1959. A note on two problems in connexion with graphs. *Numerische
mathematik,* 1(1), pp. 269-271.

Divecha, D., 2011. Augumented Reality (AR) used in architecture and design. *designMENA*,
8.

Doerr, M., 2005. *The cidoc crm, an ontological approach to schema heterogeneity.* Schloss
Dagstuhl, s.n.

Doerr, M. et al., 2010. *The europeana data model (edm).* s.l., s.n., pp. 10-15.

Dorai, C., Wang, G., Jain, A. K. & Mercer, C., 1998. Registration and integration of multiple object views for 3D model construction. *IEEE Transactions on Pattern Analysis and Machine Intelligence* , pp. 83-89.

Dorn, M., Browne, M. & Ghidary, S. S., 2003. *Landmark detection by a rotary laser scanner for autonomous robot navigation in sewer pipes.* Jecheon, s.n.

Dorrington, A. A., Payne, A. D. & Cree, M. J., 2010. An evaluation of time-of-flight range cameras for close range metrology applications. *International archives of photogrammetry, remote sensing and spatial information sciences*, pp. 201-206.

Dorsch, R. G., Häusler, G. & Herrmann, J. M., 1994. Laser triangulation: fundamental uncertainty in distance measurement. *Applied Optics*, pp. 1306-1314.

Du, G. et al., 2015. *A 3D modeling and measurement system for cultural heritage preservation.* s.l., SPIE.

Durupt, A., Remy, S., Ducellier, G. & Eynard, B., 2008. From a 3D point cloud to an engineering CAD model: a knowledge-product-based approach for reverse engineering. *Virtual and Physical Prototyping*, pp. 51-59.

Dynamake, 2015. *Dynamake Trinity 3D printer.* [Online]
Available at: http://dynamake.com/
[Accessed 10 10 2015].

Eidenbenz, S., 2002. Approximation algorithms for terrain guarding. *Information Processing Letters*, pp. 99-105.

Erič, M. et al., 2013. *The impact of the latest 3D technologies on the documentation of underwater heritage sites.* s.l., IEEE.

European Commision, 2016. *EU FP7 Framework.* [Online]
Available at: https://ec.europa.eu/research/fp7/index_en.cfm
[Accessed 18 11 2016].

European Commision, 2016. *Horizon 2020 framework.* [Online]
Available at: https://ec.europa.eu/programmes/horizon2020/en/what-horizon-2020
[Accessed 18 11 2016].

Evatronix, 2017. *Skanery 3D.* [Online]
Available at: http://evixscan3d.pl/skanery-3d/
[Accessed 02 09 2017].

Facebook, 2016. *Oculus VR.* [Online]
Available at: https://www.facebook.com/oculusvr/
[Accessed 09 11 2016].

Fan, K. C. & Leu, M. C., 1998. Intelligent planning of CAD-directed inspection for coordinate measuring machines. *Computer Integrated Manufacturing Systems*, 2, pp. 43-51.

Fanuc Ltd., 2016. *Fanuc Robotics.* [Online]
Available at: http://www.fanuc.eu/uk/en/robots/robot-filter-page/lrmate-series
[Accessed 11 08 2016].

Faro, 2016. *Faro Laser Scanners.* [Online]
Available at: http://www.faro.com/products/3d-surveying/laser-scanner-faro-focus-3d/overview
[Accessed 10 11 2016].

FARO, 2016. *FARO Robo-Imager Mobile.* [Online]
Available at: http://www.faro.com/products/metrology/faro-factory-robo-imager-mobile/overview
[Accessed 12 10 2016].

FARO2, 2016. *FARO Robo-Imager video demonstration.* [Online]
Available at: https://www.youtube.com/watch?v=TlkbzvovwaE
[Accessed 11 10 2016].

FARO3, 2016. *FARO Robo-Imager.* [Online]
Available at: http://www.faro.com/es-mx/productos/metrologia/faro-factory-array-imager/vision-general
[Accessed 12 10 2016].

FARO4, 2016. *FARO Cobalt.* [Online]
Available at: http://cobalt.faro.com/
[Accessed 12 10 2016].

Finocchiaro, C. W., 2012. Personal Factory or Catalyst for Piracy: The Hype, Hysteria, and Hard Realities of Consumer 3-D Printing. *Cardozo Arts & Ent.*.

Fraser, C., 2015. *Advances in Close-Range Photogrammetry.* s.l., Wachmann/VDE Verlag.

Fröhlich, C. & Mettenleiter, M., 2004. Terrestrial laser scanning–new perspectives in 3D surveying. *International archives of photogrammetry, remote sensing and spatial information sciences.*

Gao, J., Gindy, N. & Chen, X., 2006. An automated GD&T inspection system based on non-contact 3D digitization. *International Journal of Production Research*, 01, pp. 117-134.

General Electric, 2016. *GE PACRX3i.* [Online]
Available at: http://www.geautomation.com/products/pacsystems-rx3i-controller
[Accessed 22 09 2016].

Geomagic, 2016. *Geomagic Control.* [Online]
Available at: http://www.geomagic.com/en/products/control/overview
[Accessed 11 10 2016].

Georgopoulos, A., Ioannidis, C. & Valanis, A., 2010. *Assessing the performance of a structured light scanner.* s.l., s.n.

Germani, F., Mandorli, F., Mengoni, M. & Raffaeli, R., 2010. CAD-based environment to bridge the gap between product design and tolerance control. *Precision Engineering*.

Gibson, I., 2006. *Advanced manufacturing technology for medical applications: reverse engineering, software conversion and rapid prototyping.* s.l.:John Wiley & Sons.

Ginsburg, B., 2016. Naughty America Invites You to Experience Virtual Reality Adult Entertainment During South by Southwest. *Business Wire*.

Glinkowski, W., Michoński, J., Sitnik, R. & Witkowski, M., 2010. 3D diagnostic system for anatomical structures detection based on a parametrized method of body surface analysis. *Journal of Biomedical Optics*, pp. 153-164.

Gokturk, S. B., Yalcin, H. & Bamji, C., 2004. *A time-of-flight depth sensor-system description, issues and solutions.* s.l., IEEE.

GOM, 2016. *GOM Atos ScanBox.* [Online]
Available at: http://www.gom.com/metrology-systems/atos-scanbox.html
[Accessed 11 10 2016].

GOM2, 2016. *Atos Digitizer.* [Online]
Available at: http://www.gom.com/metrology-systems/atos/atos-triple-scan.html
[Accessed 11 10 2016].

Google, 2016. *Google VR.* [Online]
Available at: https://vr.google.com/
[Accessed 09 11 2016].

Haasbroek, N. D., 1968. Gemma Frisius, Tycho Brahe and Snellius and their triangulations. *Delft, Rijkscommissie voor Geodesie*.

Haas, N., 2016. *Multisensor evidence integration and optimization in object inspection.* United States of America, Patent No. 9,260,122..

Hähnel, D. & Burgard, W., 2002. *Probabilistic matching for 3D scan registration.* Ludwigsburg , s.n.

Harris, M. et al., 1998. The role of laser coherence length in continuous-wave coherent laser radar. *Journal of Modern Optics*, pp. 1567-1581.

Hartley, R. & Zisserman, A., 2003. *Multiple View Geometry in Computer Vision.* 2 ed. s.l.:Cambridge University Press.

Hebert, M. & Krotkov, E., 1992. 3D measurements from imaging laser radars: how good are they?. *Image Vision and Computing*, pp. 170-178.

Helling, 2015. *3D Laserscanning Entspiegelungsspray.* [Online]
Available at: http://www.helling-ndt.de/optische-pruefung/3-d-laserscanning-entspiegelungsspray
[Accessed 10 10 2015].

Henricson, M. & Nyquist, E., 1997. *Industrial Strength C++.* 1 ed. s.l.:Prentice Hall.

Henry, P. et al., 2014. RGB-D mapping: Using depth cameras for dense 3D modeling of indoor environments. *Experimental robotics*, pp. 477-491.

Hołowko, E. et al., 2016. Application of multi-resolution 3D techniques in crime scene documentation with bloodstain pattern analysis. *Forensic Science International*, pp. 218-227.

Hołowko, E., Wojsz, J., Sitnik, R. & Karaszewski, M., 2014. Color-based algorithm for automatic merging of multiview 3D point clouds. *Journal on Computing and Cultural Heritage* .

Horn, B., 1984. *Extended Gaussian images.* s.l., IEEE, pp. 1671-1686.

Hosseininaveh, A. et al., 2014. Towards fully automatic reliable 3D acquisition: From designing imaging network to a complete and accurate point cloud. *Robotics and Autonomous Systems*, pp. 1197-1207.

HTC, 2016. *HTC Vive.* [Online]
Available at: https://www.vive.com/eu/
[Accessed 09 11 2016].

Hwang, C. Y., Tsai, C. Y. & Chang, C. A., 2004. Efficient inspection planning for coordinate measuring machines. *The International Journal of Advanced Manufacturing Technology*, 9, pp. 732-742.

IDS Imaging Development Systems GmbH, 2017. *IDS Camera Finder.* [Online]
Available at: https://en.ids-imaging.com/store/products/cameras.html
[Accessed 22 05 2017].

Impoco, G., Cignoni, P. & Scopigno, R., 2004. *Closing gaps by clustering unseen directions.* s.l., IEEE.

Intel Corporation, 2016. *Intel Realsense.* [Online]
Available at: http://www.intel.com/content/www/us/en/architecture-and-technology/realsense-overview.html
[Accessed 09 11 2016].

Kai-Browne, A. et al., 2016. *3D Acquisition, Processing and Visualization of Archaeological Artifacts.* s.l., Springer International Publishing.

Kamrani, A. et al., 2015. Feature-based design approach for integrated CAD and computer-aided inspection planning. *International Journal of Advanced Manufacturing Technology*, pp. 2159-2183.

Karaszewski, M. et al., 2013. *Automated full-3D digitization system for documentation of paintings.* Munich, SPIE.

Karaszewski, M. et al., 2012. *Automated view integration techniques for numerous 3d clouds of points.* s.l., Springer Berlin Heidelberg.

Karaszewski, M., Lech, K., Bunsch, E. & Sitnik, R., 2014. *In the pursuit of perfect 3D digitization of surfaces of paintings: geometry and color optimization.* Limassol, Cyprus, Springer.

Karaszewski, M., Sitnik, R. & Adamczyk, M., 2016. Assessment of next-best-view algorithms performance with various 3D scanners and manipulator. *ISPRS Journal of Photogrammetry and Remote Sensing*, pp. 320-333.

Karaszewski, M., Sitnik, R. & Bunsch, E., 2012. On-line, collision-free positioning of a scanner during fully automated three-dimensional measurement of cultural heritage objects. *Robotics and Autonomous Systems*, pp. 1205-1219.

Karaszewski, M., Sitnik, R. & Bunsch, E., 2012. On-line, collision-free positioning of a scanner during fully automated three-dimensional measurement of cultural heritage objects. *Robotics and Autonomous Systems*, Issue 60.9, pp. 1205-1219.

Karaszewski, M., Sitnik, R. & Bunsch, E., 2013. *The Process of Automated Digitization of Shape and Colour of Outdoor Historical Objects.* s.l., s.n., pp. 74-79.

Katts, R., 2012. Elizabeth Arden brings new fragrance to life with augmented reality. *Mobile Marketer*, 09.

Kawasaki Robotics, 2016. *Kawasaki Robotics.* [Online]
Available at: https://robotics.kawasaki.com/en1/products/robots/small-medium-payloads/RS005L/
[Accessed 12 09 2016].

Kazhdan, M., Bolitho, M. & Hoppe, H., 2006. *Poisson surface reconstruction.* s.l., s.n.

Kazhdan, M. & Hoppe, H., 2013. Screened poisson surface reconstruction. *ACM Transactions on Graphics (TOG).*

Kerney, A. T., 2015. *3D Printing: A Manufacturing Revolution,* s.l.: s.n.

Khalfaoui, S., Seulin, R., Fougerolle, Y. & Fofi, D., 2013. An efficient method for fully automatic 3D digitization of unknown objects. *Computers in Industry*, pp. 1152-1160.

Konica Minolta, 2016. *Konica Minolta 3D Digitizer.* [Online]
Available at: https://www.konicaminolta.eu/en/measuring-instruments/products/3d-measurement/range-7/introduction.html
[Accessed 22 10 2016].

Konica Minolta, 2017. *Konica Minolta Vivid 910 Laser Scanner.* [Online]
Available at:
http://www.konicaminolta.com/instruments/download/instruction_manual/3d/pdf/vivid-910_vi-910_instruction_eng.pdf
[Accessed 09 09 2016].

Koppel, P., 2012. *Agisoft PhotoScan: Point Cloud accuracy in close range configuration,* s.l.: Koppel Engineering Messdienstleistungen.

Kotem Software, 2016. *GageSite.* [Online]
Available at: http://www.gagesite.com/smartprofile-software-p-220000-l-en.html
[Accessed 10 10 2016].

Ko, T. J., Park, J. W., Kim, H. S. & Kim, S. H., 2007. On-machine measurement using a noncontact sensor based on a CAD model. *The international journal of advanced manufacturing technology*, 7, pp. 739-746.

Kriegel, S., Bodenmüller, T., Suppa, M. & Hirzinger, G., 2011. *A surface-based next-best-view approach for automated 3D model completion of unknown objects.* s.l., IEEE, pp. 4869-4874.

Kriegel, S., Bodenmüller, T., Suppa, M. & Hirzinger, G., 2011. *A surface-based next-best-view approach for automated 3D model completion of unknown objects.* s.l., s.n., pp. 4869-4874.

Kriegel, S. et al., 2012. *Next-Best-Scan Planning for Autonomous 3D Modeling.* s.l., IEEE, p. 2850–2856.

Kriegel, S., Rink, C., Bodenmüller, T. & Suppa, M., 2015. Efficient next-best-scan planning for autonomous 3D surface reconstruction of unknown objects. *Journal of Real-Time Image Processing*, 01 12, pp. 611-631.

Krzesłowski, J., Sitnik, R. & Mączkowski, G., 2011. Integrated three-dimensional shape and reflection properties measurement system. *Applied Optics*, pp. 532-541.

Kweon, S. & Medeiros, D. J., 1998. Improvement of coordinate measuring machine probing accessibility. *Computer-Aided Design*, 8, pp. 741-749.

Labster, 2016. *Labster- stoliki obrotowe.* [Online]
Available at: http://www.labster.com.pl/index.php/pl/fotografia-obrotowa-360
[Accessed 20 07 2016].

Lange, R., 2000. *3D time-of-flight distance measurement with custom solid-state image sensors in CMOS/CCD-technology, Diss., Department of Electrical Engineering and Computer Science.* s.l.:University of Siegen.

Larue, J.-F., Brown, D. & Viala, M., 2015. How optical CMMs and 3D scanning will revolutionize the 3D metrology world. *Integrated Imaging and Vision Techniques for Industrial Inspection*, pp. 141-176.

LaserDesign, 2016. *Rexscan DS3.* [Online]
Available at: http://www.laserdesign.com/products/rexcan-ds3/
[Accessed 08 11 2016].

LaserDesign2, 2016. *Rexscan DS3 videoclip.* [Online]
Available at: http://www.laserdesign.com/rexcan-ds-short-video-clip/
[Accessed 09 11 2016].

LaserDesign3, 2016. *CyberGage360.* [Online]
Available at: http://www.laserdesign.com/products/CyberGage360/
[Accessed 10 11 2016].

Lazebnik, S., Schmid, C. & Ponce, J., 2005. A sparse texture representation using local affine regions. *IEEE Transactions on Pattern Analysis and Machine Intelligence*, pp. 1265-1278.

Lee, N., 2016. 'Gone' is a VR thriller from 'Walking Dead' team and Samsung. *Engadget*.

Leica Geosystems, 2016. *Leica Laser Scanners.* [Online]
Available at: http://leica-geosystems.com/products/laser-scanners/scanners
[Accessed 18 11 2016].

Lenstra, J. K., Kan, A. R. & Shmoys, D. B., 1985. *The traveling salesman problem: a guided tour of combinatorial optimization.* New York: Wiley.

Limaiem, A. & ElMaraghy, H. A., 1997. *Automatic Planning for Coordinate Measuring Machines.* Marina del Rey, IEEE.

Little, C. Q., Small, D. E., Peters, R. R. & Rigdon, J. B., 2000. *Forensic 3D scene reconstruction.* s.l., International Society for Optics and Photonics.

Li, Y. & Gu, P., 2004. Free-form surface inspection techniques state of the art review. *Computer-Aided Design*, pp. 1395-1417.

Logan, W. S., 2007. Closing Pandora's box: human rights conundrums in cultural heritage protection. *Cultural Heritage and Human Rights*, pp. 33-52.

Loriot, B., Seulin, R., Gorria, P. & Meriaudeau, F., 2007. *Simulation for an automation of 3D acquistion and post-processing.* s.l., SPIE, pp. 635604-635604.

Lowe, D. G., 2004. Distinctive image features from scale-invariant keypoints.. *International journal of computer vision*, pp. 91-110.

Loy Rodas, N. P. N., 2014. 3D Global Estimation and Augmented Reality Visualization of Intra-operative X-ray Dose". Proceedings of Medical Image Computing and Computer-Assisted Intervention (MICCAI). *Oral*.

Luhmann, T., Robson, S., Kyle, S. & Harley, I., 2006. *Close range photogrammetry: Principles, methods and applications.* s.l.:Whittles.

MacDonald, L., 2010. *The limits of resolution.* s.l., British Computer Society.

MakerBot, 2016. *MakerBot Digitizer.* [Online]
Available at: http://www.makerbot.com/media-center/2013/08/22/makerbot-digitizer-desktop-3d-scanner-order-today
[Accessed 17 11 2016].

Mansouri, A. et al., 2007. Toward a 3d multispectral scanner: an application to multimedia. *IEEE Multimedia*.

Markets, M. a., 2016. *3D scanner market,* s.l.: marketsandmarkets.com.

Markiewicz, J. S. & Zawieska, D., 2015. *Quality assessment of the TLS data in conservation of monuments.* s.l., SPIE.

Markmoryak, 2015. *Sculpture- Königsberg - Hermann Brachert - Nimfa.* [Online]
Available at: http://www.thingiverse.com/thing:855724
[Accessed 12 08 2015].

Martins, F. A. R., Garcia-Bermejo, J. G., Casanova, E. Z. & Gonzalez, J. R. P., 2005.
Automated 3D surface scanning based on CAD model. *Mechatronics*, pp. 837-857.

Matter and Form, 2016. *Matter and Form 3D scanner.* [Online]
Available at: https://matterandform.net/scanner
[Accessed 29 10 2016].

May, S., Werner, B., Surmann, H. & Pervolz, K., 2006. *3D time-of-flight cameras for mobile robotics.* s.l., IEEE, pp. 790-795.

McAlinden, C., Khadka, J. & Pesudovs, K., 2011. A comprehensive evaluation of the precision (repeatability and reproducibility) of the Oculus Pentacam HR. *Investigative ophthalmology & visual science*, pp. 7731-7737.

Meeri, K., 2016. Virtual reality apps aim to make exercise less tedious. *Tyler Morning Telegraph*, pp. A1-A11.

Microsoft Corporation, 2016. *Microsoft Hololens.* [Online]
Available at: https://www.microsoft.com/microsoft-hololens/en-us
[Accessed 09 11 2016].

Microsoft, 2016. *Microsoft Visual Studio 2015.* [Online]
Available at: https://msdn.microsoft.com/pl-pl/library/dd831853.aspx
[Accessed 3 10 2017].

Młynarska, P., 2017. *Research on application possibilites of 3D scanning in 3D printing technology - Masters Degree Thesis,* Warsaw: Warsaw University of Technology.

Munkelt, C. et al., 2013. Handheld 3D scanning with automatic multi-view registration based on optical and inertial pose estimation. *Fringe 2013*, pp. 809-814.

Muzeum Pałacu Króla Jana III w Wilanowie, 2016. *Zatrzymać Czas.* [Online]
Available at: https://www.youtube.com/watch?v=JOjyahe1LpM
[Accessed 22 11 2016].

National Institute of Justice, 2016. *Landscape Study on 3D Crime Scene Scanning Devices,* s.l.: RTI International.

NextEngine, 2016. *NextEngine 3D scanner.* [Online]
Available at: https://www.nextengine.com/
[Accessed 29 10 2016].

Occipital, 2016. *Structure Sensor.* [Online]
Available at: https://store.structure.io/store
[Accessed 28 09 2016].

Papadimitriou, C. H., 1977. The Euclidean travelling salesman problem is NP-complete. *Theoretical Computer Science*, pp. 237-244.

Papadopoulos-Orfanos, D. & Francis, S., 1997. *Automatic 3-D digitization using a laser rangefinder with a small field of view.* s.l., IEEE, pp. 60-67.

Papadopoulos-Orfanos, D. & Schmitt, F., 1997. *Automatic 3-D digitization using a laser rangefinder with a small field of view.* s.l., IEEE, pp. 60-67.

Perceptron, 2016. *Perceptron Robotic Scanning.* [Online]
Available at: http://perceptron.com/products/3d-scanning-solutions/robotic-scanning/
[Accessed 29 09 2016].

Photoneffect, 2016. *ColDet 3D Collision Detection.* [Online]
Available at: https://sourceforge.net/projects/coldet/
[Accessed 29 09 2016].

Pigan, R. & Metter, M., 2008. *Automating with PROFINET.* 2 ed. s.l.:s.n.

Pito, R., 1996. *A sensor-based solution to the "next best view" problem.* s.l., IEEE, pp. 941-945.

Pito, R., 1999. A solution to the next best view problem for automated surface acquisition. *IEEE Transactions on Pattern Analysis and Machine Inteligence*, pp. 1016-1030.

Ponomarenko, N. et al., 2009. Ponomarenko, N., Lukin, V., Zelensky, A., Egiazarian, K., Carli, M., & Battisti, F. (2009). TID2008-a database for evaluation of full-reference visual quality assessment metrics. *dvances of Modern Radioelectronics*, pp. 30-45.

Poussart, D. & Laurendeau, D., 1989. 3-D sensing for industrial computer vision. *Advances in Machine Vision*, pp. 122-159.

PragmaVision Sp. z o. o., 2017. *SLScan - skanery 3D.* [Online]
Available at: http://pragmavision.pl/slscan/
[Accessed 22 05 2017].

Prieto, F., Redarce, T., Boulanger, P. & Lepage, R., 1999. *CAD-Based Range Sensor Placement for Optimum 3D Data Acquisition.* s.l., IEEE.

Qt Company, 2017. *Qt Company.* [Online]
Available at: https://www.qt.io/
[Accessed 2 10 2017].

Raju, S., Mansouri, A. & Hardeberg, J. Y., 2011. *Multispectral imaging using a stereo camera: Concept, design and assessment..* s.l., s.n.

ReconstructMe, 2015. *Reconstructme.* [Online]
Available at: http://reconstructme.net/
[Accessed 10 10 2015].

Reed, M. & Allen, P., 2000. Constraint-based sensor planning for scene modeling. *IEEE Transactions Pattern Analysis and Machine Intelligence*, pp. 1460-1467.

Reed, M. K. & Allen, P. K., 2000. Constraint-based sensor planning for scene modeling. *IEEE Transactions on Pattern Analysis and Machine Inteligence*, pp. 1460-1467.

Remondino, F., 2011. Heritage recording and 3D modeling with photogrammetry and 3D scanning. *Remote Sensing*, pp. 1104-1138.

Richter, R. & Döllner, J., 2014. Concepts and techniques for integration, analysis and visualization of massive 3D point clouds. *Computers, Environment and Urban Systems*, pp. 114-124.

Riegl, 2016. *Riegl Terrestial Scanning.* [Online]
Available at: http://www.riegl.com/nc/products/terrestrial-scanning/produktdetail/product/scanner/33/
[Accessed 18 11 2016].

Roettgers, J., 2016. Fox Sports Streams College Football Match in Virtual Reality. *Variety*.

Rosato, D. V. & Rosato, M. G., 2012. *Injection molding handbook.* s.l.:Springer Science & Business Media.

Rublee, E., Rabaud, V., Konolige, K. & Bradski, G., 2011. *ORB: An efficient alternative to SIFT or SURF.* s.l., IEEE, pp. 2564-2571.

Rusinkiewicz, S. & Levoy, M., 2001. *Efficient variants of the ICP algorithm.* s.l., IEEE.

Rusli, E., 2015. WSJ.D Technology: Oculus VR Seeks to Go Beyond Games — Facebook Unit to Create Lab to Help Studios Create Films Using Virtual Reality Technology. *The Wall Street Journal*.

Rusu, R. B. & Cousins, S., 2011. *3d is here: Point cloud library (pcl).* s.l., IEEE.

Rüther, H., Smit, J. & Kamamba, D., 2012. A Comparison of Close-Range Photogrammetry to Terrestrial Laser. *South African Journal of Geomatics*, 8.

Sansoni, G., Trebeschi, M. & Docchio, F., 2009. State-of-the-art and applications of 3D imaging sensors in industry, cultural heritage, medicine, and criminal investigation.. *Sensors*, pp. 658-601.

Santos, P., 2014. *CultLab3D - the system* [Interview] (6 11 2014).

Schäfer, A. et al., 2011. *Large scale Angkor style reliefs: high definition 3D acquisition and improved visualization using local feature estimation.* s.l., s.n.

Schäfer, S. et al., 2015. *Collaborating robots in a museum environment: Modular systems for 3D documentation.* s.l., IEEE.

Sciavicco, L. & Siciliano, B., 1996. *Modeling and control of robot manipulators.* New York: McGraw-Hill.

Scopigno, R. et al., 2015. Digital Fabrication Techniques for Cultural Heritage: A Survey. *Computer Graphics Forum*, 11.

Scott, W. R., 2009. Model-based view planning. *Machine Vision and Applications*, pp. 47-69.

Scott, W., Roth, G. & Rivest, J., 2003. View planning for automated 3D object reconstruction inspection. *ACM Computing Surveys*.

Sculpteo, 2016. *Sculpteo - 3D printing hub.* [Online]
Available at: https://www.sculpteo.com/en/glossary/3d-scan-definition/
[Accessed 09 11 2016].

Shapegrabber, 2016. *Shapergrabber Automated Scanning Systems.* [Online]
Available at: http://www.shapegrabber.com/product/automated-3d-scanners/shapegrabber-ai310/
[Accessed 10 10 2016].

Sheng, W. & Xi, N., 2000. *Automated CAD-Guided Automobile Part Dimensional Inspection.* s.l., IEEE, pp. 1157-1162.

Sitnik, R. & Karaszewski, M., 2010. *Zautomatyzowany system do trójwymiarowej digitalizacji obiektów polskiego i europejskiego dziedzictwa kulturowego. Raport merytoryczny projektu badawczo-rozwojowego NR17 001 02,* s.l.: s.n.

Sładek, J. et al., 2011. The hybrid contact–optical coordinate measuring system. *Measurement*, pp. 503-510.

Smarttech, 2017. *Smarttech Skanery 3D.* [Online]
Available at: http://www.smarttech.pl/
[Accessed 20 08 2017].

Sokovic, M. & Kopac, J., 2006. RE (reverse engineering) as necessary phase by rapid product development.. *Journal of Materials Processing Technology*, pp. 398-403.

Stanco, F., Battiato, S. & Gallo, G., 2011. *Digital imaging for cultural heritage preservation: Analysis, restoration, and reconstruction of ancient artworks..* s.l.:CRC Press.

Stuart, E., 2012. Augmenting Phenomenology: Using Augmented Reality to Aid Archaeological Phenomenology in the Landscape. *Journal of archaeological method and theory*, pp. 582-600.

Tarbox, G. H. & Gottschlich, S. N., 1995. Planning for complete sensor coverage in inspection. *Computer Vision and Image Understanding*, pp. 84-111.

Taylor, A., Unver, E. & Ball, A., 2016. *Interdisciplinary 3d Mobile Scanning Technology Case Studies: Canvasman, Faro, Artec & Structure Sensor For Ipad.* s.l., s.n.

Thali, M. J. et al., 2007. VIRTOPSY–the Swiss virtual autopsy approach. *Legal Medicine*, pp. 100-104.

The Economist, 2016. Print me a Stradivarius. *The Economist*.

Triggs, B., McLauchlan, P. F., Hartley, R. I. & Fitzgibbon, A. W., 1999. *Bundle adjustment—a modern synthesis.* s.l., Springer Berlin Heidelberg, pp. 298-372.

Trimble, 2016. *Trimble Laser Scanners.* [Online]
Available at: http://www.trimble.com/3d-laser-scanning/index.aspx
[Accessed 10 10 2016].

TRoesner, F. et al., 2014. *"Augmented Reality".* s.l., ACM.

Turner, D., Lucieer, A. & Watson, C., 2012. An automated technique for generating georectified mosaics from ultra-high resolution unmanned aerial vehicle (UAV) imagery, based on structure from motion (SfM) point clouds. *Remote Sensing*, pp. 1392-1410.

Vasquez-Gomez, J., Sucar, L., Murrieta-Cid, R. & Lopez, D., 2014. Volumetric Next Best View Planning for 3D Object Reconstruction with Positioning Error. *International Journal of Advanced Robotic Systems*.

VDI/VDE, 2008. *Standard: VDI/VDE 2634 BLATT 3,* s.l.: VDI/VDE-Gesellschaft Mess- und Automatisierungstechnik.

VRTD, 2017. *VRTD.* [Online]
Available at: http://ztrw.mchtr.pw.edu.pl/en/about-vrtd/
[Accessed 2 10 2017].

Wadhwa, T., 2013. CrowdOptic and L'Oreal To Make History By Demonstrating How Augmented Reality Can Be A Shared Experience. *Forbes*, 06.

Webley, K., 2010. The 50 Best Inventions of 2010. *Time*, 11.

Westoby, M. J. et al., 2012. Structure-from-Motion'photogrammetry: A low-cost, effective tool for geoscience applications. *Geomorphology*, pp. 300-314.

Witkowski, M. et al., 2008. Surface shape parameters and analysis of data captured with use of 4D surface scanners. *Biomedical Optics*.

Wittbrodt, B. T. et al., 2013. Life-cycle economic analysis of distributed manufacturing with open-source 3-D printers. *Mechatronics*.

Woo, S., Dipanda, A., Marzani, F. & Voisin, Y., 2002. *Determination of an Optimal Configuration for a Direct Correspondence in an Active Stereovision System.* s.l., s.n.

Woźniak, A. & Dobosz, M., 2003. Metrological feasibilities of CMM touch trigger probes. Part I: 3D theoretical model of probe pretravel. *Measurement*, pp. 273-286.

Wu, S. et al., 2014. *Quality-driven Poisson-guided autoscanning.* s.l., ACM.

Wu, Y., Liu, S. & Zhang, G., 2004. Improvement of coordinate measuring machine probing accessibility. *Precision Engineering*, 1, pp. 89-94.

XYZ Printing, 2016. *http://us.xyzprinting.com/product/dv10aio.* [Online]
Available at: http://us.xyzprinting.com/product/dv10aio
[Accessed 22 09 2016].

Yang, C. C. & Ciarallo, F. W., 2001. Optimized Sensor Placement for Active Visual Inspection. *Journal of Robotic Systems*, 1, pp. 1-15.

Yashyna, K., Krupnyk, O. & Karpenko, O., 2016. Application of 3D Printing and 3D Scanning Technologies in Educational Activities. *ICT in Education, Research and Industrial Applications*.

Yuan, X., 1993. *3D reconstruction as an automatic modeling system (Doctoral dissertation).* Edmonton: University of Alberta.

Yuan, X., 1995. A mechanism of automatic 3D object modeling. *IEEE Transactions on Pattern Analysis and Machine Intelligence*, pp. 307-311.

Zeiss Optotechnik, 2016. *ZEISS T-Scan Automated.* [Online]
Available at: http://optotechnik.zeiss.com/en/products/3d-scanning/laserscanner-t-scan-automated
[Accessed 12 10 2016].

ZEISS Optotechnik2, 2016. *ZEISS Comet Automated.* [Online]
Available at: http://optotechnik.zeiss.com/en/products/3d-scanning/comet-automated
[Accessed 12 10 2016].

ZEISS Optotechnik3, 2016. *ZEISS Visio7.* [Online]
Available at: http://optotechnik.zeiss.com/en/products/software/visio-7
[Accessed 12 10 2016].

ZEISS Optotechnik4, 2016. *ZEISS Comet.* [Online]
Available at: http://optotechnik.zeiss.com/en/products/3d-scanning/comet-6
[Accessed 12 10 2016].

Zhao, F., Xu, X. & Xie, S., 2009. Computer-Aided Inspection Planning - The state of the art. *Computers in Industry*, pp. 453-466.

List of figures

184

List of tables